SUPPORTING INFORMATION

CCC–NHC Au(III) Pincer Complexes as a Reliable Platform for Isolating Elusive Species

Hugo Valdés,[1,*] Nora Alpuente,[1] Pedro Salvador,[1] A. Stephen K. Hashmi,[2,3*] Xavi Ribas [1,*]

Table of Contents

1 General Considerations

Experimental details: All reagents and solvents were purchased from Sigma Aldrich, Fischer Scientific, TCI, Fluorochem or Honeywall and were used without further purification. Compounds 1–isopropyl–1H–benzo[*d*]imidazole and 1–butyl–1H–benzo[*d*]imidazole were synthesized following established procedures outlined in the literature.[1, 2] NMR spectra were recorded on Bruker spectrometers operating at 400 MHz (^{1}H NMR), 101 MHz (^{13}C{^{1}H} NMR), 376 MHz (^{19}F NMR) and referenced to residual solvent, (δ in ppm and *J* in hertz). ESI mass spectra were recorded on a Bruker Esquire 6000 Ion Trap (MS)at Serveis Tècnics de Recerca, University of Girona. For reactions carried out under inert atmosphere, a N_2 drybox with O_2 and H_2O concentrations <1 ppm was employed.

Computational details: All DFT calculations were carried out using GAUSSIAN16 program.[3] Geometry optimizations were performed in gas-phase without any symmetry restrictions. The hybrid PBE0 functional[4] and Grimme's D3 dispersion corrections[5] with Becke–Johnson damping[6, 7] were used based on previous studies of Au(III) complexes.[8-10] Au atoms were always described with a triple–zeta Stuttgart–Köln basis set including a quasi–relativistic pseudopotential.[11, 12] For the other atoms, the cc–pVDZ basis set was used for geometry optimization and harmonic frequency calculations. Additional single–point calculations at the equilibrium geometries ($E_{solv,sp}$) were carried out using the cc–pVTZ basis set and implicit solvent effects (*via* the Self–Consistent Reaction Field –SCRF–method using the SMD solvation model).[13] Only in the case of Bezuidenhout's complexes, the C and H atoms of the isopropyl and isobutyl groups were described with the cc–pVDZ basis set.

The total Gibbs Energy values (G) were calculated using the following equation:

$$G = E_{solv,sp} + G_{corr.} + \Delta G^{\circ/*}$$

The Gibbs Energy correction ($G_{corr.}$) were obtained from the thermodynamical analysis at 333.15 K, using Grimme's Quasi–Harmonic Approximation[14] for harmonic frequencies below 100 cm^{-1}. The additional term $\Delta G^{\circ/*}$ accounts for the correction to 1M standard state. These corrections were obtained with the GoodVibes code.[15]
The two reactions considered in this work are

$AuH(L) + NaH \rightarrow Au(L)^{-} + Na^{+} + H_2$ (in THF implicit solvent) (1)

$AuH(L) + HCOOH \rightarrow Au(L)(HCOO) + H_2$ (in formic acid implicit solvent) (2)

where L represents the pincer ligand.

The effective fragment orbitals (EFOs) for Au, H and pincer ligands were obtained using Natural Atomic Orbitals (NAO) partitioning[16] with the APOST–3D code.[17]
The Cartesian coordinates of all optimized structures can be found in a separate document uploaded (Aupincer.xyz file).

2 Synthesis of diazonium–bis(azolium) salts

2.1 Synthesis of 1,3–bis(bromomethyl)–2–nitrobenzene (2)

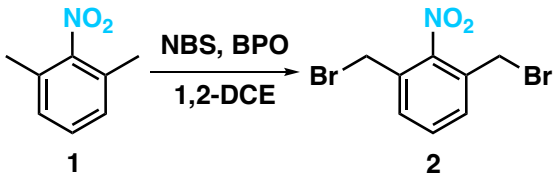

Scheme S1. Synthesis of **2**

1,3–dimethyl–2–nitrobenzene (4.4 mL, 32.4 mmol) was dissolved in 1,2–dichloroethane (30 mL), followed by the addition of N–bromosuccinimide (11.6 g, 65.2 mmol) and Luperox® A70S (benzoyl peroxide, 2.0g, 5.8 mmol). The resulting solution underwent reflux for 24h. Subsequently, the solution was cooled to room temperature, and washed with water (50 mL x 3). Then, Na_2SO_4 was added to the organic phase. The solution was filtered, and the volatiles were removed until the obtention of a red–brown oil. Cyclohexane (50 mL) was added to the oil and heated to reflux for 2 minutes, followed by hot filtration. Upon cooling to room temperature, a semicrystalline compound formed in the solution. The product was collected through filtration, washed with a minimal amount of cyclohexane, and dried under high vacuum. The first crystallization affords a yellowish solid, which can be used in the next step reaction. An extra crystallization from cyclohexane affords a white–off solid. Yield: 1.5g (14%).

^{1}H NMR (400 MHz, $CDCl_3$) δ 7.58 – 7.44 (m, 3H, CH_{Ar}), 4.50 (s, 4H, CH_2).

^{13}C{^{1}H} NMR (101 MHz, $CDCl_3$) δ 149.5 (*C*–NO_2), 132.0 (*C*H_{Ar}), 131.6 (*C*$_{Ar}$), 131.0 (*C*H_{Ar}), 26.6 (*C*H_2Br).

ESI$^+$ (m/*z*): 309.88 $[M+H]^+$

2.2 Synthesis of 3a and 3b

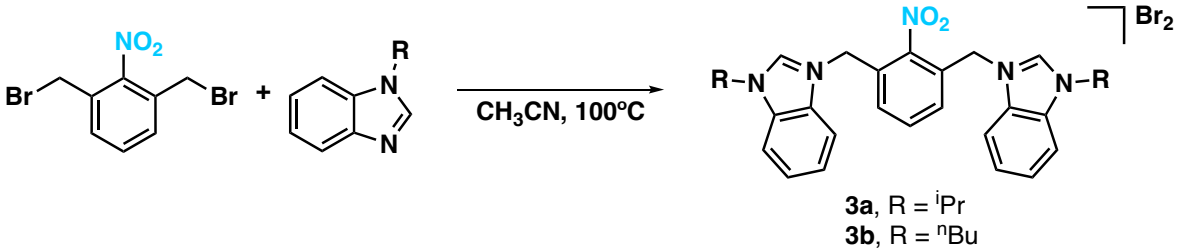

Scheme S2. Synthesis of **3a** and **3b**

A sealed vial with a solution of 1,3–bis(bromomethyl)–2–nitrobenzene (**2**, 1 equivalent) and 1–*subtituted*–1*H*–benzo[*d*]imidazole (2.7 equivalent) in CH_3CN (0.8 mL) was heated at

110 °C for 18h. Then, the solution was warm to room temperature, and filtered. The solid was washed three times with CH_3CN (3mL), followed by diethyl ether (10 mL). The desired compound was obtained as a white solid.

Compound 3a. For the synthesis of **3a** was employed 1,3–bis(bromomethyl)–2–nitrobenzene (1.8315 g, 5.9 mmol) and 1–isopropyl–1*H*–benzo[*d*]imidazole (2.5641 g, 16.0 mmol). Yield: 2.6831g (72%).

^{1}H NMR (400 MHz, DMSO–d_6) δ 10.08 (s, 2H, NC*H*N), 8.21 (d, *J* = 8.3 Hz, 2H, CH_{BIm}), 7.78 (d, *J* = 8.2 Hz, 2H, CH_{BIm}), 7.71 (td, *J* = 7.9, 1.2 Hz, 2H, CH_{BIm}), 7.67 – 7.55 (m, 3H, 3H CH_{BIm} and 1H CH_{Ar}), 7.31 (d, *J* = 7.9 Hz, 2H, 2H CH_{Ar}), 6.03 (s, 4H, NCH_2), 5.14 (hept, *J* = 6.6 Hz, 2H, CH_{ipr}), 1.67 (d, *J* = 6.6 Hz, 12H, CH_{3iPr}).

^{13}C{^{1}H} NMR (101 MHz, DMSO–d_6) δ 147.1 (C–NO_2), 142.2 (NCHN), 133.0 (CH_{Ar}), 131.2 (C_{BIm}), 130.7 (C_{BIm}), 129.6 (CH_{Ar}), 128.5 (C_{AR}), 126.9 (CH_{BIm}), 126.8 (CH_{BIm}), 114.4 (CH_{BIm}), 113.8 (CH_{BIm}), 51.0 (CH_{iPr}), 46.9 (CH_2), 21.5 (CH_{3iPr}).

Electrospray MS (m/*z*):548.2 $[M–BF_4]^+$

Compound 3b. For the synthesis of **3b** was employed 1,3–bis(bromomethyl)–2–nitrobenzene (0.8190 g, 2.7 mmol) and 1–butyl–1*H*–benzo[*d*]imidazole (1.0227 g, 5.9 mmol). Yield: 1.7348 g (99%).

^{1}H NMR (400 MHz, DMSO) δ 10.14 (s, 2H, (NC*H*N)), 8.20 (d, *J* = 7.7 Hz, 2H, CH_{BIm}), 7.89 (d, *J* = 8.0 Hz, 2H, CH_{BIm}), 7.76 – 7.61 (m, 5H, 4H CH_{BIm} and 1H CH_{Ar}), 7.51 (d, *J* = 7.5 Hz, 2H, CH_{Ar}), 6.05 (s, 4H, NCH_2), 4.60 (t, *J* = 7.2 Hz, 4H, CH_{2Bu}), 1.92 (p, *J* = 7.6 Hz, 4H, CH_{2Bu}), 1.36 (h, *J* = 7.3 Hz, 4H, CH_{2Bu}), 0.92 (t, *J* = 7.4 Hz, 6H, CH_{3Bu}).

^{13}C{^{1}H} NMR (101 MHz, DMSO) δ 147.7 (*C*–NO_2), 143.2 (NCHN), 133.2 (CH_{Ar}), 131.2 (C_{BIm}), 131.0 (C_{BIm}), 130.7 (CH_{Ar}), 128.2 (C_{Ar}), 126.9 (CH_{BIm}), 126.8 (CH_{BIm}), 114.1 (CH_{BIm}), 113.8 (CH_{BIm}), 46.9 (CH_2), 46.7 (CH_{2Bu}), 30.6 (CH_{2Bu}), 19.0 (CH_{2Bu}), 13.4 (CH_{3Bu}).

Electrospray MS (m/*z*): 578.2 $[M–BF_4]^+$

2.3 Synthesis of 4a and 4b

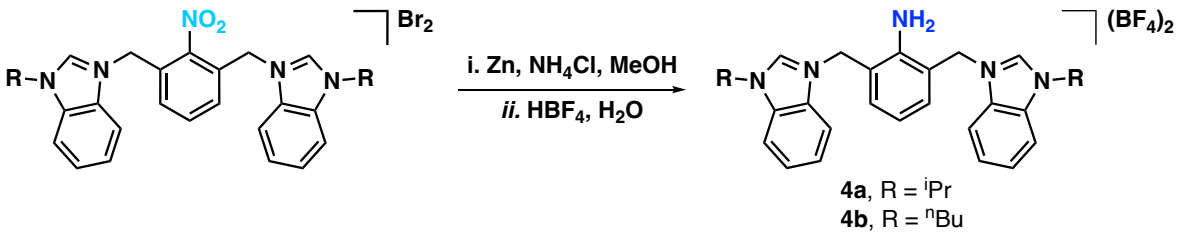

Scheme S3. Synthesis of **4a** and **4b**

A solution of **1a** or **1b** (1.6 mmol) and NH_4Cl (432.9 mg, 7.9 mmol) in methanol (350 mL) was stirred at room temperature until a clear solution was observed. Then, Zn (2.0920 g, 32.0 mmol) was added in one portion, and the resulting suspension was refluxed for 30 min. The reaction was warmed to room temperature and filtered over celite®, then all the volatiles were removed under high vacuum. The solid residue was washed with chloroform (20 mL), followed by the addition of distilled water (50 mL) and HBF_4 (1 mL, 4wt.%). The solution was stirred for 2 h. After this time a white solid was recovered by filtration and washed three times with water (10 mL), followed by 10 mL of diethylether:methanol (8:2) solution.

For the synthesis of **4a** was employed 3,3'–((2–nitro–1,3–phenylene)bis(methylene))bis(1–^{i}propyl–1*H*–benzo[*d*]imidazol–3–ium) bromide (1.021 g, 1.6 mmol). Yield: 926.5 mg (95%).

^{1}H NMR (400 MHz, DMSO–d_6) δ 9.74 (s, 2H, NC*H*N), 8.15 (d, *J* = 8.3 Hz, 2H, CH_{BIm}), 7.80 (d, *J* = 8.2 Hz, 2H, CH_{BIm}), 7.67 (t, *J* = 8.4 Hz, 2H, CH_{BIm}), 7.59 (t, *J* = 7.3 Hz, 2H, CH_{BIm}), 7.23 (d, *J* = 7.6 Hz, 2H, CH_{Ar}), 6.69 (t, *J* = 7.6 Hz, 1H, CH_{Ar}), 5.66 (s, 6H, 2H –NH_2 and 4H C*H*2), 5.08 (hept, *J* = 6.7 Hz, 2H, CH_{iPr}), 1.62 (d, *J* = 6.7 Hz, 12H, C$H_{3\ iPr}$).

^{13}C{^{1}H} NMR (101 MHz, DMSO–d_6) δ = 144.9 (*C*–NH_2), 140.7 (N*C*HN), 131.3 (*C*$_{BIm}$), 131.2 (*C*H_{Ar}), 130.7 (*C*$_{BIm}$), 126.6 (*C*H_{BIm}), 117.7 (*C*$_{Ar}$), 117.1 (*C*H_{Ar}), 114.2 (*C*H_{BIm}), 114.0 (*C*H_{BIm}), 50.7 (*C*H_{iPr}), 47.4 (*C*H_2), 21.5 (*C*H_{3iPr}).

Electrospray MS (m/*z*):526.4 [M–BF_4]$^{+}$

For the synthesis of **4b** was employed 3,3'–((2–nitro–1,3–phenylene)bis(methylene))bis(1–butyl–1*H*–benzo[*d*]imidazol–3–ium) bromide (1.052 g, 1.6 mmol). Yield: 1.019 g (99%).

^{1}H NMR (400 MHz, DMSO–d_6) δ 9.50 (s, 2H, NC*H*N), 8.12 (d, *J* = 7.8 Hz, 2H, CH_{BIm}), 7.94 (d, *J* = 7.5 Hz, 2H, CH_{BIm}), 7.75 – 7.61 (m, 4H, CH_{BIm}), 7.32 (d, *J* = 7.6 Hz, 2H, CH_{Ar}), 6.75 (t, *J* = 7.6 Hz, 1H, CH_{Ar}), 5.65 (br s, 6H, 2H NH_2 and 4H CH_2), 4.50 (t, *J* = 7.2 Hz, 4H, CH_{2Bu}), 1.85 (p, *J* = 7.4 Hz, 4H, CH_{2Bu}), 1.32 (h, *J* = 7.4 Hz, 4H, CH_{2Bu}), 0.90 (t, *J* = 7.3 Hz, 6H, CH_{3Bu}).

^{13}C{^{1}H} NMR (101 MHz, DMSO–d_6) δ 145.7 (*C*$_{Ar}$–NH_2), 141.6 (NC*H*N), 132.5 (CH_{Ar}), 131.4 (*C*$_{BIm}$), 131.3 (*C*$_{BIm}$), 126.7 (*C*H_{BIm}), 126.5 (*C*H_{BIm}), 117.0 (*C*$_{Ar}$), 116.9 (CH_{Ar}), 114.1 (*C*H_{BIm}), 113.8 (*C*H_{BIm}), 47.5 (*C*H_2), 46.4 (*C*H_{2Bu}), 30.7 (*C*H_{2Bu}), 19.0 (*C*H_{2Bu}), 13.3 (*C*H_{3Bu}).

Electrospray MS (m/*z*):554.3 [M–BF_4]$^{+}$

2.4 Synthesis of 5a and 5b

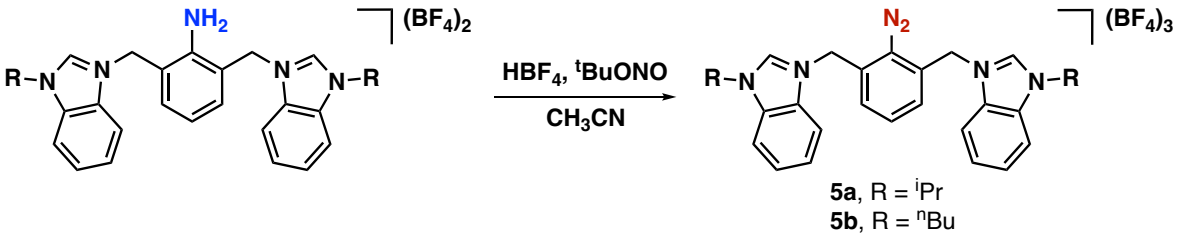

Scheme S4. Synthesis of **5a** and **5b**.

A solution of **4a** or **4b** (1.7 mmol) in CH_3CN (40 mL) was cooled at 0°C, followed by the addition of HBF_4 (0.8 mL, 6.3 mmol). Then, ^{t}BuONO (240.4 µL, 1.8 mmol) was added, and the reaction mixture was stirred for 15 min at 0°C. After this time, diethyl ether (80 mL) was added, and the solution was kept at 0°C for 20 min. The white solid was filtered and washed with diethyl ether (3 x 10 mL).

For the synthesis of **5a** was used 3,3'–((2–amino–1,3–phenylene)bis(methylene))bis(1–^{i}propyl–1*H*–benzo[*d*]imidazol–3–ium) tetrafluoroborate (1.032 g, 1.7 mmol). Yield: 1.1709 g (96%).

^{1}H NMR (400 MHz, DMSO–d_6) δ 10.05 (s, 2H, NC*H*N), 8.26 (d, *J* = 8.3 Hz, 2H, CH_{BIm}), 8.07 (t, *J* = 7.9 Hz, 1H, CH_{Ar}), 7.82 (d, *J* = 8.2 Hz, 2H, CH_{BIm}), 7.76 (t, *J* = 7.9 Hz, 2H, CH_{BIm}), 7.70 (t, *J* = 7.8 Hz, 2H, , CH_{BIm}), 7.62 (d, *J* = 7.9 Hz, 2H, CH_{Ar}), 6.39 (s, 4H, CH_2), 5.15 (hept, *J* = 6.6 Hz, 2H, CH_{ipr}), 1.72 (d, *J* = 6.7 Hz, 5H, CH_{3ipr}).

^{13}C{^{1}H} NMR (101 MHz, DMSO–d_6) δ = 142.6 (N*C*HN), 141.2 (*C*H_{Ar}), 138.9 (*C*$_{Ar}$), 130.9 (*C*H_{BIm}), 130.7 (*C*H_{BIm}), 130.4 (*C*H_{Ar}), 127.1 (*C*H_{BIm}), 127.0 (*C*H_{BIm}), 114.7 (*C*H_{BIm}), 113.9 (C–N_2), 113.8 (*C*H_{BIm}), 51.3 (*C*H_{iPr}), 46.4 (*C*H_2), 21.4 (*C*H_{3iPr}).

Electrospray MS (m/*z*):625.2 $[M–BF_4]^+$.

For the synthesis of **5b** was used 3,3'–((2–amino–1,3–phenylene)bis(methylene))bis(1–butyl–1*H*–benzo[*d*]imidazol–3–ium) tetrafluoroborate (1.090 g, 1.7 mmol). Yield: 1.158 mg (92%).

^{1}H NMR (400 MHz, DMSO–d_6) δ 10.00 (s, 2H, NC*H*N), 8.24 (d, *J* = 8.2 Hz, 2H, CH_{BIm}), 8.09 (t, *J* = 8.0 Hz, 1H, CH_{Ar}), 7.84 (d, *J* = 8.2 Hz, 2H, CH_{BIm}), 7.78 (t, *J* = 7.3 Hz, 2H, CH_{BIm}), 7.71 (t, *J* = 7.4 Hz, 2H, CH_{BIm}), 7.62 (d, *J* = 7.9 Hz, 2H, CH_{Ar}), 6.42 (s, 4H, CH_2), 4.60 (t, *J* = 7.4 Hz, 4H, CH_{2Bu}), 1.99 (p, *J* = 7.6 Hz, 4H, CH_{2Bu}), 1.46 (h, *J* = 7.4 Hz, 4H, CH_{2Bu}), 0.99 (t, *J* = 7.3 Hz, 6H, CH_{3Bu}).

Electrospray MS (m/*z*):653.3 $[M–BF_4]^+$

We were unable to acquire the ^{13}C{^{1}H} NMR spectra due to the compound's instability in DMSO solution.

Note: *Compounds **5a** and **5b** exhibited instability in a DMSO–d_6 solution at room temperature. In the ^{1}H NMR spectrum, significant signals of decomposition products began to emerge after a few minutes. However, these compounds can be stored in a solid state at room temperature and under air for several months (~1 year) without apparent decomposition.*

3 Synthesis of Au(III) complexes

3.1 Synthesis of complexes 6a and 6b

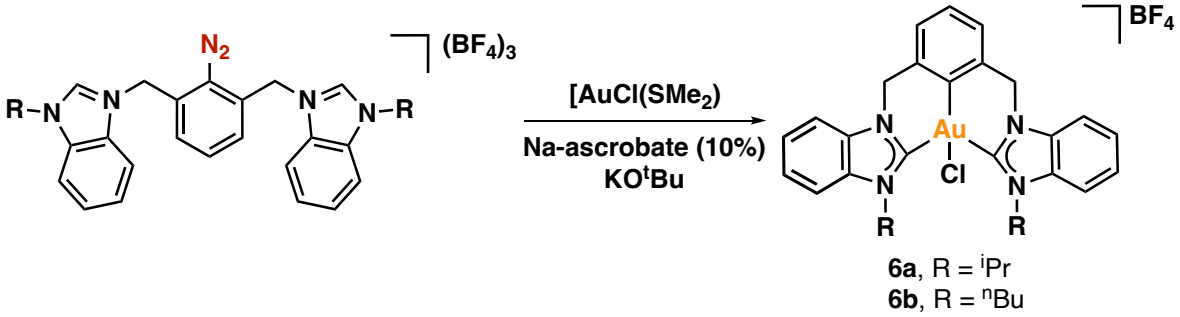

Scheme S5. Synthesis of **6a** and **6b.**

In glovebox, a solution of compound **5a** or **5b** (0.28 mmol), LiCl (35.2 mg, 0.83 mmol), and [Au(S(CH_3)$_2$)Cl] (82.8 mg, 0.28 mmol) in DMSO (0.8 mL) was stirred at room temperature for 20 min at room temperature in the absence of light. Then, a solution of sodium ascorbate (16.8 mg, 0.09 mmol) in DMSO (1mL) was added dropwise and the mixture was stirred for 1h. During this time the color of the solution changed from yellowish to red, and the appearance of bubbles was evident. Then, a solution of KO^{t}Bu (78.6mg, 0.70 mmol) in DMSO (1.2 mL) was added dropwise. The reaction was removed from the glovebox and was stirred at 50 °C for at least 18h. After this time, the reaction mixture was poured into 25 mL of distilled water. The formed solid was filtered and washed with water (3 x 1mL). The solid was dried in the funnel under vacuum, and then, was dissolved in CH_2Cl_2 and filtered through celite®, and all volatiles were removed under vacuum. The residue was then purified using a chromatographic column of neutral aluminum oxide and eluting with CH_2Cl_2. If after the solid remains yellow, it can be washed with THF to produce a pure white product.

Complex 6a. For the synthesis of **6a** was used compound **5a** (200mg, 0.28mmol). Yield: 83.2 mg (40%).

^{1}H NMR (400 MHz, CD_3CN) δ 7.97 (dd, *J* = 10.3, 8.7 Hz, 4H, C*H*$_{Blm}$), 7.65 – 7.57 (m, 2H, , C*H*$_{Blm}$), 7.57 – 7.50 (m, 2H, , C*H*$_{Blm}$), 7.45 (d, *J* = 7.4 Hz, 2H, C*H*$_{Ar}$), 7.24 (t, *J* = 7.7 Hz, 1H, , C*H*$_{Ar}$), 5.84 (hept, *J* = 6.9 Hz, 2H, C*H*$_{iPr}$), 5.55 (s, 4H, C*H*$_2$), 1.91 (d, *J* = 7.0 Hz, 6H, C*H*$_{3iPr}$), 1.60 (d, *J* = 7.1 Hz, 6H, C*H*$_{3iPr}$).

$^{13}C\{^1H\}$ NMR (101 MHz, CD_3CN) δ 170.3 ($C_{carbene}$–Au), 137.2 (C_{Ar}), 134.9 (C_{Ar}–Au), 135.6 (C_{BIm}), 132.7 (C_{BIm}), 129.4 (CH_{Ar}), 129.2 (CH_{Ar}), 126.4 (CH_{BIm}), 126.1 (CH_{BIm}), 116.0 (CH_{BIm}), 113.7 (CH_{BIm}), 55.4 (CH_{iPr}), 53.6 (CH_2), 22.3 (CH_{3iPr}), 21.5 (CH_{3iPr}).

Electrospray MS (m/*z*): 653.2 $[M–BF_4]^+$.

Complex 6b. For the synthesis of **6b** was used compound **5b** (207mg, 0.28mmol). Yield: 86.4 mg (40%).
^1H NMR (400 MHz, DMSO–d_6) δ 8.21 (d, *J* = 8.0 Hz, 2H, CH_{BIm}), 8.01 (d, *J* = 7.9 Hz, 2H, CH_{BIm}), 7.70 – 7.57 (m, 4H, CH_{BIm}), 7.53 (d, *J* = 7.5 Hz, 2H, CH_{Ar}), 7.27 (t, *J* = 7.5 Hz, 1H, CH_{Ar}), 5.88 (d, *J* = 14.9 Hz, 2H, CH_2), 5.63 (d, *J* = 14.9 Hz, 2H, CH_2), 4.95 – 4.78 (m, 4H, CH_{2Bu}), 2.00 – 1.91 (m, 4H, CH_{2Bu}), 1.41 – 1.21 (m, 4H, CH_{2Bu}), 0.90 (t, *J* = 7.4 Hz, 6H, CH_{3Bu}).

$^{13}C\{^1H\}$ NMR (101 MHz, DMSO–d_6) δ 168.8 ($C_{carbene}$–Au), 136.6 (C_{Ar}), 133.1 (C_{BIm}), 132.4 (C_{BIm}), 128.3 (CH_{Ar}), 128.1 (CH_{Ar}), 125.6 (CH_{BIm}), 113.3 (CH_{BIm}), 112.7 (CH_{BIm}), 52.1 (CH_2), 47.5 (CH_{2Bu}), 31.7 (CH_{2Bu}), 19.3 (CH_{2Bu}), 13.6 (CH_{3Bu}).

Electrospray MS (m/*z*): 681.2 $[M–BF_4]^+$.

3.2 Identification of complex 7b–Au

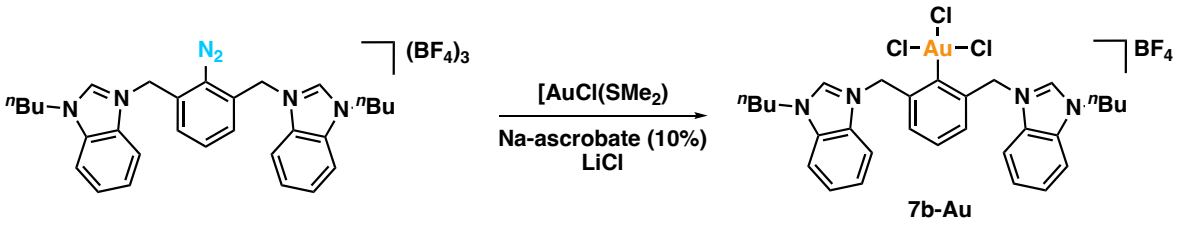

Scheme S6. Synthesis of **7b–Au**

In glovebox, a solution of **5b** (10.4 mg, 0.014 mmol), LiCl (1.8 mg, 0.042 mmol), and $[Au(S(CH_3)_2)Cl]$ (4.1 mg, 0.014 mmol) in DMSO (0.5 mL) was stirred at room temperature for 20 min at room temperature in the absence of light. Then, a solution of sodium ascorbate (1.0 mg, 5.0 μmol) in DMSO (0.5mL) was added dropwise and the mixture was stirred for 1h. After this time an aliquot of 0.5mL of the reaction mixture was collected and analyzed by ESI–MS in positive mode.

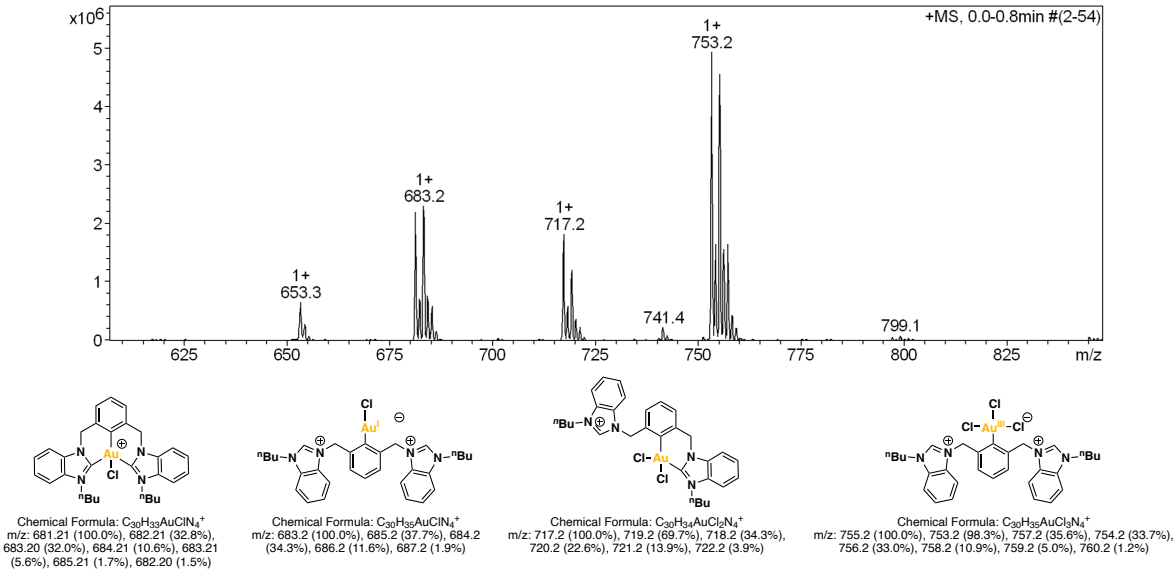

Figure S1. ESI–MS of the reaction mixture for the synthesis of complex **6b**.

3.3 Synthesis of complexes 8a and 8b

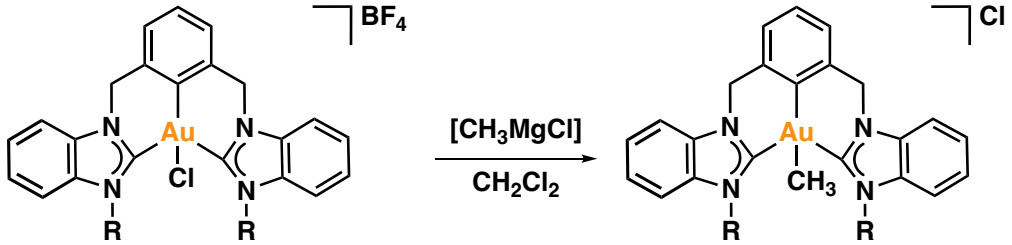

Scheme S7. Synthesis of **8a** and **8b**

In a glovebox, the gold complex (13.5 μmol) was introduced into a vial and dissolved in CH_2Cl_2 (3 mL). The vial, once sealed, was transferred out of the glovebox, connected to a Schlenk line, and purged with nitrogen. Subsequently, CH_3MgCl (10 μL, 3 M solution in THF, 0.03 mmol) was injected into the solution using a syringe. The reaction was stirred at room temperature for 24h. Then, all the volatiles were removed under high vacuum, obtaining a white solid. The vial was then opened, and the resulting white solid was subjected to a washing step with CH_2Cl_2 (3 x 2 mL). After filtration, the solution was concentrated under high vacuum, resulting in the isolation of a white solid.

Complex 8a. For the synthesis of **8a** was used compound **6a** (10.0mg, 13.5 μmol). Yield: 8.8 mg (97%).

^{1}H NMR (400 MHz, CD_3CN) δ 7.98 (d, *J* = 7.5 Hz, 2H, C*H*$_{BIm}$), 7.95 (d, *J* = 7.5 Hz, 2H, C*H*$_{BIm}$), 7.56 (td, *J* = 7.9, 1.2 Hz, 2H, C*H*$_{BIm}$), 7.50 (td, *J* = 7.8, 1.2 Hz, 2H, C*H*$_{BIm}$), 7.42 (d, *J* = 7.5 Hz, 2H, C*H*$_{Ar}$), 7.07 (t, *J* = 7.5 Hz, 1H, C*H*Ar), 5.53 (d, *J* = 14.8 Hz, 2H, C*H*$_2$), 5.38 – 5.26 (m, 4H, 2H

CH_2 and 2H CH_{iPr}), 1.90 (d, *J* = 7.0 Hz, 6H, CH_{3iPr}), 1.53 (d, *J* = 7.0 Hz, 6H, CH_{3iPr}), 1.02 (s, 3H, Au–CH_3).

$^{13}C\{^1H\}$ NMR (101 MHz, CD_3CN) δ 172.1 ($C_{carbene}$–Au), 155.2 (C_{Ar}–Au), 138.7 (C_{Ar}), 135.5 (C_{BIm}), 132.7 (C_{BIm}), 127.6 (CH_{Ar}), 127.4 (CH_{Ar}), 126.0 (CH_{BIm}), 125.5 (CH_{BIm}), 115.6 (CH_{BIm}), 113.5 (CH_{BIm}), 54.8 (CH_2), 54.7 (CH_{iPr}), 22.2 (CH_{3IPr}), 21.6 (CH_{3iPr}), –1.7 (Au–CH_3).

Electrospray MS (m/*z*): 633.2 $[M–Cl]^+$.

Complex 8b. For the synthesis of **8b** was used compound **6b** (10.4mg, 0.013mmol). Yield: 9.1 mg (97%)
^1H NMR (400 MHz, CD_3CN) δ 7.98 (d, *J* = 7.2 Hz, 2H, CH_{BIm}), 7.83 – 7.72 (m, 2H, CH_{BIm}), 7.62 – 7.49 (m, 4H, CH_{BIm}), 7.44 (d, *J* = 7.5 Hz, 2H, CH_{Ar}), 7.08 (t, *J* = 7.5 Hz, 1H, CH_{Ar}), 5.56 (d, *J* = 14.9 Hz, 2H, CH_2), 5.23 (d, *J* = 14.8 Hz, 2H, CH_2), 4.67 – 4.51 (m, 4H, CH_{2Bu}), 1.94 – 1.77 (m, 4H, CH_{2Bu}), 1.34 – 1.10 (m, 4H, CH_{2Bu}), 1.09 (s, 3H, Au–CH_3), 0.85 (t, *J* = 7.4 Hz, 6H, CH_{3Bu}).

$^{13}C\{^1H\}$ NMR (101 MHz, CD_3CN) δ 172.0 ($C_{carbene}$–Au), 155.4 (C_{Ar}–Au), 138.7 (C_{Ar}), 134.7 (C_{BIm}), 134.5 (C_{BIm}), 127.7 (CH_{Ar}), 127.5 (CH_{Ar}), 126.2 (CH_{BIm}), 125.9 (CH_{BIm}), 113.8 (CH_{BIm}), 113.1 (CH_{BIm}), 55.0 (CH_2), 48.5 (CH_{2Bu}), 32.6 (CH_{2Bu}), 20.5 (CH_{2Bu}), 13.8 (CH_{3Bu}), –2.4 ($Au–CH_3$).

Electrospray MS (m/*z*): 661.2 $[M–Cl]^+$.

3.4 Synthesis of complexes 9a and 9b

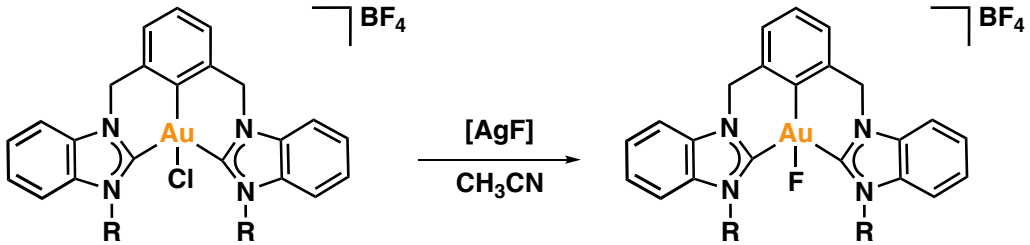

Scheme S8. Synthesis of **9a** and **9b**.

In a glovebox, a mixture of the corresponding gold(III)–Cl complex **6a** or **6b** (13.5 μmol), AgF (10 mg, 78.8 μmol), and CH_3CN (0.8 mL) was carefully transferred into an amber vial. The vial was tightly sealed and stirred at room temperature for 24h. Subsequently, the reaction mixture was carefully removed from the glovebox and the volatile components were evaporated under vacuum using the Schlenk line. Returning the vial inside the glovebox, dichloromethane was added to the remaining solid residue, and the resulting suspension was filtered, obtaining a clear colorless solution. Finally, white crystals were obtained by slow diffusion of n–hexane into the latter solution.

Complex 9a. For the synthesis of **9a** was used compound **6a** (10.0 mg, 13.5 μmol). Yield: 9.1 mg (93%)

^{1}H NMR (400 MHz, CD_3CN) δ 8.04 – 7.90 (m, 4H, CH_{BIm}), 7.64 – 7.50 (m, 4H, CH_{BIm}), 7.52 – 7.41 (m, 2H, CH_{Ar}), 7.26 (t, J = 7.5 Hz, 1H, CH_{Ar}), 5.90 – 5.76 (m, 2H, CH(CH_3)$_2$), 5.62 (d, J = 15.2 Hz, 4H, CH_2), 5.53 (d, J = 15.2 Hz, 2H, CH_2), 1.83 (d, J = 6.8 Hz, 6H, CH(CH_3)$_2$), 1.67 (d, J = 6.5 Hz, 6H, CH(CH_3)$_2$).

^{13}C{^{1}H} NMR (101 MHz, CD_3CN) δ 170.0 (d, $^{2}J_{CF}$ = 2.6 Hz, $C_{carbene}$–Au), 137.1 (d, $^{3}J_{CF}$ = 3.3 Hz, C_{Ar}), 134.3 (C_{BIm}), 132.8 (C_{BIm}), 129.5 (d, J = 3.3 Hz, CH$_{Ar}$), 129.1 (CH$_{Ar}$), 126.3 (CH$_{BIm}$), 126.0 (CH$_{BIm}$), 124.1 (d, ^{2}J = 37.0 Hz, C_{Ar}–Au), 115.7 (CH$_{BIm}$), 113.7 (CH$_{BIm}$), 54.19 (d, J = 10.6 Hz, CH(CH_3)$_2$), 53.2 (CH$_2$), 22.1 (CH(CH$_3$)$_2$), 21.5 (CH(CH$_3$)$_2$).

^{19}F NMR (377 MHz, CD_3CN) δ –152.78 (BF_4), –152.84 (BF_4), –256.06 (F–Au).

Electrospray MS (m/z): 637.2 [M–BF_4]$^{+}$.

Complex 9b. For the synthesis of **9b** was used compound **6b** (10.4 mg, 13.5 μmol). Yield: 9.3 mg (91%)
^{1}H NMR (400 MHz, CD_2Cl_2) δ 7.94 (d, *J* = 8.1 Hz, 2H, CH_{BIm}), 7.72 – 7.55 (m, 6H, CH_{BIm}), 7.50 (d, *J* = 7.7 Hz, 2H, CH_{Ar}), 7.33 (t, *J* = 7.6 Hz, 1H, CH_{Ar}), 5.59 (d, *J* = 15.3 Hz, 2H, CH_2), 5.47 (d, *J* = 15.2 Hz, 2H, CH_2), 5.25 – 5.13 (m, 2H, CH_{2Bu}), 4.64 – 4.53 (m, 2H, CH_{2Bu}), 2.03 – 1.89 (m, 4H, CH_{2Bu}), 1.53 – 1.28 (m, 4H, CH_{2Bu}), 0.97 (t, *J* = 7.3 Hz, 6H, CH_{3Bu}).

^{13}C{^{1}H} NMR (101 MHz, CD_2Cl_2) δ 169.2 ($C_{carbene}$–Au), 136.0 (C_{Ar}), 134.1 (C_{BIm}), 132.8 (C_{BIm}), 129.6 (CH$_{Ar}$), 129.2 (CH$_{Ar}$), 126.86 (dd, *J* = 241.0, 26.1 Hz, C_{Ar}–Au), 126.5 (CH$_{BIm}$), 126.3 (CH$_{BIm}$), 113.0 (CH$_{BIm}$), 112.6 (CH$_{BIm}$), 53.3 (CH$_2$, overlapped with the solvent), 47.4 (CH$_{2Bu}$), 32.7 (CH$_{2Bu}$), 20.5 (CH$_{2Bu}$), 13.8 (CH$_{3Bu}$).

^{19}F NMR (377 MHz, CD_2Cl_2) δ –153.2 (BF_4), –153.3 (BF_4), –260.1 (Au–F).

Electrospray MS (m/*z*): 665.2 [M–BF_4]$^{+}$.

NOTE: *If the complex is dissolved in non–anhydrous acetonitrile, it decomposes after a few hours.*

3.5 Synthesis of complex 10a

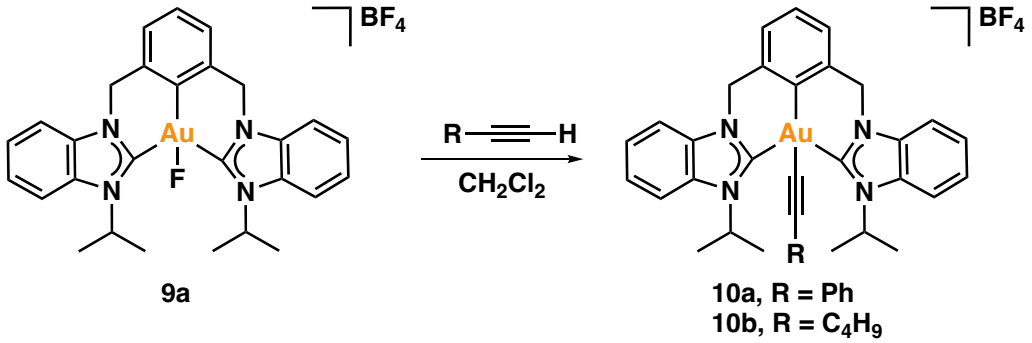

Scheme S9. Synthesis of complex **10a** and **10b.**

The reaction was conducted in an NMR tube. Phenylacetylene (100μL, 0.91mmol) or 1-hexyne (100μL, 0.870mmol) was added to a solution of freshly prepared complex **9a** (10.0 mg, 13.5 μmol) in 0.7 mL of CD_2Cl_2. After 2h, the ^1H and ^{19}F NMR spectra of the reaction mixture were acquired, confirming the completion of the reaction. Crystals of complex **10a** were growth by slow diffusion of n–hexane into the reaction mixture.

Complex 10a. Yield: >99%, *quantitative (NMR)*.

^1H NMR (400 MHz, CD_2Cl_2) δ 7.94 (d, *J*=8.3, 2H, C*H*$_{BIm}$), 7.86 (d, *J*=8.3, 2H, C*H*$_{BIm}$), 7.66 – 7.57 (m, 2H, C*H*$_{BIm}$), 7.57 – 7.51 (m, 2H, C*H*$_{BIm}$), 7.49 (d, *J*=7.5, 2H, C*H*$_{Ar}$), 7.42 – 7.35 (m, 2H, C*H*$_{PhC≡C}$), 7.35 – 7.26 (m, 3H, C*H*$_{PhC≡C}$), 7.23 (t, *J*=7.5, 1H, C*H*$_{Ar}$), 6.08 (hept, *J*=7.0, 2H, C*H*(CH$_3$)), 5.54 (d, *J*=15.0, 2H, C*H*$_2$), 5.41 (d, *J*=14.9, 2H, C*H*$_2$), 1.84 (d, *J*=6.8, 6H, CH(C*H*$_3$)), 1.64 (d, *J*=7.1, 6H, CH(C*H*$_3$)).

$^{13}C\{^1H\}$ NMR (101 MHz, CD_2Cl_2) δ 166.0 ($C_{carbene}$–Au), 140.2 (*C*$_{Ar}$–Au), 137.3 (*C*$_{Ar}$), 134.7 (*C*$_{BIm}$), 132.1 (*C*$_{BIm}$), 131.5 (*C*H$_{PhC≡C}$), 128.8 (*C*H$_{PhC≡C}$), 128.2 (*C*H$_{Ar}$), 128.2 (*C*H$_{Ar}$), 127.9 (*C*H$_{PhC≡C}$), 126.0 (*C*H$_{BIm}$), 125.6 (*C*H$_{BIm}$), 125.5 (*C*$_{PhC≡C}$), 115.0 (*C*H$_{BIm}$), 112.8 (*C*H$_{BIm}$), 111.5 (PhC≡*C*–Au), 100.5 (Ph*C*≡C–Au), 55.7 (*C*H(CH$_3$), 54.3 (*C*H$_2$, overlapped with the solvent), 21.8 (CH(*C*H$_3$), 21.7(CH(*C*H$_3$).

^{19}F NMR (377 MHz, CD_2Cl_2) δ = –153.6 (BF_4), –153.7 (BF_4).

Electrospray MS (m/z): 719.2 $[M–BF_4]^+$.

Complex 10b. Yield: >99%, *quantitative (NMR)*.

^1H NMR (400 MHz, CD_2Cl_2) δ 7.92 – 7.84 (m, 4H, C*H*$_{Bim}$), 7.60 (td, *J*=7.8, 1.2, 2H, C*H*$_{BIm}$), 7.54 (td, *J*=7.9, 1.2, 2H, C*H*$_{BIm}$), 7.44 (d, *J*=7.5, 2H, C*H*$_{Ar}$), 7.20 (t, *J*=7.5, 1H, C*H*$_{Ar}$), 6.09 (hept, *J*=6.8, 2H, C*H*(CH$_3$)), 5.47 (d, *J*=14.9, 2H, C*H*$_2$), 5.36 (s, 2H, C*H*$_2$), 2.39 (td, *J*=7.2, 2.8, 2H, C*H*$_{2Bu}$), 1.92 (d, *J*=6.8, 6H, CH(C*H*$_3$)), 1.63 (d, *J*=7.1, 6H, CH(C*H*$_3$)), 1.53 – 1.46 (m, 2H, C*H*$_{2Bu}$), 1.46 – 1.34 (m, 2H, C*H*$_{2Bu}$), 0.90 (t, *J*=7.3, 3H, C*H*$_{3Bu}$).

$^{13}C\{^{1}H\}$ NMR (101 MHz, CD_2Cl_2) δ 166.2 ($C_{carbene}$–Au), 140.9 (C_{Ar}–Au), 137.4 (C_{Ar}), 134.6 (C_{BIm}), 132.1 (C_{BIm}), 128.0 (CH_{Ar}), 128.0 (CH_{Ar}), 125.9 (CH_{BIm}), 125.5 (CH_{BIm}), 115.0 (CH_{BIm}), 112.7 (CH_{BIm}), 55.3 ($CH(CH_3)$), 54.3 (CH_2, overlapped with the solvent), 32.2 (CH_{2Bu}), 22.7 (CH_{2Bu}), 21.7 ($CH(CH_3)$), 21.6 ($CH(CH_3)$), 21.2 (CH_{2Bu}), 13.9 (CH_{3Bu}).

^{19}F NMR (377 MHz, CD_2Cl_2) δ = –153.1 (BF_4), –153.1 (BF_4).

Electrospray MS (m/z): 699.3 $[M–BF_4]^+$.

3.6 Synthesis of complex 11a

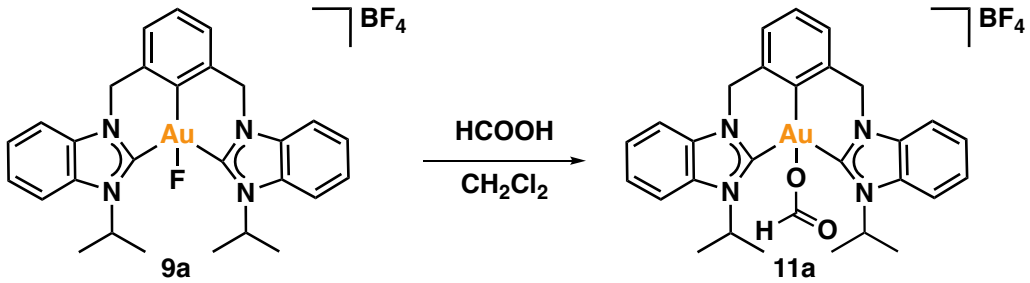

Scheme S10. Synthesis of complex **11a**

The reaction was conducted in an NMR tube. Formic acid (0.05 mL, 1.3mmol) was added to a solution of freshly prepared complex **9a** (10.0 mg, 13.5 μmol) in 0.7 mL of CD_2Cl_2. After 15 min, the ^{1}H and ^{19}F NMR spectra of the reaction mixture were acquired, confirming the completion of the reaction. Crystals of complex **11a** were grown by slow diffusion of diethyl ether into the reaction mixture.

Yield: *quantitative (NMR)*.

^{1}H NMR (400 MHz, CD_2Cl_2) δ 8.91 (s, 1H, *H*COO), 7.92 (d, *J* = 8.3 Hz, 2H, CH_{BIm}), 7.83 (d, *J* = 8.3 Hz, 2H, CH_{Bim}), 7.66 – 7.58 (m, 2H. CH_{Bim}), 7.58 – 7.50 (m, 2H. CH_{Bim}), 7.47 (d, *J* = 7.6 Hz, 2H, CH_{Ar}), 7.30 (t, *J* = 7.5 Hz, 1H, CH_{Ar}), 5.62 – 5.48 (m, 4H, CH_2), 5.31 (h, *J* = 7.3 Hz, 2H, $CH(CH_3)$), 1.81 (d, *J* = 7.0 Hz, 6H, $CH(CH_3)$), 1.66 (d, *J* = 7.0 Hz, 6H, $CH(CH_3)$).

$^{13}C\{^{1}H\}$ NMR (101 MHz, CD_2Cl_2) δ 169.0 ($C_{carbene}$–Au), 167.1 (HCOO), 136.3 (C_{Ar}), 134.2 (C_{Bim}), 132.0 (C_{Bim}), 129.3 (CH_{Ar}), 129.1 (CH_{Ar}), 127.6 (C_{Ar}–Au), 126.3 (CH_{Bim}), 125.8 (CH_{Bim}), 115.1 (CH_{Bim}), 112.9 (CH_{Bim}), 54.3 ($CH(CH_3)$), 53.2 (CH_2), 21.8 ($CH(CH_3)$), 21.3 ($CH(CH_3)$).

^{19}F NMR (377 MHz, CD_2Cl_2) δ = –153.4 (BF_4), –153.5 (BF_4).

Electrospray MS (m/*z*): 663.2 $[M–BF_4]^+$.

3.7 Synthesis of complex 12a

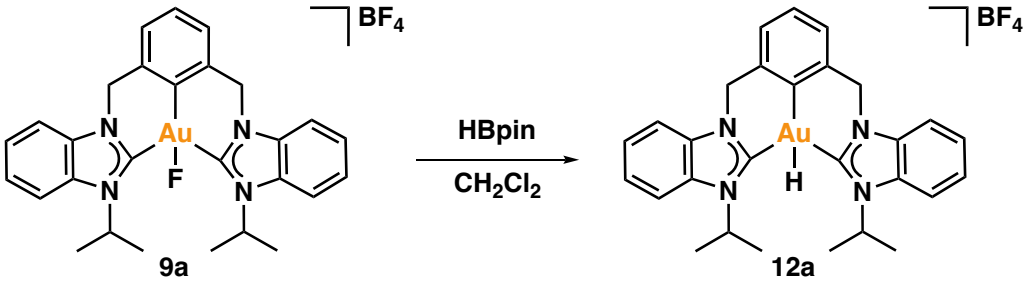

Scheme S11. Synthesis of **12a**.

In a glovebox, Hbpin (10μL, 68.9 μmol) was added to a vial containing a solution of pincer **9a** (5.0 mg, 6.9 μmol) in CH_2Cl_2 (1 mL). The vial was sealed, removed from the glovebox and stirred at room temperature for 1h. Subsequently, white crystals were obtained through slow diffusion of n–hexane into the solution. The crystals were separated by decantation, washed with THF (1.5 mL) and pentane (1.5mL), and finally dried under high vacuum. Yield: 4.3mg (89%)

^{1}H NMR (400 MHz, CD_2Cl_2) δ 7.94 – 7.85 (m, 4H, CH_{Bim}), 7.65 – 7.49 (m, 6H, 4H CH_{Bim} and 2H CH_{Ar}), 7.26 (t, *J* = 7.5 Hz, 1H, CH_{Ar}), 5.56 – 5.42 (m, 6H, 4H CH_2 and 2H CH(CH_3)$_2$), 1.79 (d, *J* = 7.1 Hz, 12H, CH(CH_3)$_2$), 1.43 (s, 1H, Au–*H*).

^{13}C{^{1}H} NMR (101 MHz, CD_2Cl_2) δ 167.5 ($C_{carbene}$–Au), 151.6 (C_{Ar}–Au), 136.8 (C_{Ar}), 135.1 (C_{Bim}), 131.7 (C_{Bim}), 127.9 (CH_{Ar}), 127.5 (CH_{Ar}), 125.8 (CH_{Bim}), 125.5 (CH_{Bim}), 114.8 (CH_{Bim}), 112.6 (CH_{Bim}), 56.7 (CH(CH_3)$_2$), 54.8 (CH_2), 21.1 (CH(CH_3)$_2$).

Electrospray MS (m/*z*): 619.2 [M–BF_4]$^+$.

4 Reaction mechanism of the synthesis of Au(III) pincer complexes

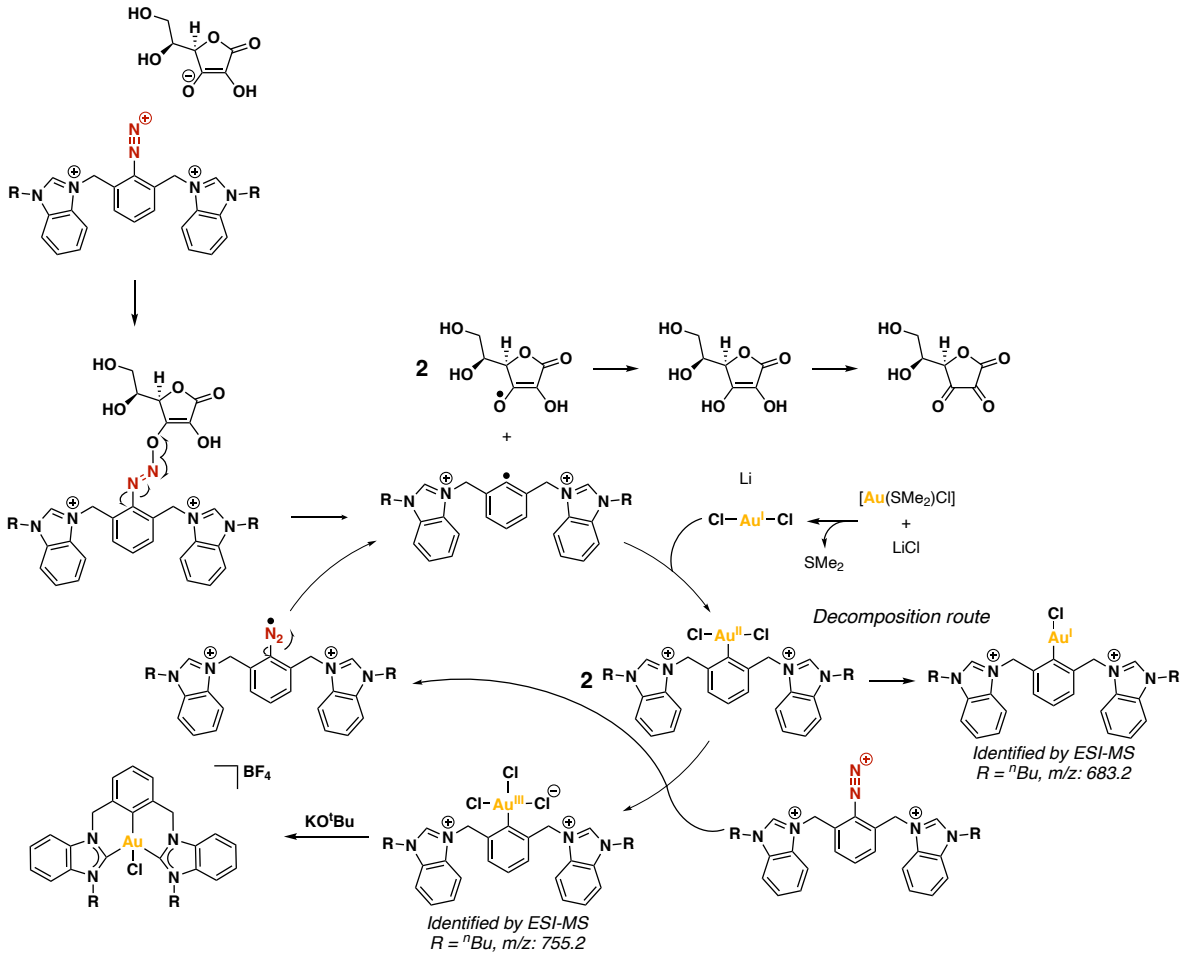

Scheme S12. Proposed reaction mechanism of the synthesis of pincer Au(III) complexes in the presence of ascorbic acid.

5 Reactivity experiments of Au(III) complexes

5.1 Thermal stability of complex 11a

A solution containing 5 mg of complex **11a** in CD_2Cl_2 or 1,2–dichloroethane was subjected to heating at 60°C or 100°C, respectively, for a duration of 24h. Following this period, the ^{1}H NMR spectra were recorded.

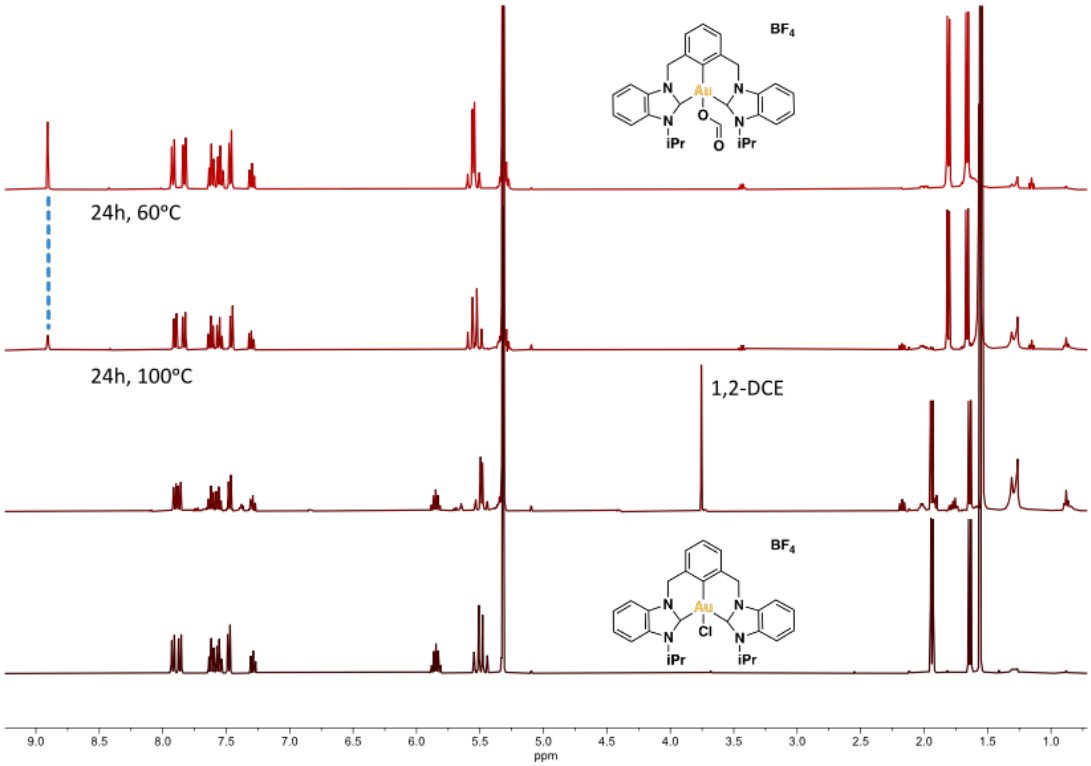

Figure S2. ^{1}H NMR (400 MHz, 298 K) of complex **11a** after undergoing heating at 60°C and 100°C in CD_2Cl_2

5.2 Reactivity of Au(III) pincer complexes towards formic acid (HCOOH)

A solution containing complex **8b**, **9a** or **12a** (13.5µmol) and formic acid (10 µL, 0.3mmol) in 0.5 mL of deuterated solvent was prepared. The solution was subjected to heating at various temperatures during the desired time. The progress of the reaction was monitored using ^{1}H NMR and ESI–MS.

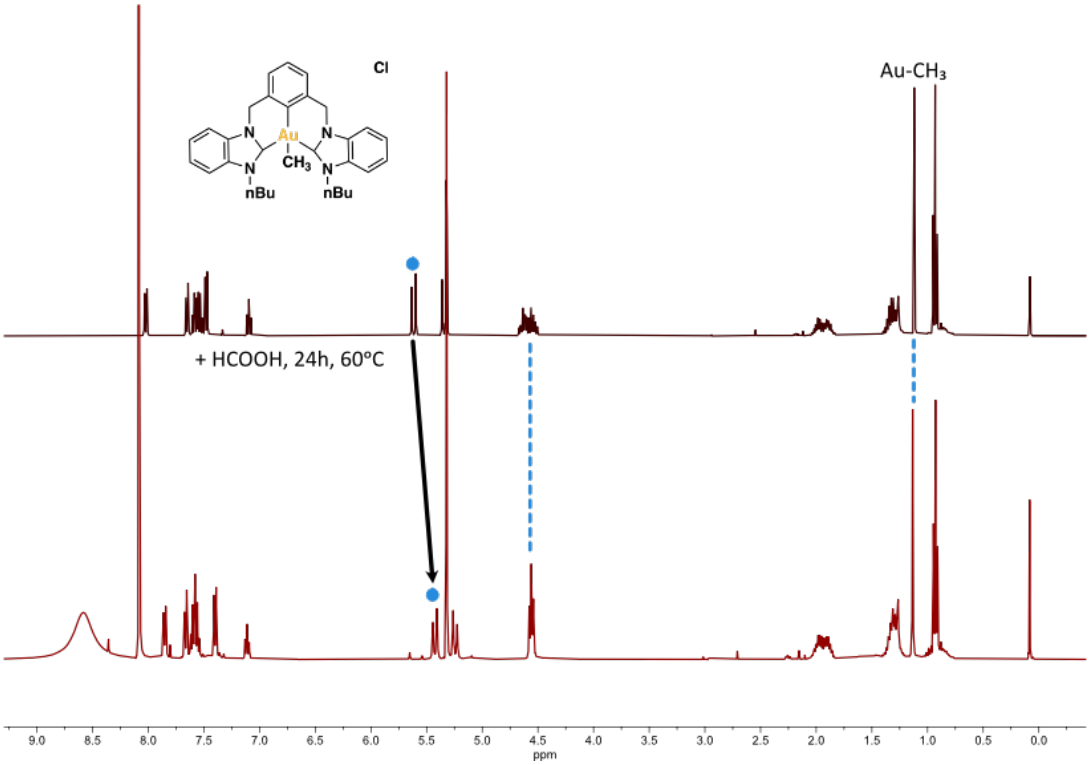

Figure S3. ^{1}H NMR (400MHz, 298K) of the reaction of complex **8b** and HCOOH in CD_2Cl_2

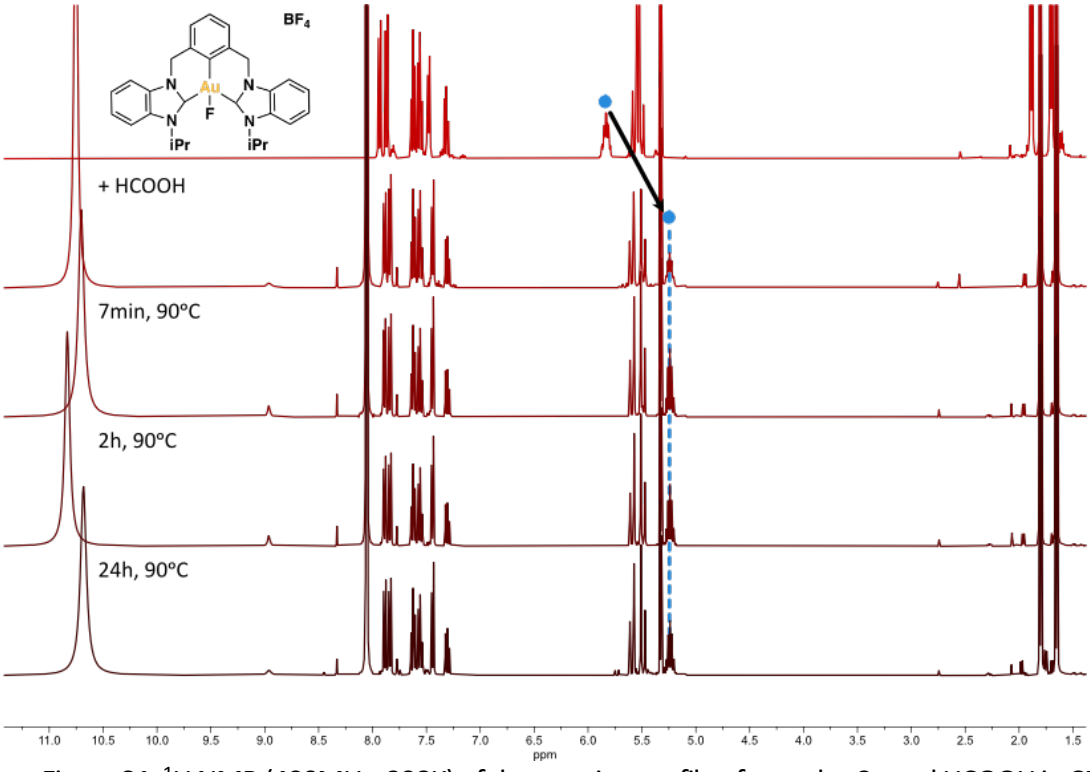

Figure S4. ^{1}H NMR (400MHz, 298K) of the reaction profile of complex **9a** and HCOOH in CD_2Cl_2

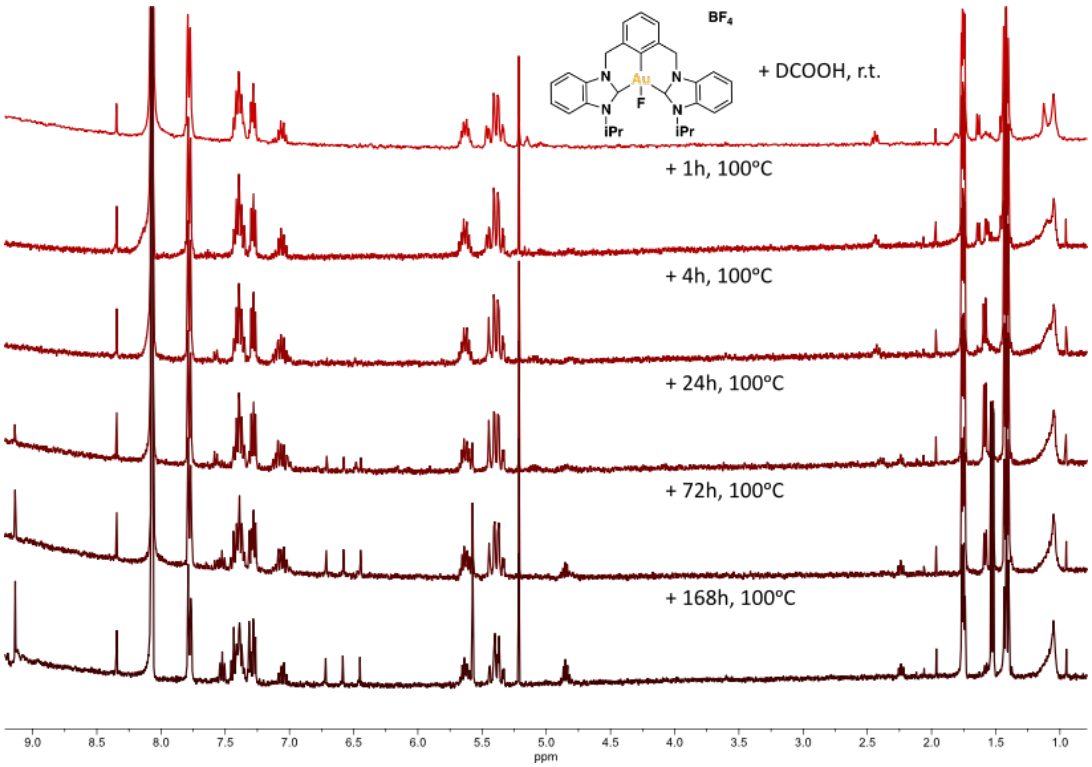

Figure S5. ^{1}H NMR (400MHz, 298K) of complex **9a** at 100°C in DCOOH

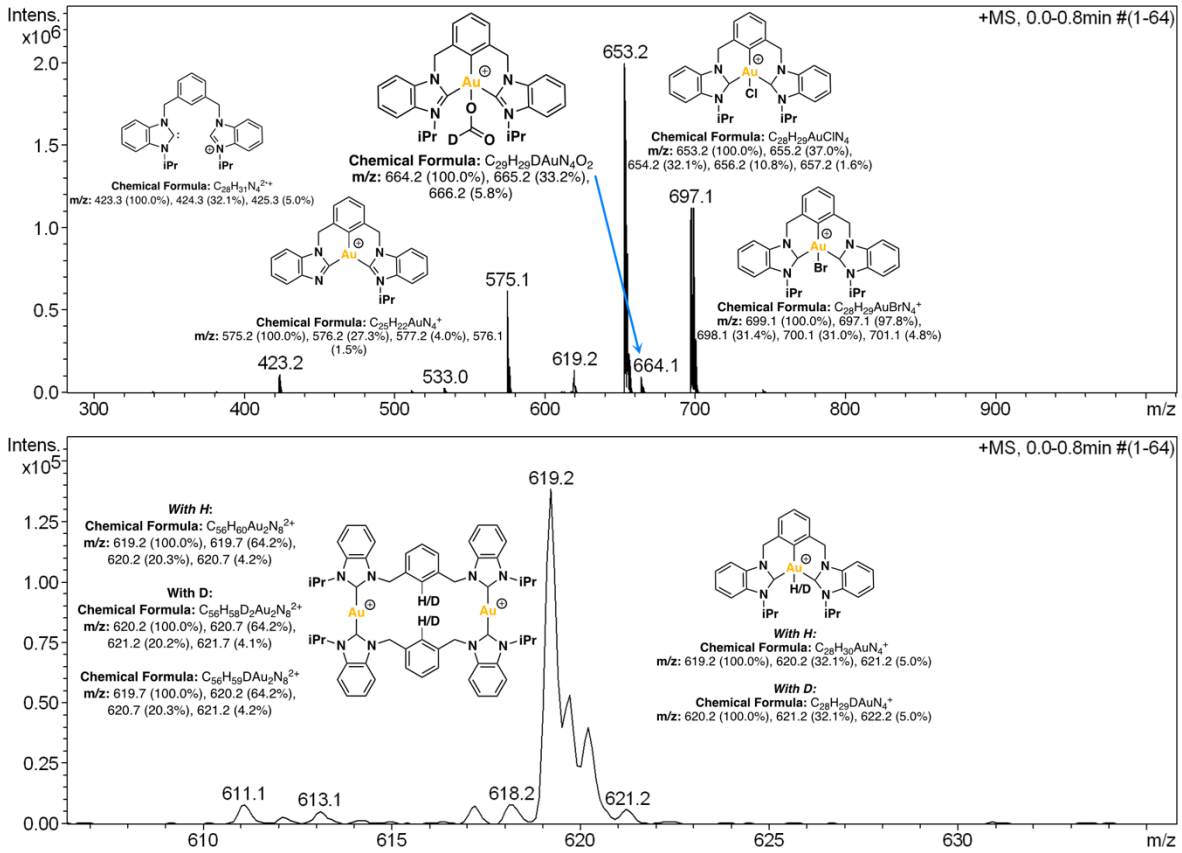

Figure S6. ESI–MS spectrum of the reaction of complex **9a** and DCOOH at 100°C for 168h

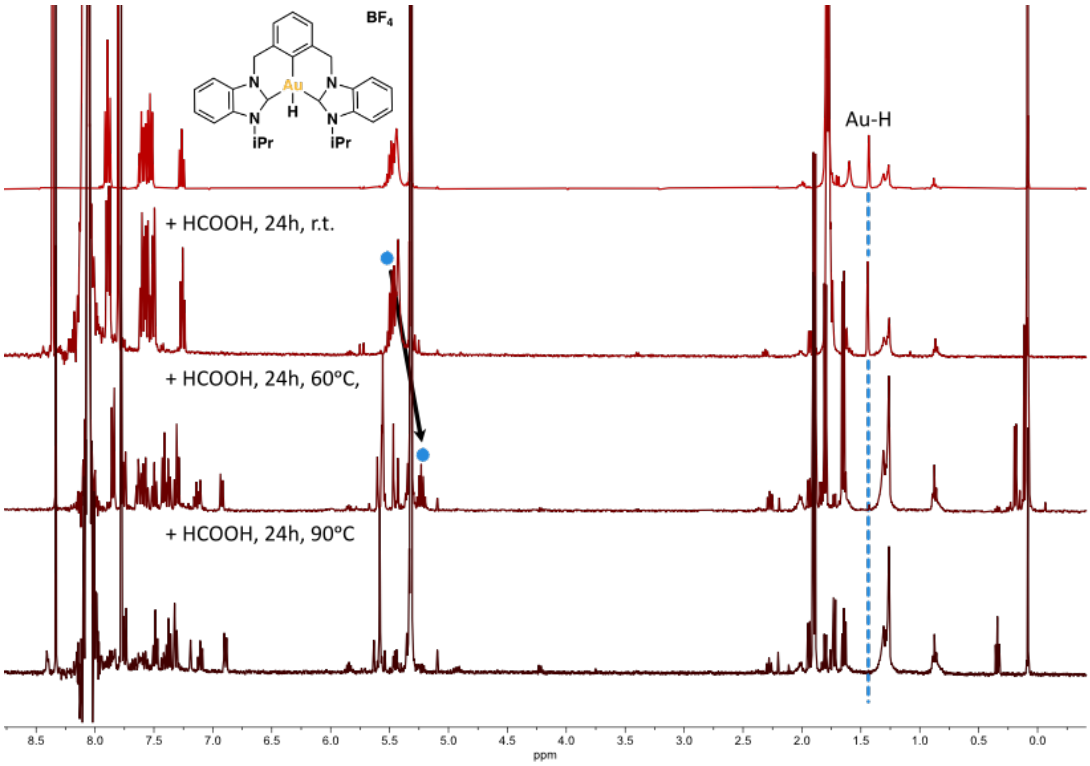

Figure S7. ^{1}H NMR (400MHz, 298K) of the reaction of complex **12a** and HCOOH at different temperatures in CD_2Cl_2

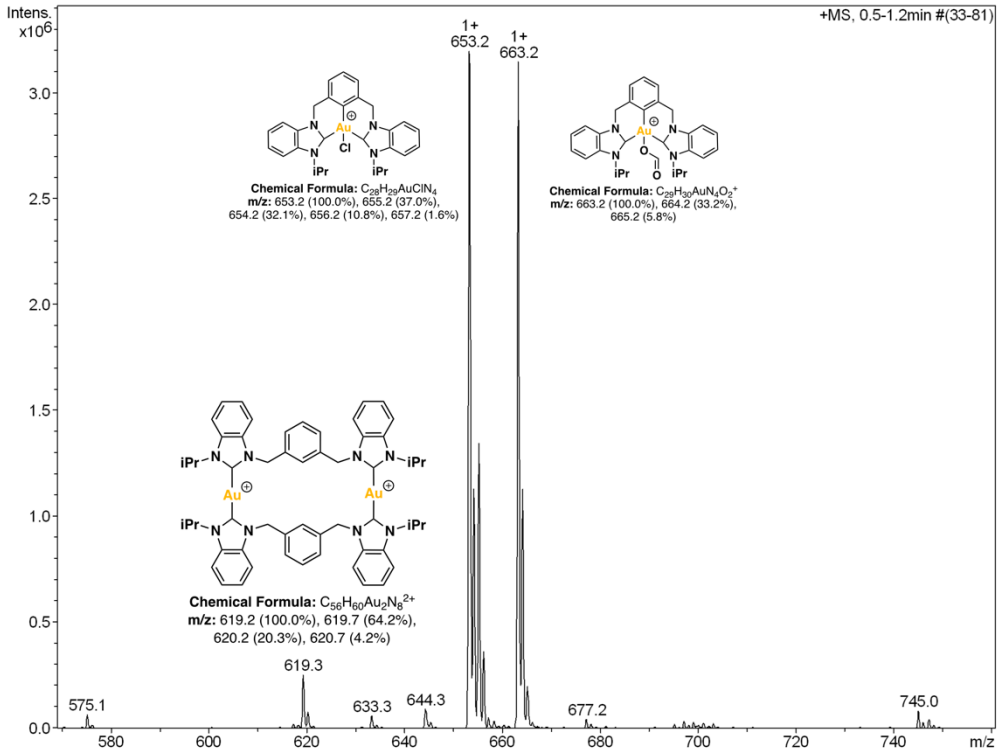

Figure S8. ESI–MS spectrum of the reaction of complex **12a** and HCOOH at 60°C

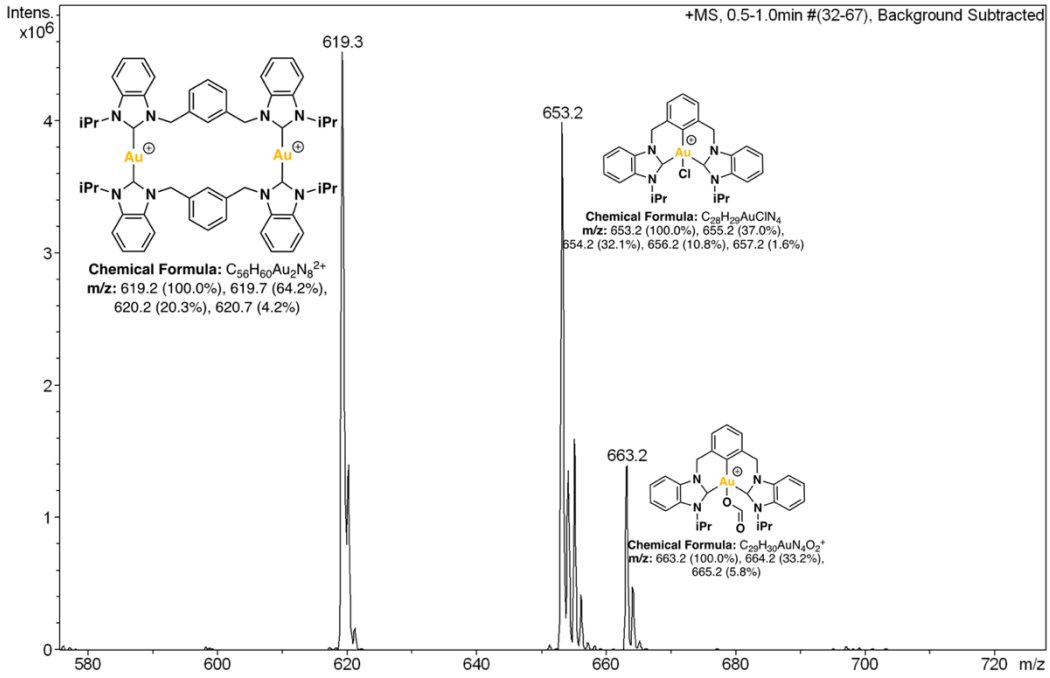

Figure S9. ESI–MS spectrum of the reaction of complex **12a** and HCOOH at 90°C

Compound **13a** was isolated from the reaction mixture of **12a** and HCOOH at 90°C. The isolation was achieved through slow diffusion of diethyl ether into the reaction mixture. Yield: 8.6mg(90%)

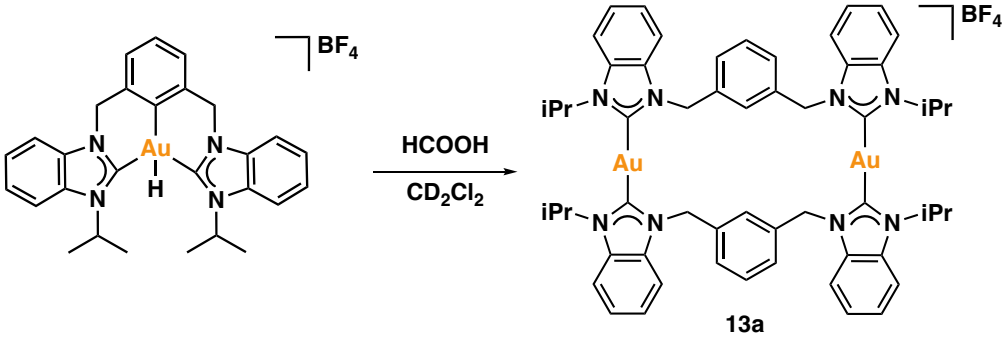

Scheme S13. Synthesis of **13a**

^{1}H NMR (400 MHz, CD_2Cl_2) δ 7.73 (d, *J* = 8.3 Hz, 2H, C*H*$_{BIm}$), 7.53 – 7.42 (m, 2H, C*H*$_{BIm}$), 7.37 (d, *J* = 4.8 Hz, 5H, 4H C*H*$_{BIm}$ and 1H C*H*$_{Ar}$), 7.06 (t, *J* = 7.8 Hz, 1H, C*H*$_{Ar}$), 6.85 (d, *J* = 2.0 Hz, 2H, C*H*$_{Ar}$), 5.65 (s, 4H, C*H*$_2$), 5.43 – 5.31 (m, 2H, C*H*$(CH_3)_2$), 1.91 (d, *J* = 6.8 Hz, 12H, CH(C*H*$_3)_2$).

^{13}C{^{1}H} NMR (101 MHz, CD_2Cl_2) δ 189.7 ($C_{carbene}$–Au), 136.6 (*C*$_{Ar}$), 134.2 (*C*$_{BIm}$), 132.8 (*C*$_{BIm}$), 129.9 (*C*H$_{Ar}$), 125.8 (*C*H$_{Ar}$), 125.7 (*C*H$_{Ar}$), 125.6 (*C*H$_{BIm}$), 125.3 (*C*H$_{BIm}$), 113.2 (*C*H$_{BIm}$), 112.8 (*C*H$_{BIm}$), 53.8 (*C*H$_2$, overlapped with the solvent), 52.2 (*C*H$(CH_3)_2$), 23.0 (CH(*C*H$_3)_2$).

Electrospray MS (m/*z*): 619.2 $[M–(BF_4)_2]^{2+}$, 1326.5 $[M– BF_4]$

5.3 Reactivity of 12a towards triflic acid

A solution containing complex **12a** (13.5 µmol) and triflic acid (2.4 µL, 27.0 µmol) in 0.5 mL of CD_2Cl_2 was prepared at room temperature. The progress of the reaction was monitored using ^1H NMR and MS, observing the formation of **13a** within minutes.

5.4 Reactivity of Au(III) pincer complexes towards sodium hydride (NaH)

A solution containing complex **8b** or **12a** (13.5µmol) and NaH (5.0mg, 0.21mmol) in 0.5mL of CD_2Cl_2 was prepared. The solution was subjected to heating at various temperatures and durations. The progress of the reaction was monitored using ^1H NMR.

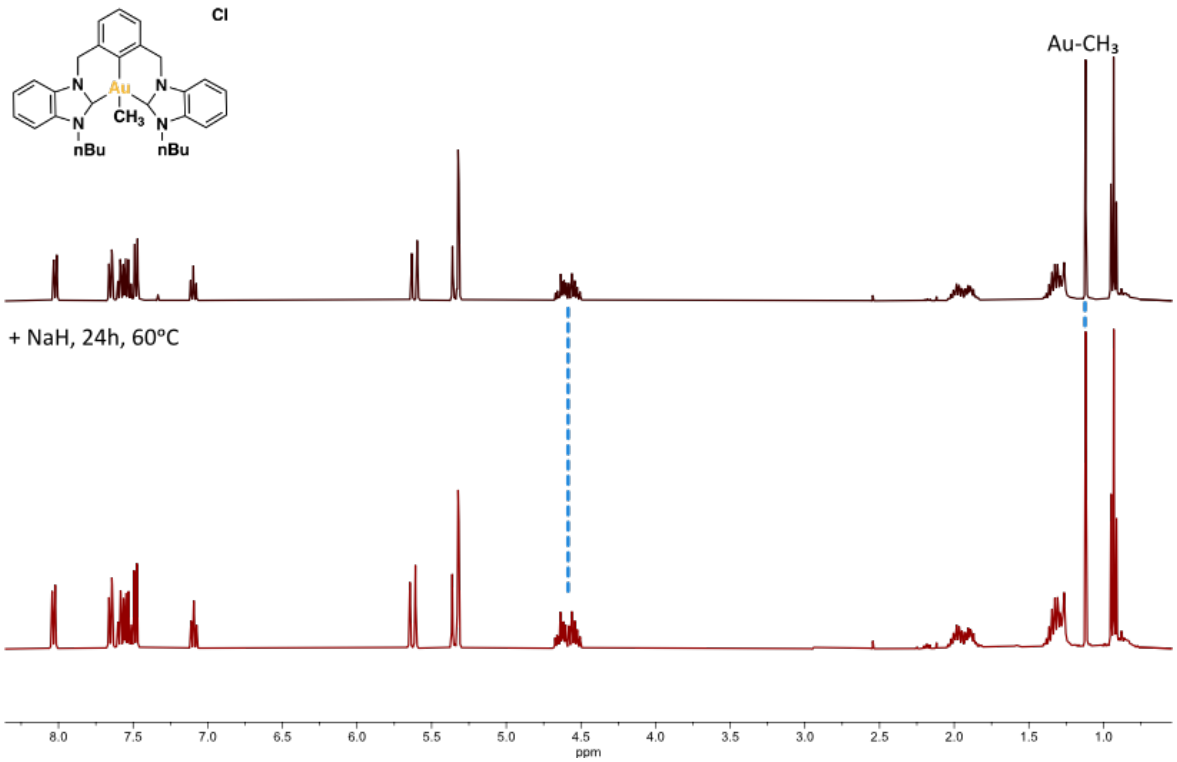

Figure S10. ^1H NMR (400MHz, 298K) of the reaction of complex **8b** and NaH at 60°C in CD_2Cl_2

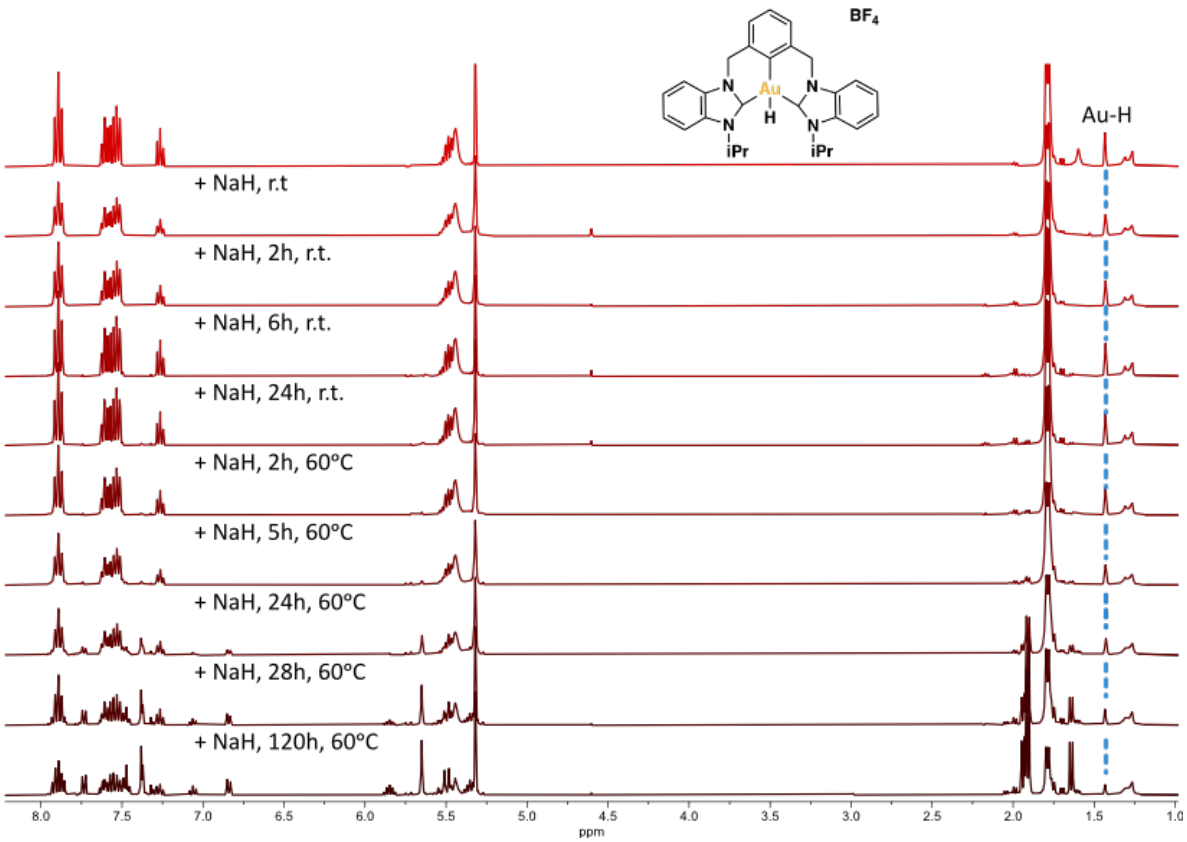

Figure S11. ^{1}H NMR (400MHz, 298K) of the reaction of complex **12a** and NaH, from r.t to 60°C in CD_2Cl_2

Compound **13a** was observed at the end of the reaction of **12a** and NaH at 60°C. This result was corroborated by ESI–MS (Figure S12).

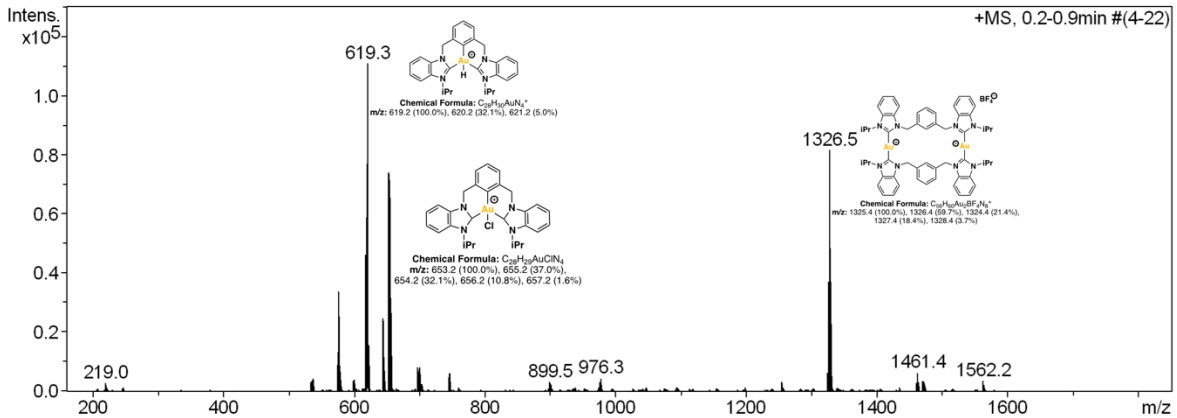

Figure S12. ESI–MS spectrum of the reaction of complex **12a** and NaH at 60°C

6 Catalytic studies of CCC–NHC Au(III) pincer complex 6a

A solution of complex **6a** (2.0 mg, 2.7 μmol), ω-alkynylfuran (0.54 mmol), [$NaSbF_6$] (5.6 mg, 21.6 μmol) in $CDCl_3$ (0.6 mL) was heated at 60°C for 16h. After this period, the reaction mixture was allowed to cool to room temperature, and ^1H NMR was collected. The reaction yield was determined by ^1H NMR using 1,3,5-trimethoxybenzene as an internal standard.

7 NMR Spectra

7.1 NMR spectra of compound 2

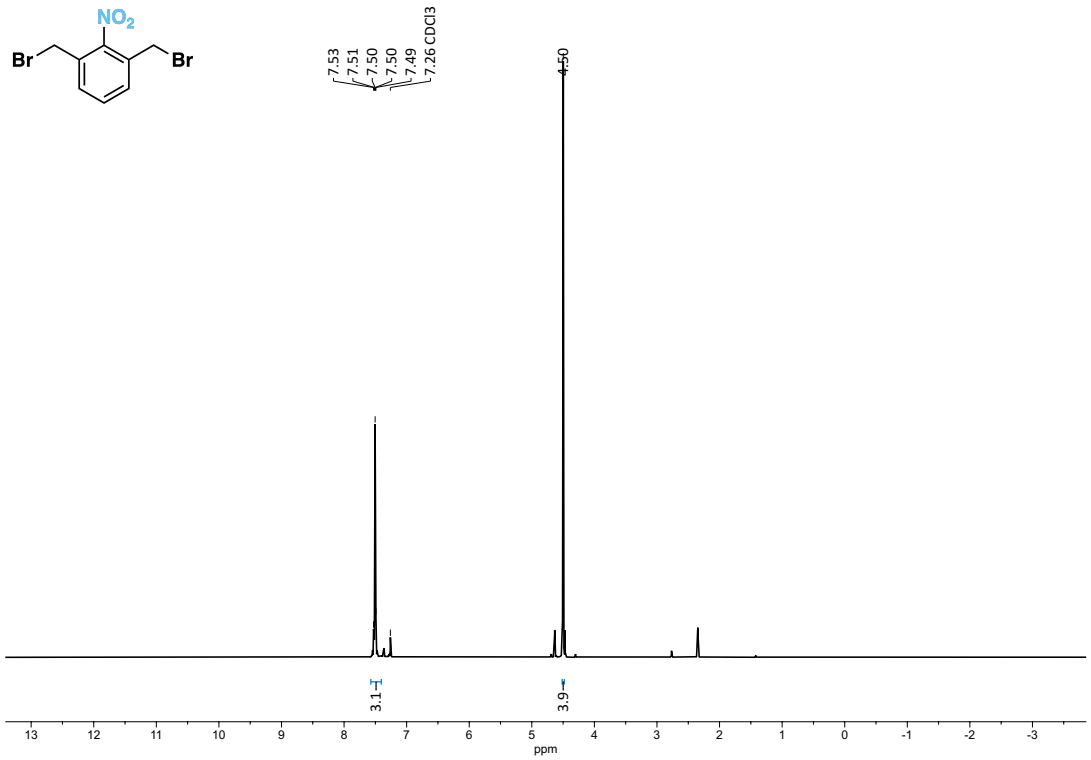

Figure S13. ^{1}H NMR (400MHz, 298K) of **2** in $CDCl_3$

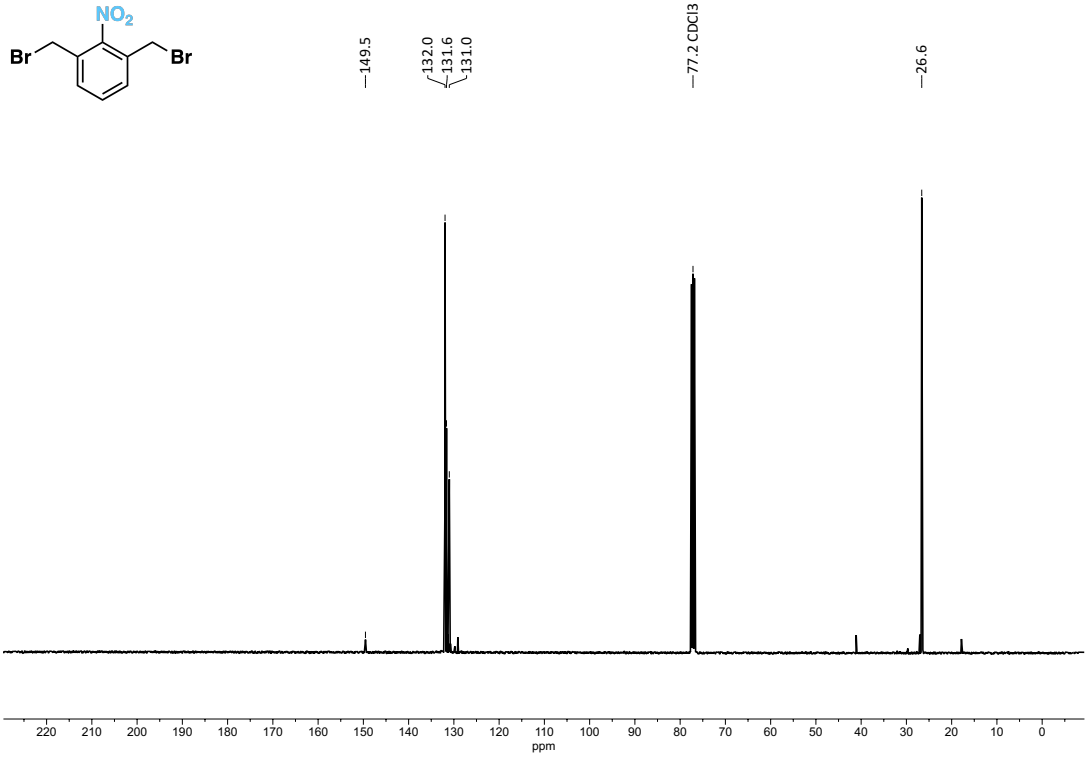

Figure S14. $^{13}C\{^{1}H\}$ NMR (101MHz, 298K) of **2** in $CDCl_3$

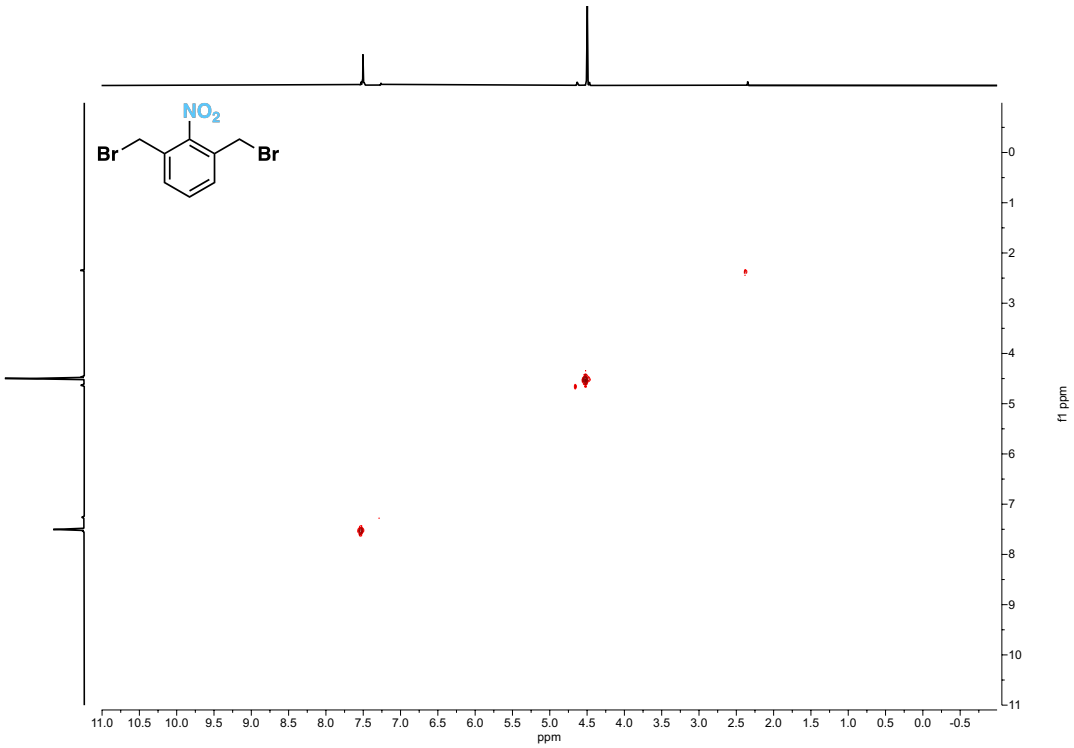

Figure S15. $^{1}H,^{1}H$ COSY NMR (400MHz, 298K) of **2** in $CDCl_3$

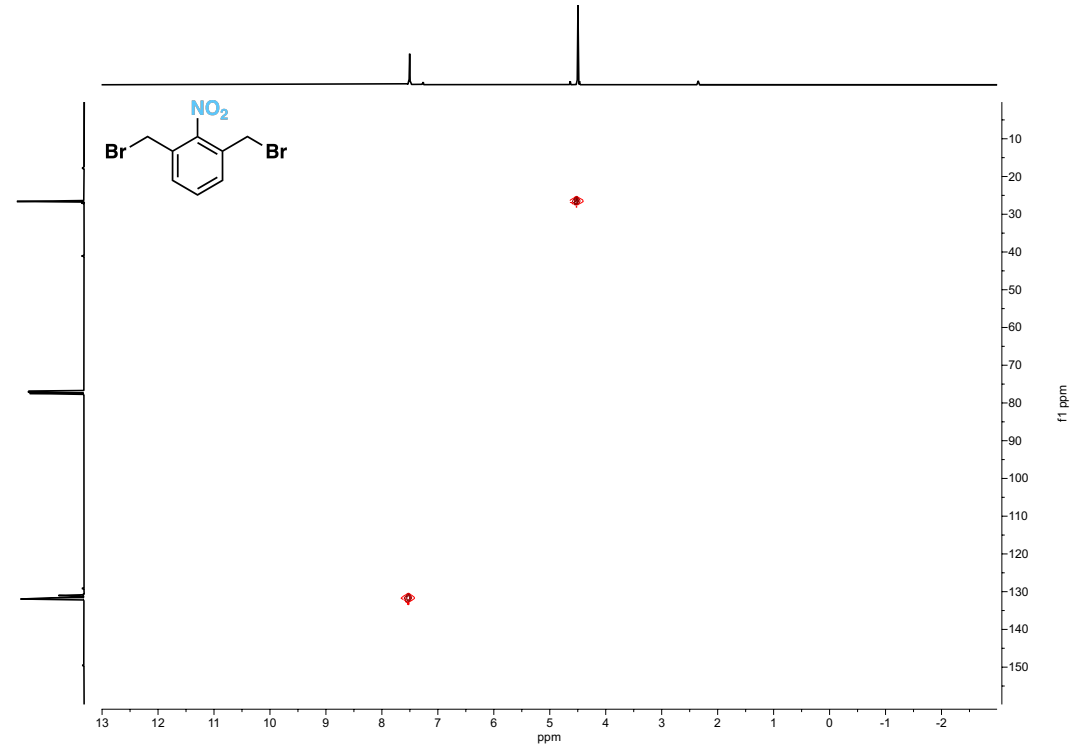

Figure S16. $^{1}H,^{13}C$ HSQC NMR (400MHz, 298K) of **2** in $CDCl_3$

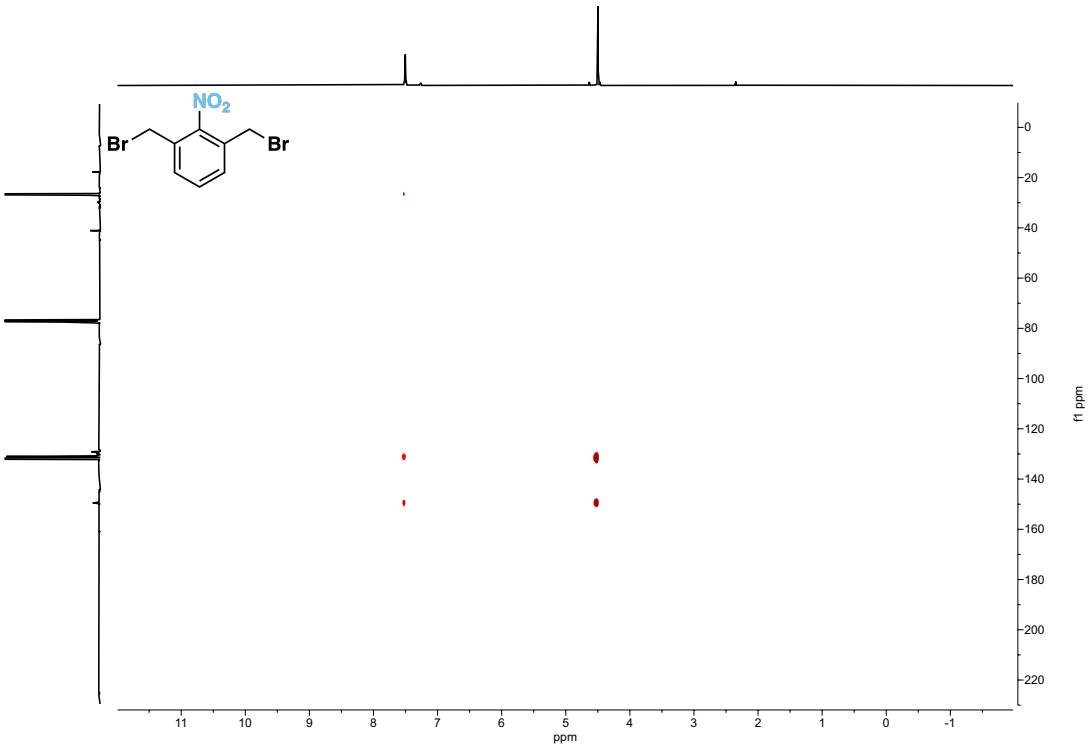

Figure S17. $^{1}H,^{13}C$ HMBC NMR (400MHz, 298K) of **2** in $CDCl_3$

7.2 NMR spectra of compound 3a

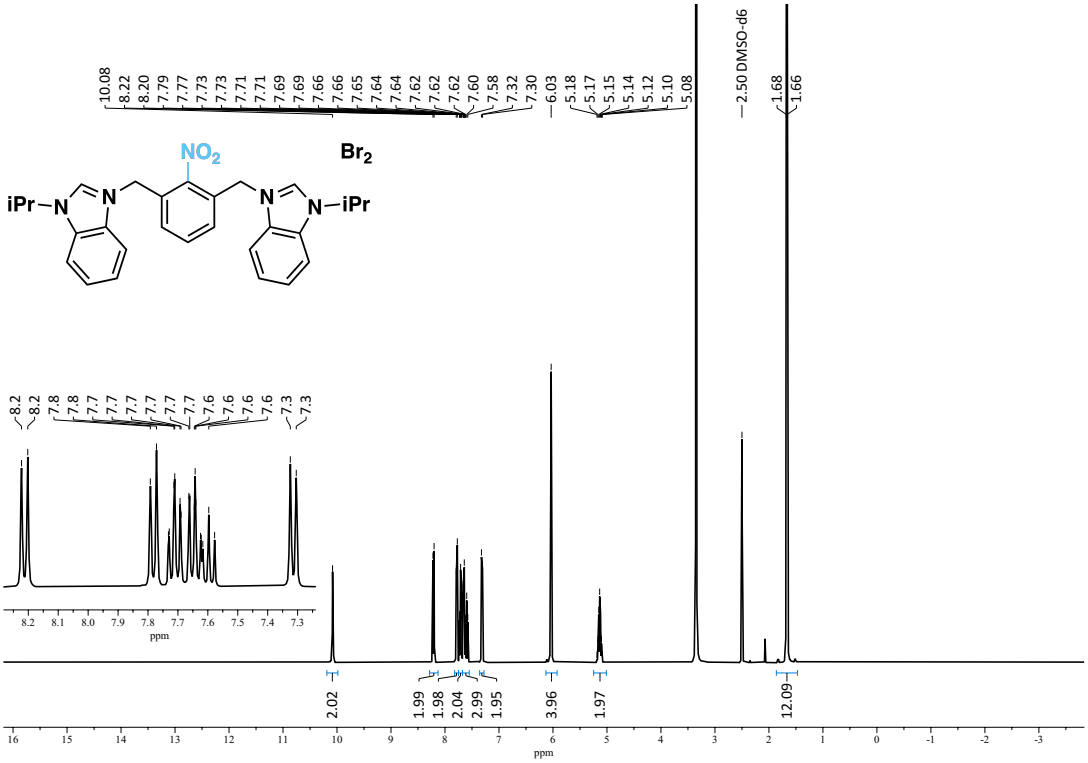

Figure S18. ^{1}H NMR (400MHz, 298K) of **3a** in DMSO–d_6

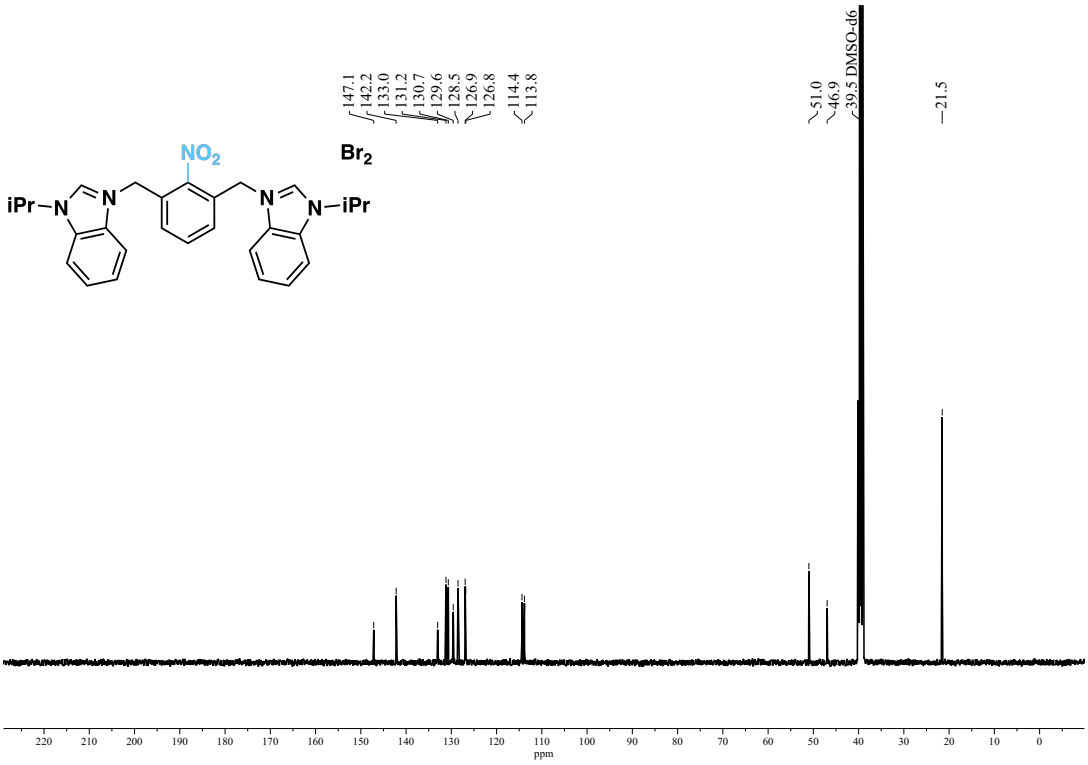

Figure S19. ^{13}C{^{1}H} NMR (101MHz, 298K) of **3a** in DMSO–d_6

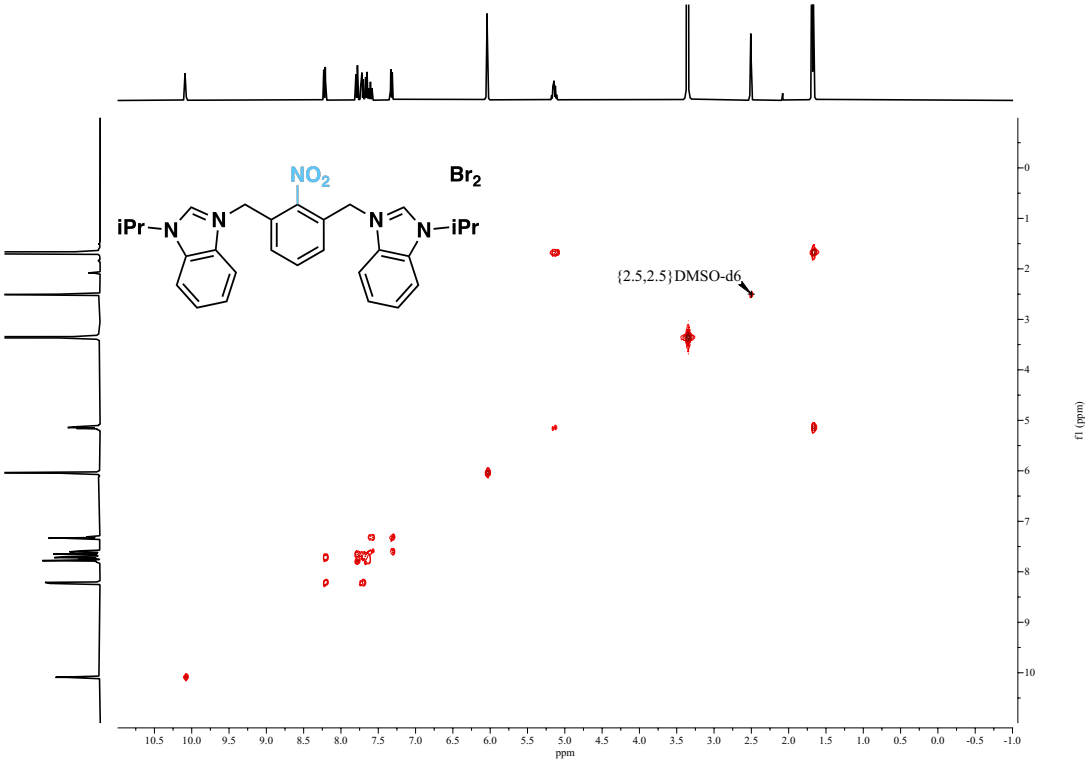

Figure S20. $^{1}H,^{1}H$ COSY NMR (400MHz, 298K) of **3a** in DMSO–d_6

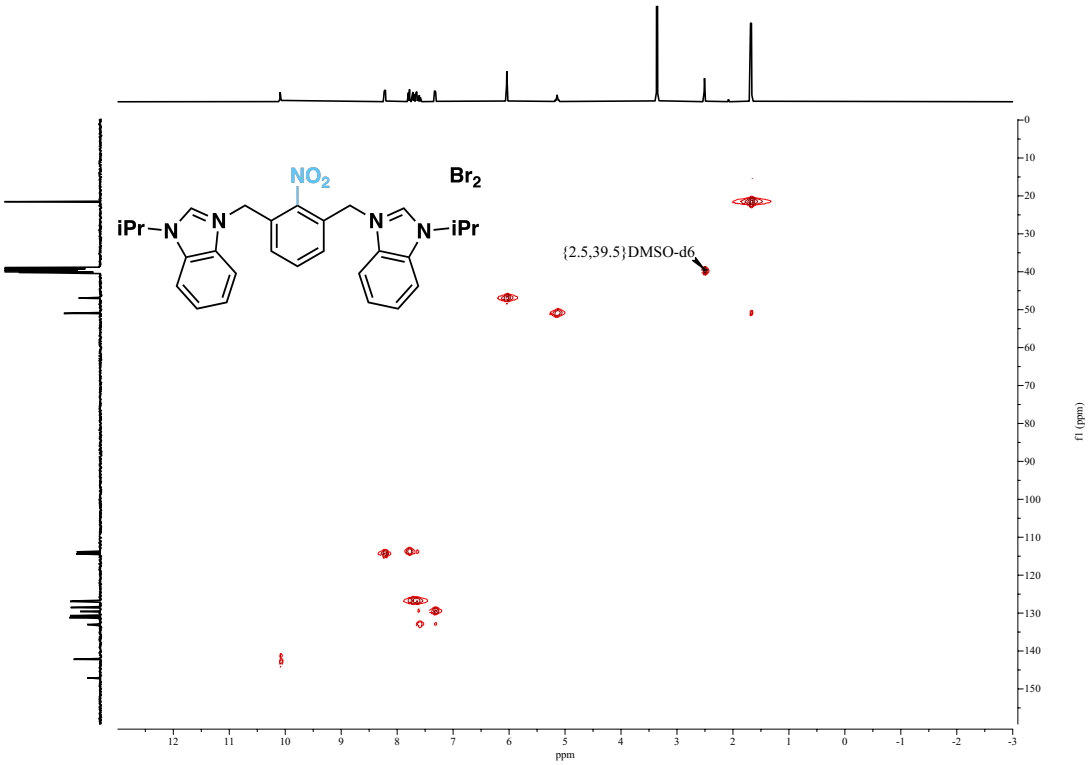

Figure S21. $^{1}H,^{13}C$ HSQC NMR (400MHz, 298K) of **3a** in DMSO–d_6

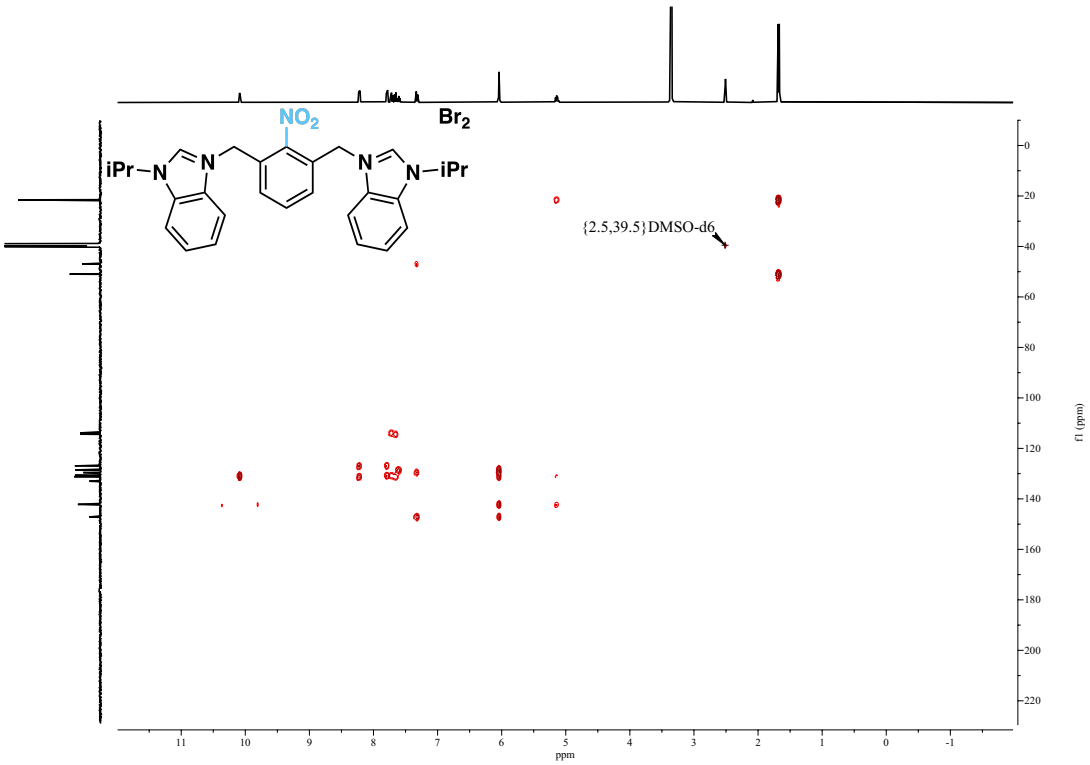

Figure S22. $^{1}H,^{13}C$ HMBC NMR (400MHz, 298K) of **3a** in DMSO–d_6

7.3 NMR spectra of compound 3b

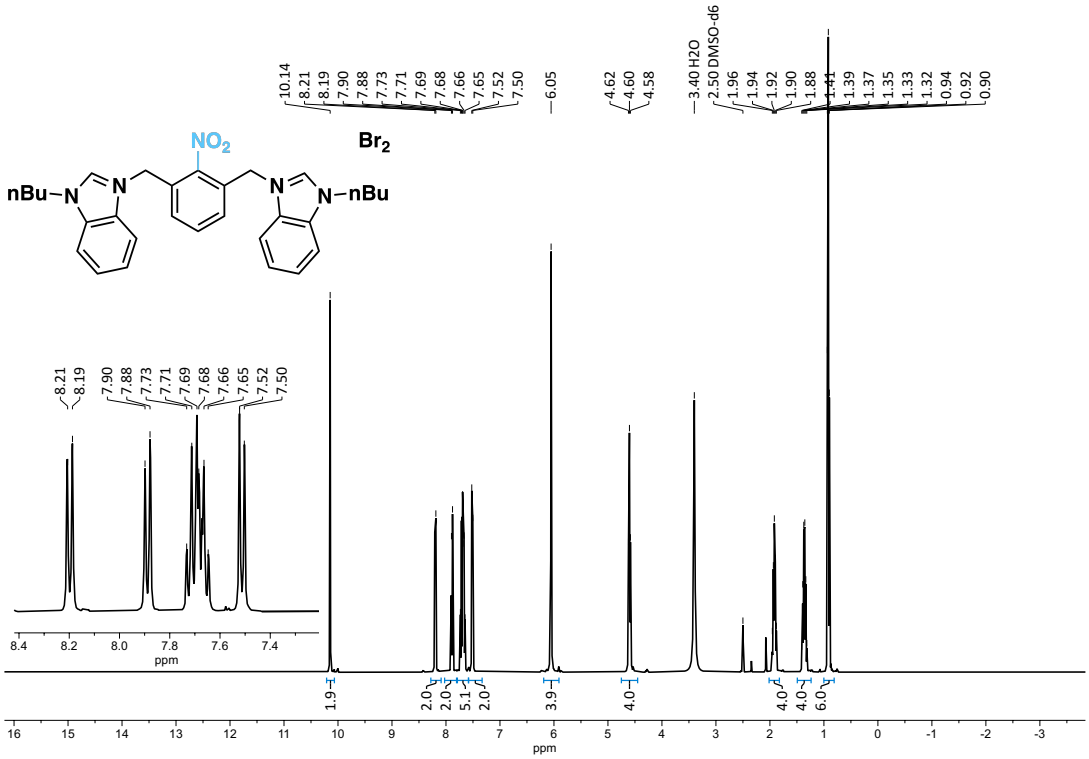

Figure S23. ^{1}H NMR (400MHz, 298K) of **3b** in DMSO–d_6

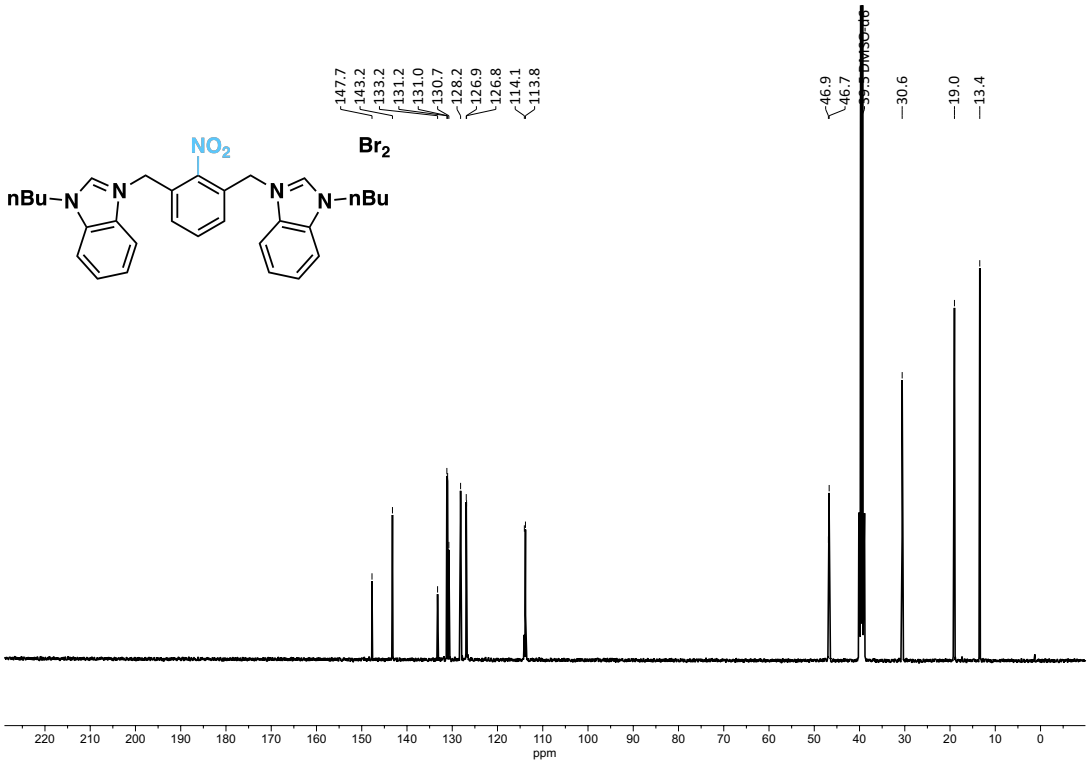

Figure S24. ^{13}C{^{1}H} NMR (101MHz, 298K) of **3b** in DMSO–d_6

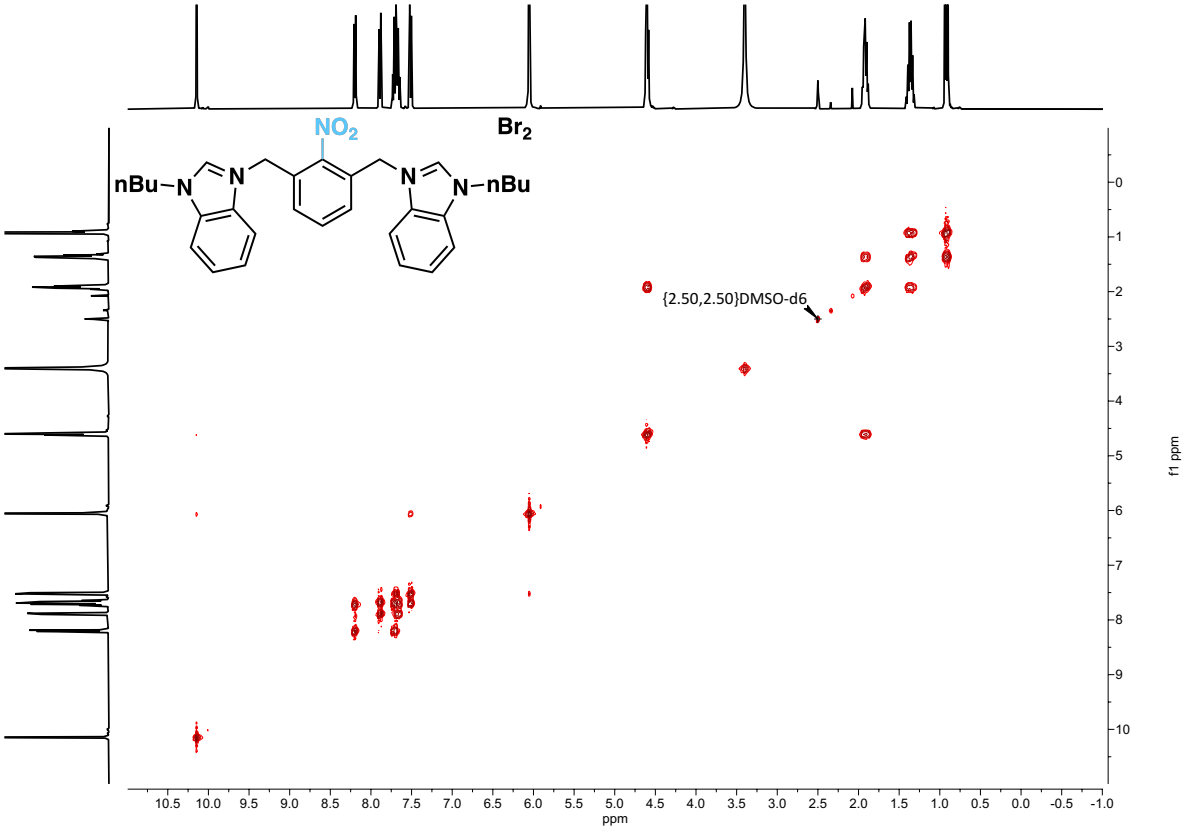

Figure S25. $^{1}H,^{1}H$ COSY NMR (400MHz, 298K) of **3b** in DMSO–d_6

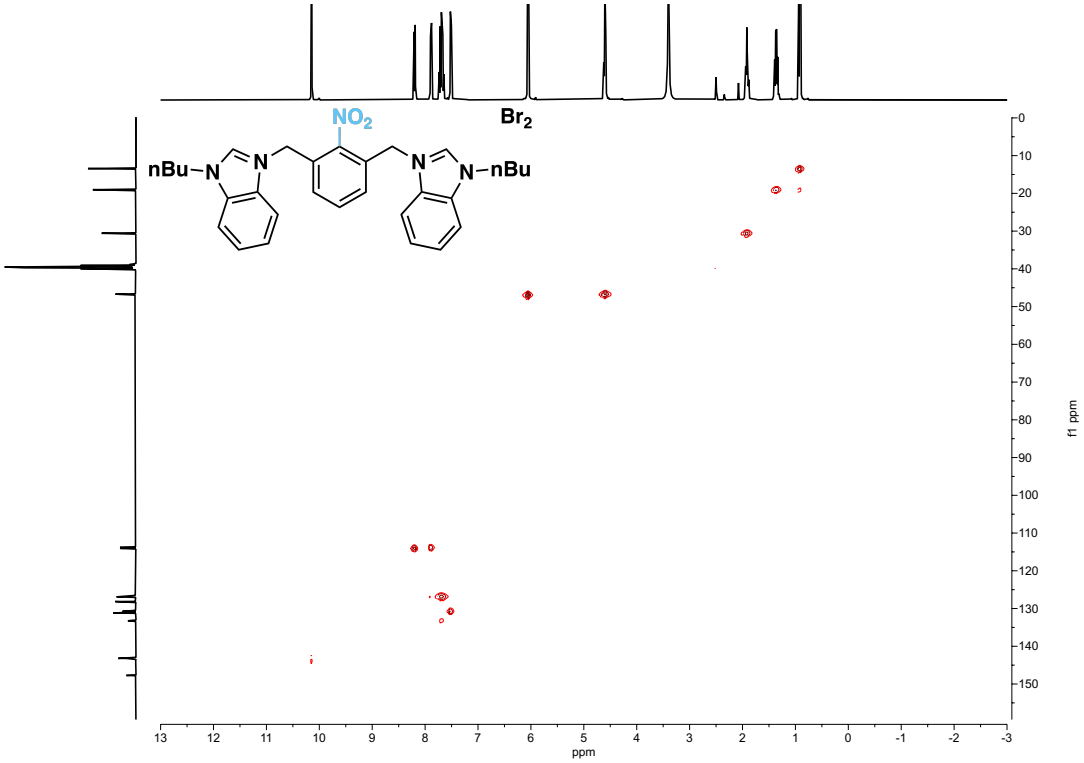

Figure S26. $^{1}H,^{13}C$ HSQC NMR (400MHz, 298K) of **3b** in DMSO–d_6

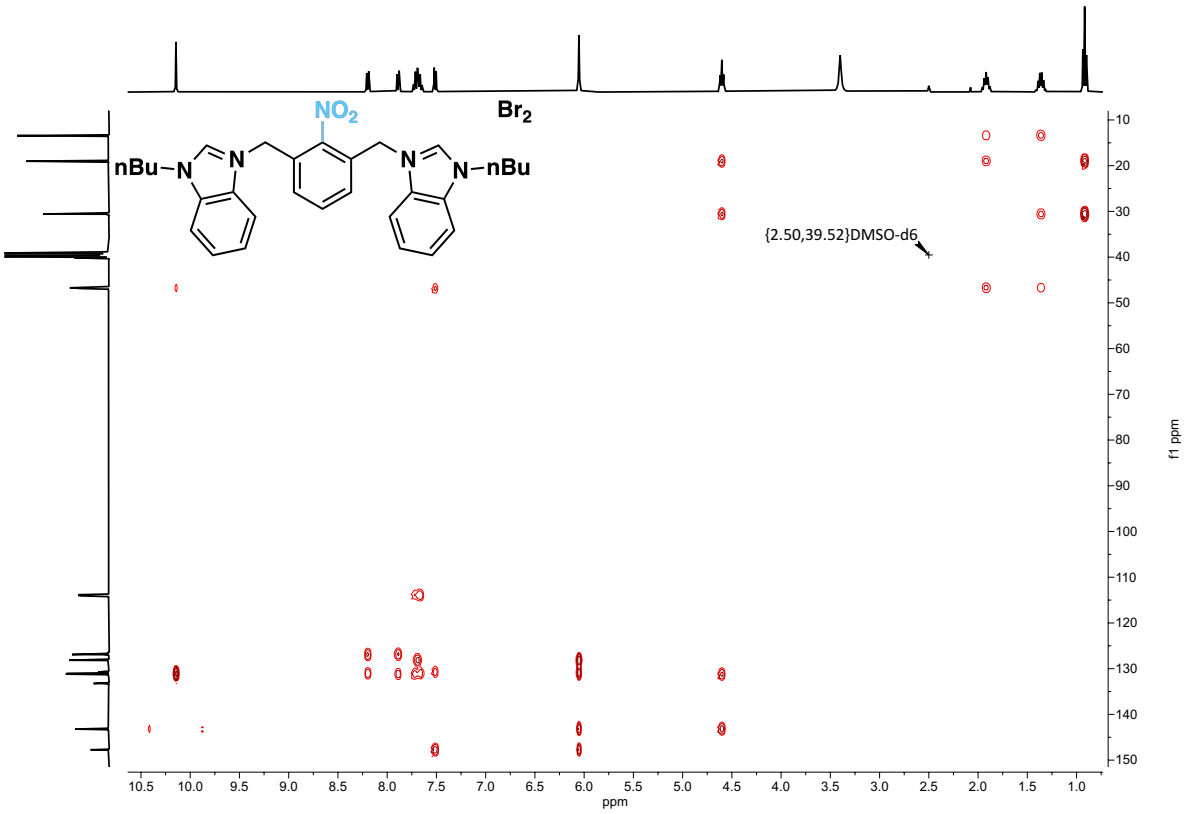

Figure S27. $^{1}H,^{13}C$ HMBC NMR (400MHz, 298K) of **3b** in DMSO–d_6

7.4 NMR spectra of compound 4a

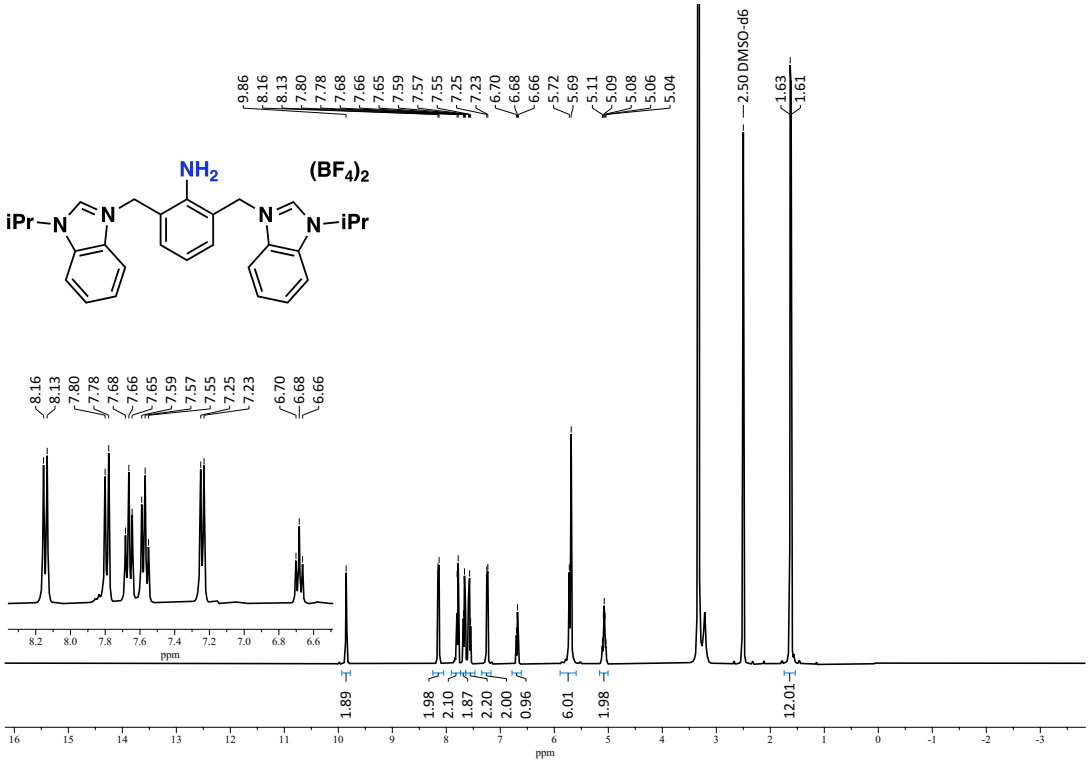

Figure S28. ^{1}H NMR (400MHz, 298K) of **4a** in DMSO–d_6

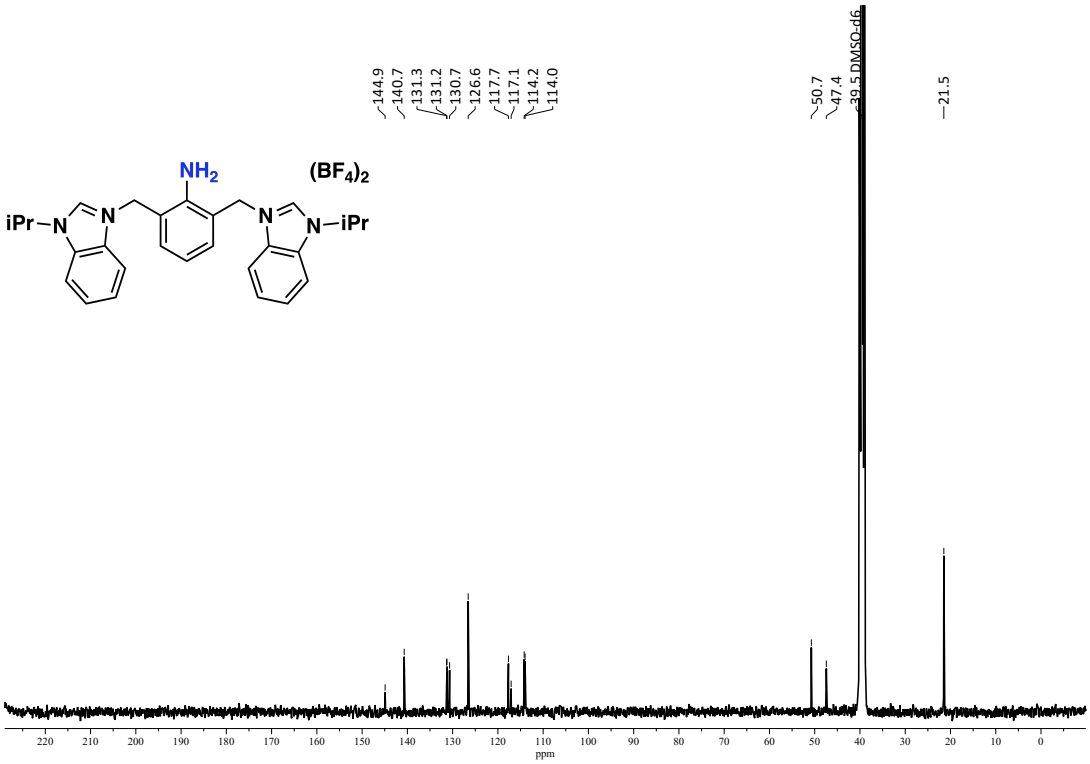

Figure S29. ^{13}C{^{1}H} NMR (101MHz, 298K) of **4a** in DMSO–d_6

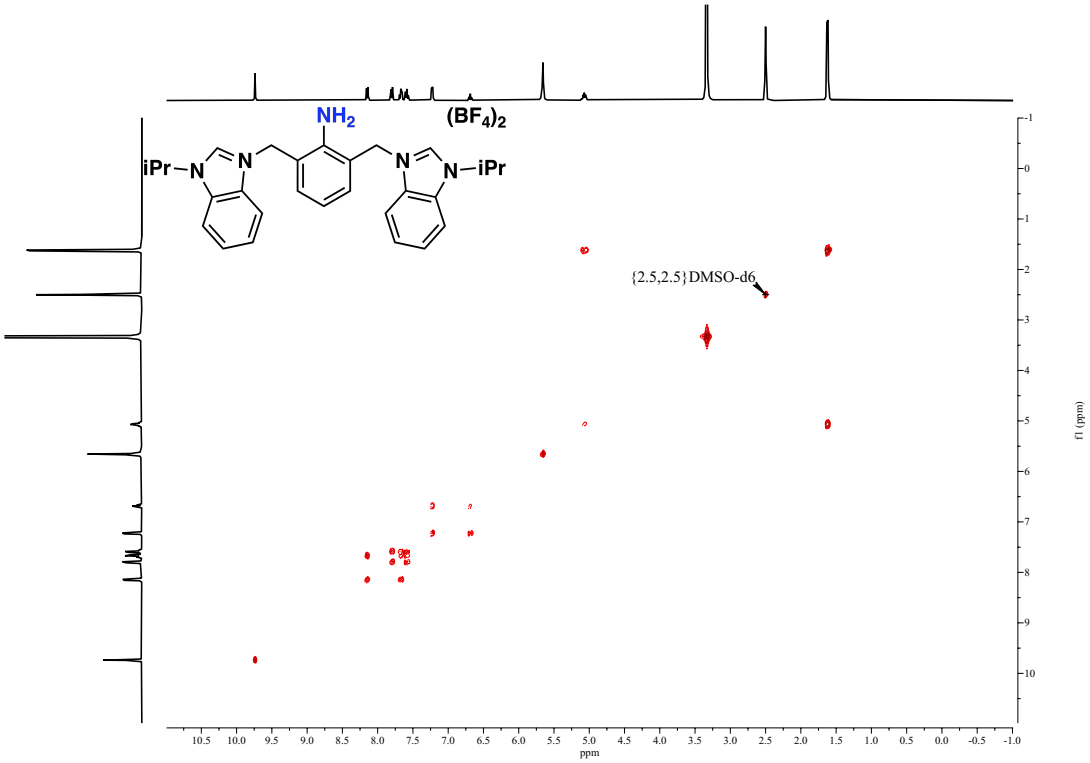

Figure S30. ^{1}H,^{1}H COSY NMR (400MHz, 298K) of **4a** in DMSO–d_6

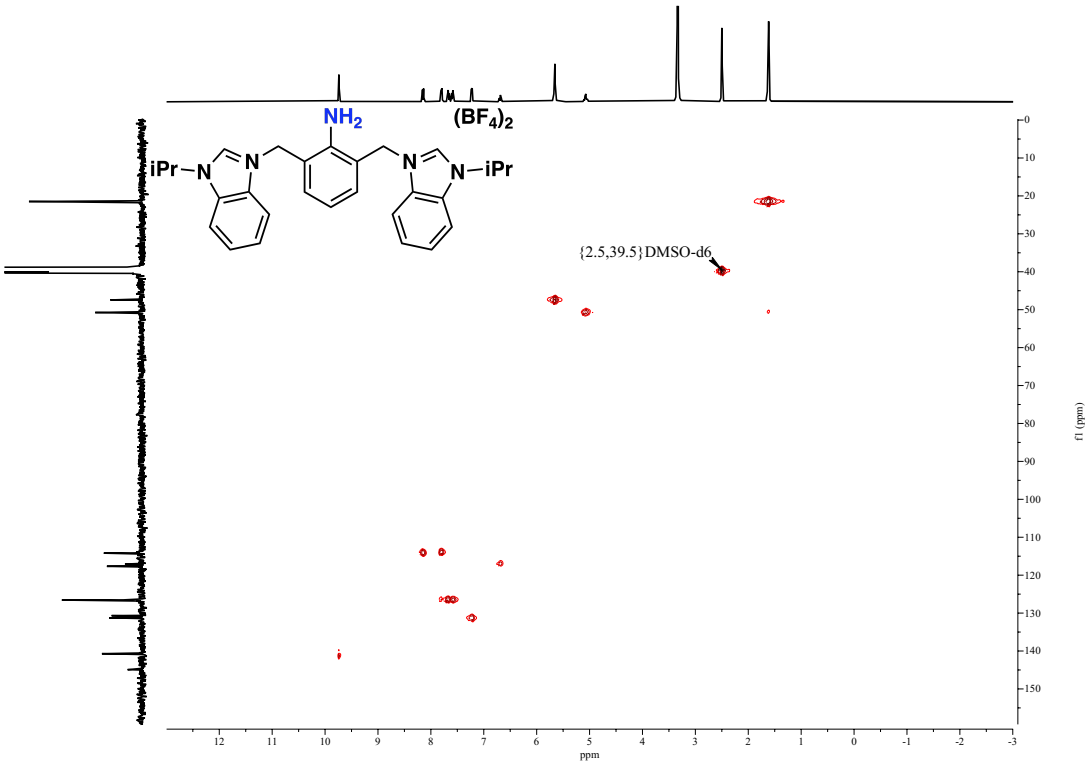

Figure S31. ^{1}H,^{13}C HSQC NMR (400MHz, 298K) of **4a** in DMSO–d_6

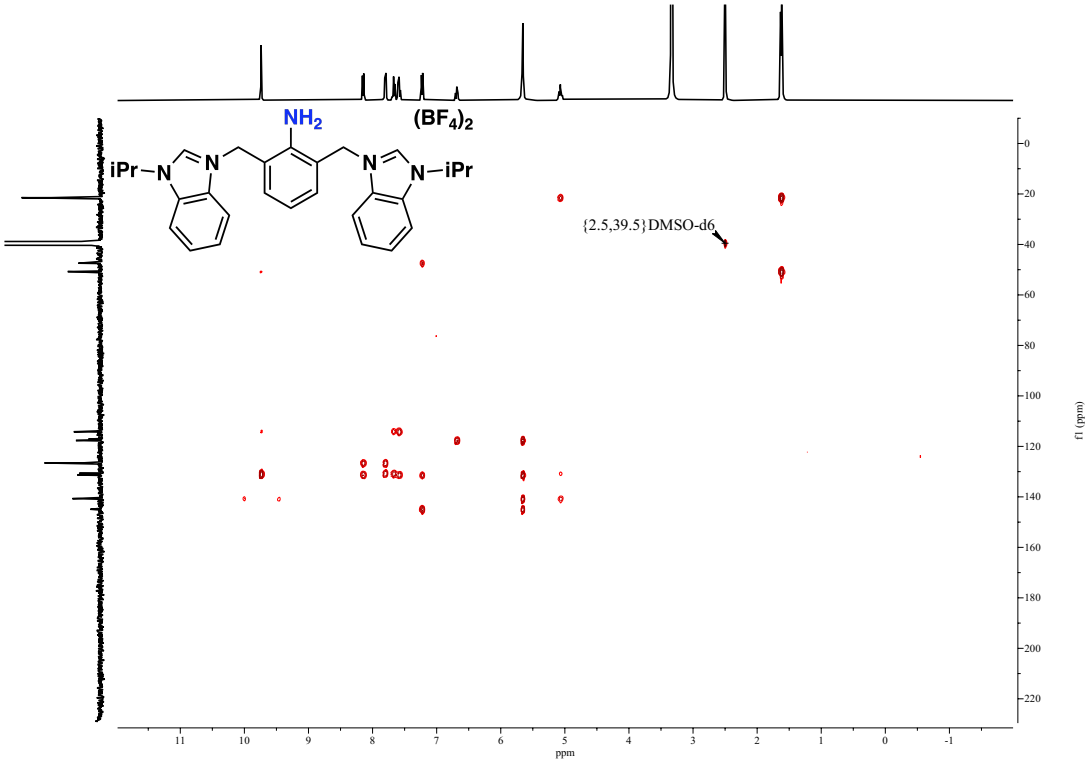

Figure S32. $^{1}H,^{13}C$ HMBC NMR (400MHz, 298K) of **4a** in DMSO–d_6

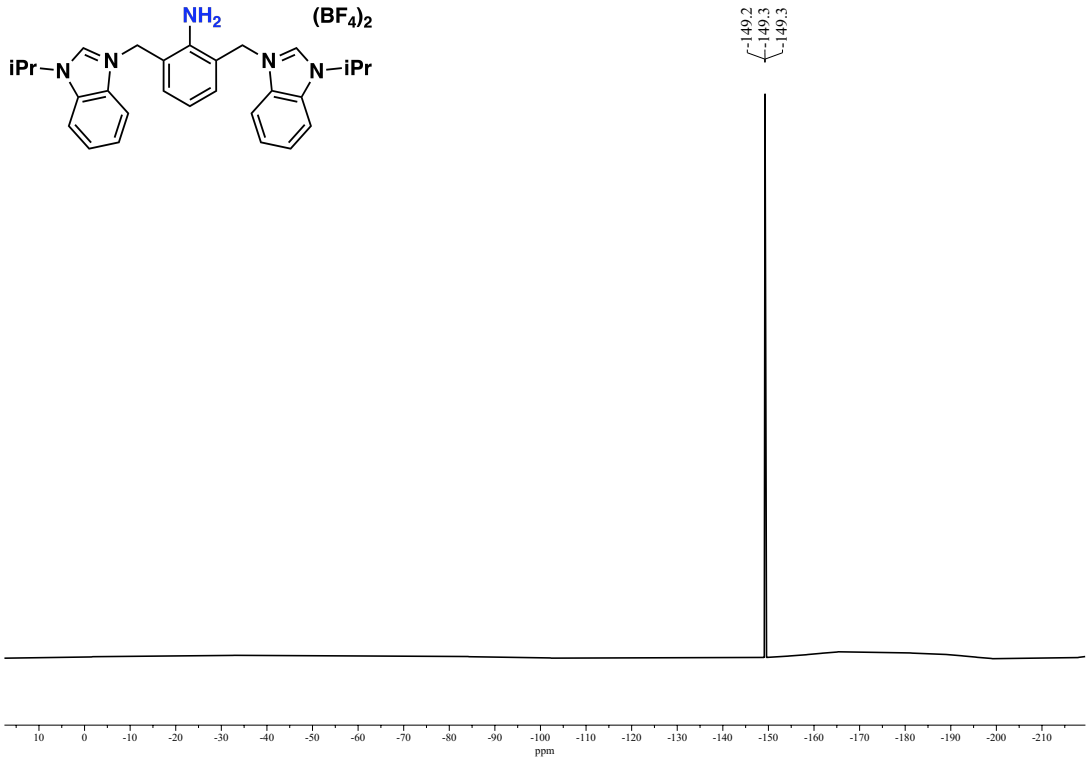

Figure S33. ^{19}F NMR (376MHz, 298K) of **4a** in DMSO–d_6

7.5 NMR spectra of compound 4b

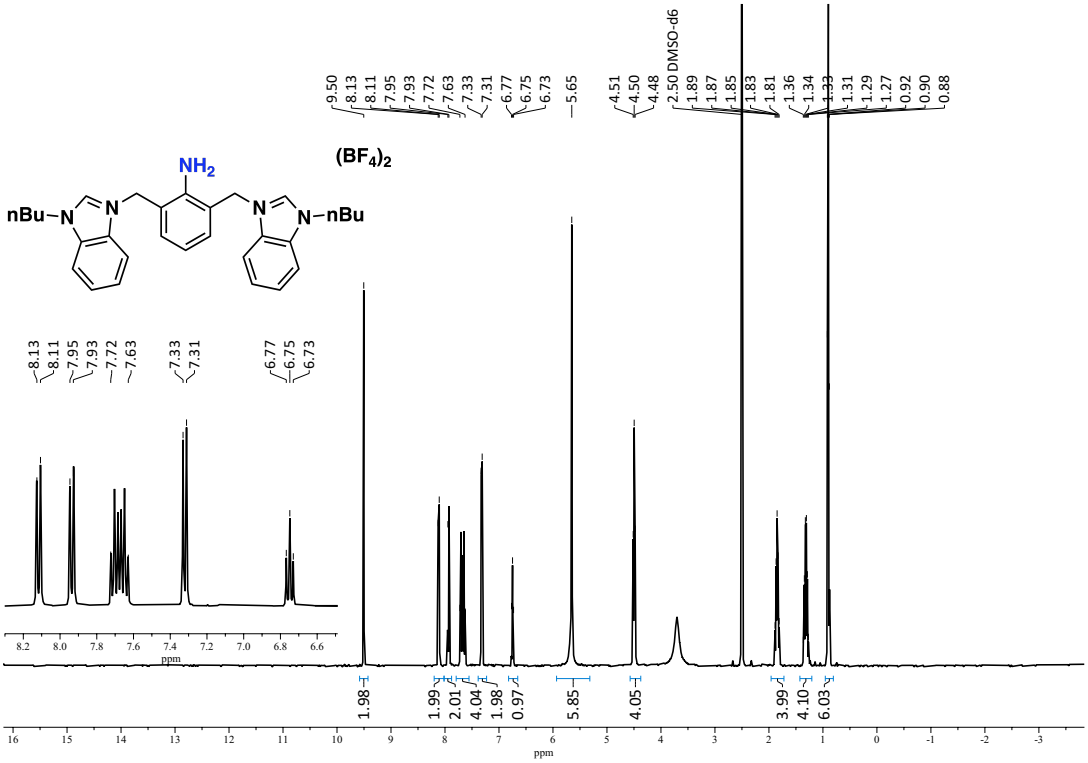

Figure S34. ^{1}H NMR (400MHz, 298K) of **4b** in DMSO–d_6

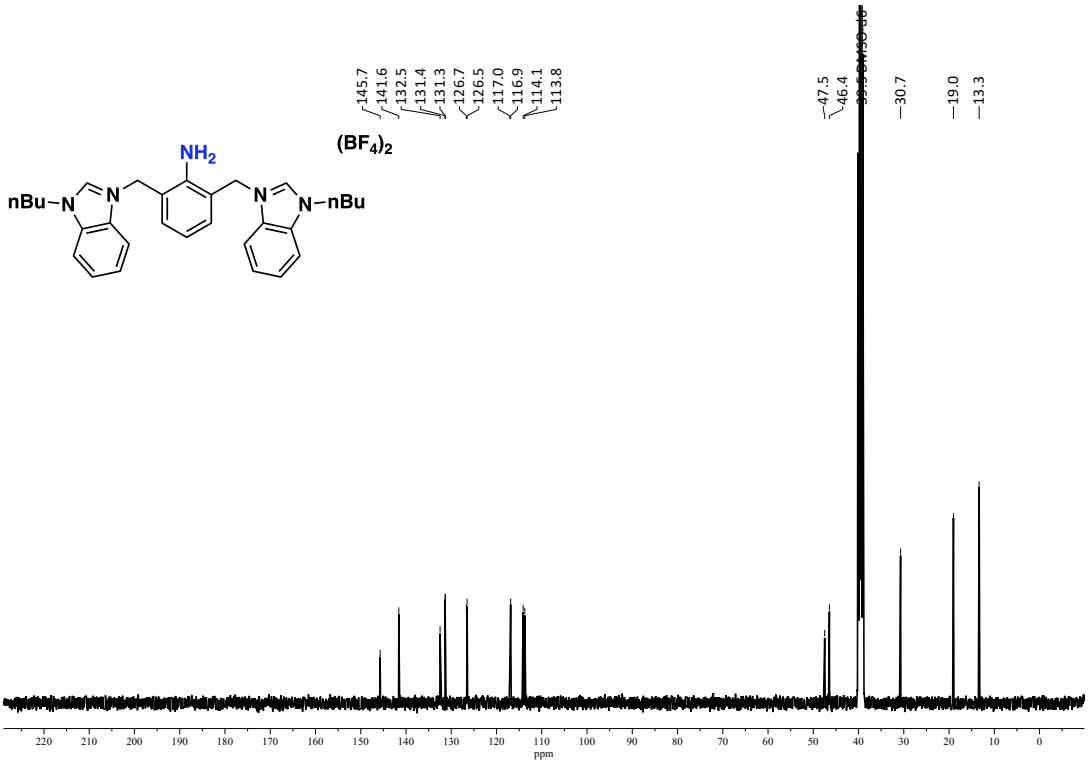

Figure S35. ^{13}C{^{1}H} NMR (101MHz, 298K) of **4b** in DMSO–d_6

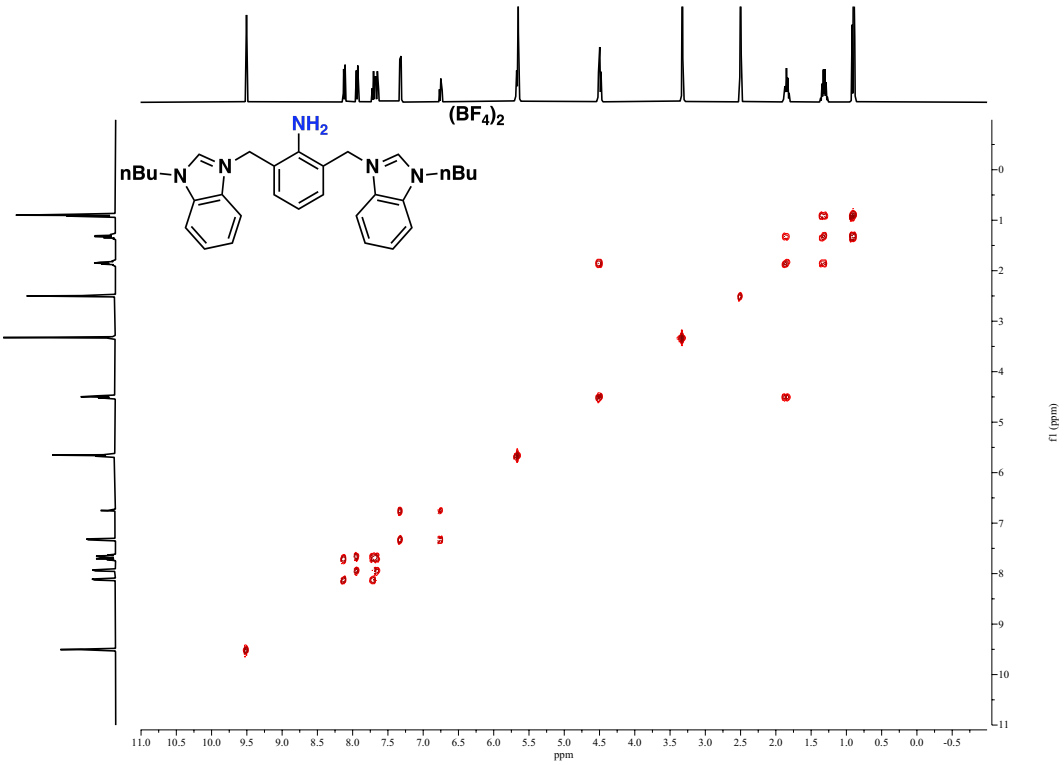

Figure S36. ^{1}H,^{1}H COSY NMR (400MHz, 298K) of **4b** in DMSO–d_6

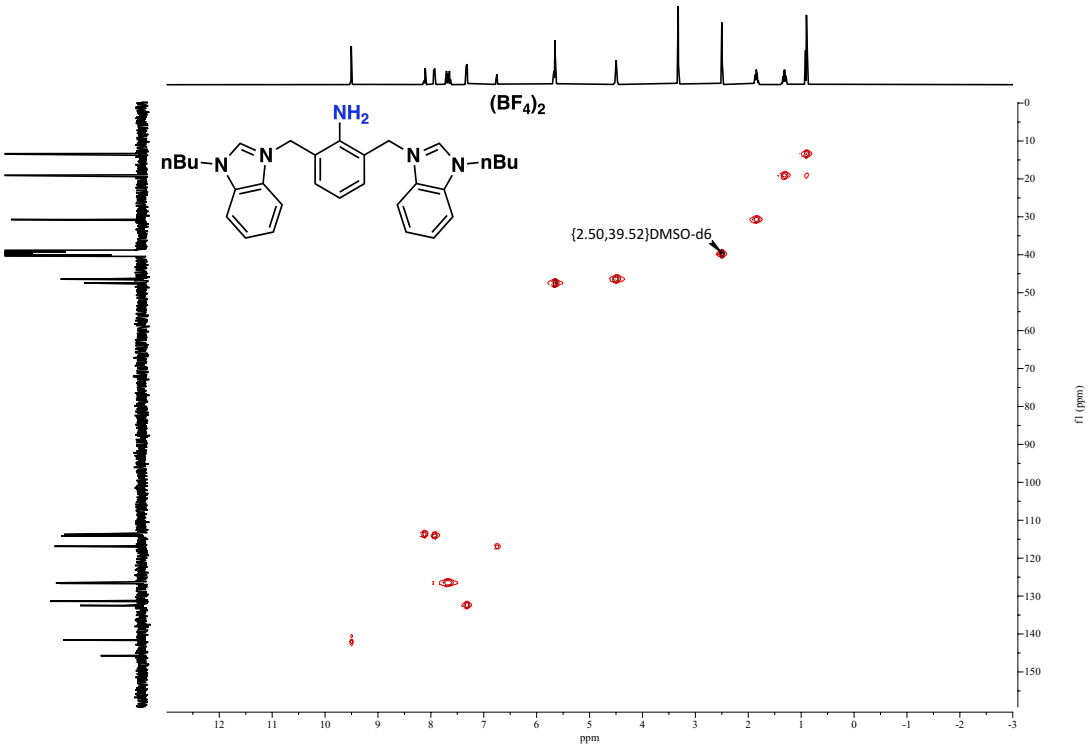

Figure S37. ^{1}H,^{13}C HSQC NMR (400MHz, 298K) of **4b** in DMSO–d_6

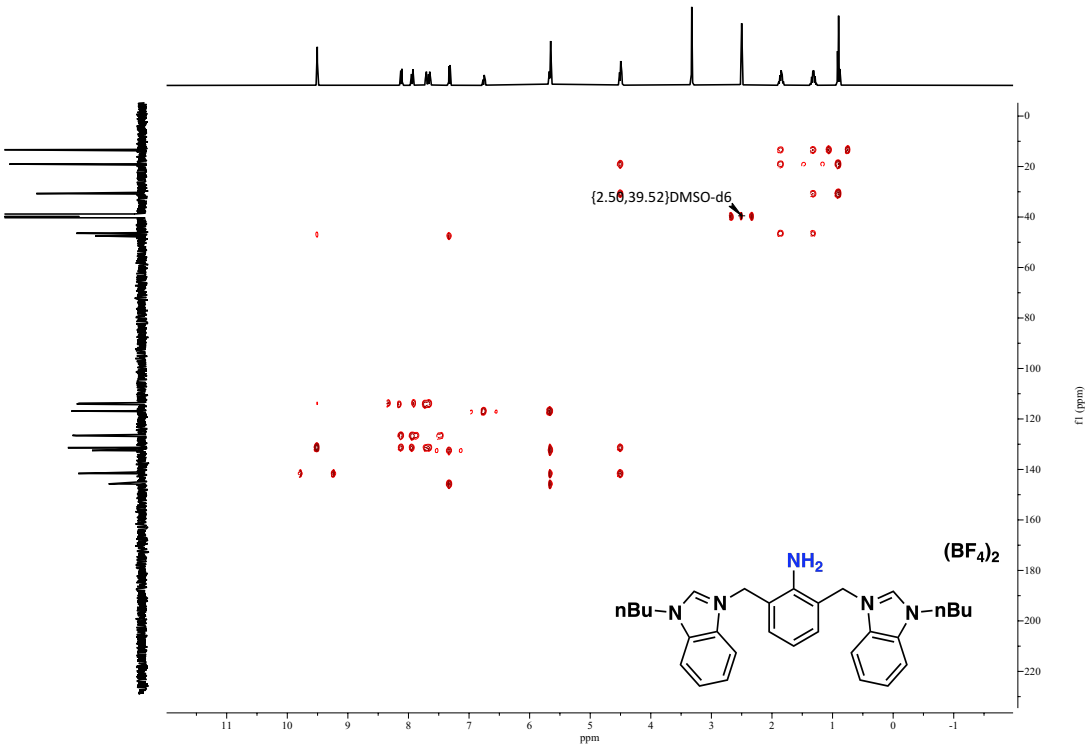

Figure S38. $^{1}H,^{13}C$ HMBC NMR (400MHz, 298K) of **4b** in DMSO–d_6

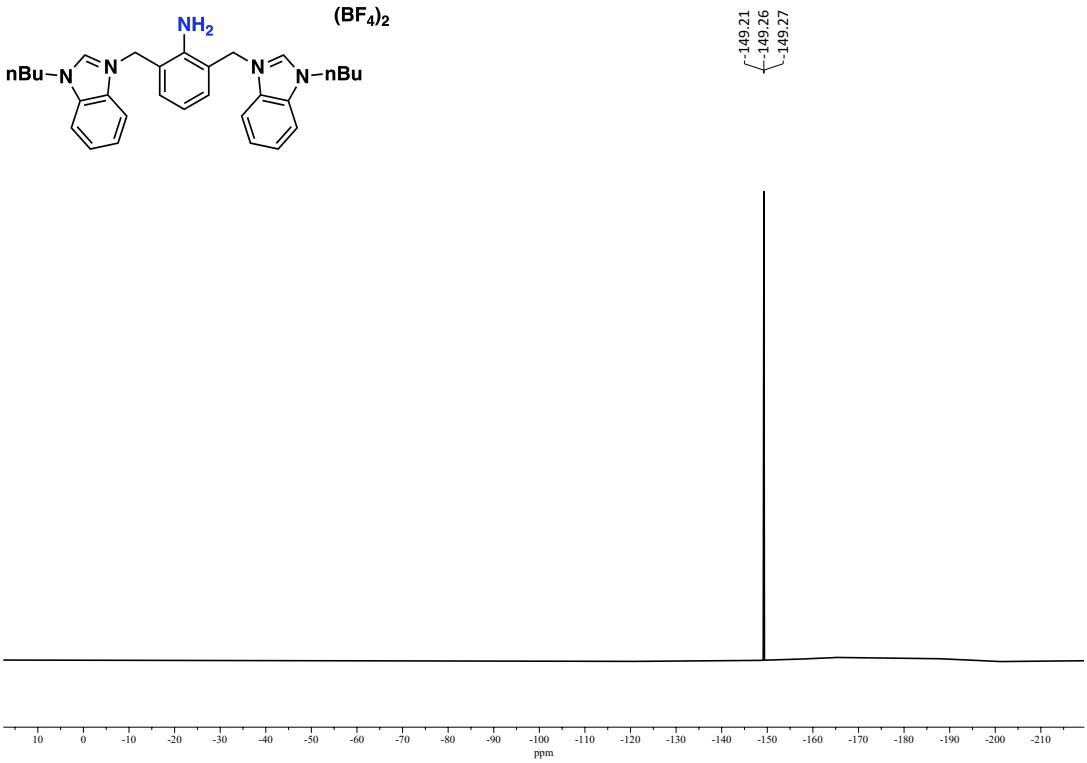

Figure S39. ^{19}F NMR (376MHz, 298K) of **4b** in DMSO–d_6

7.6 NMR spectra of compound 5a

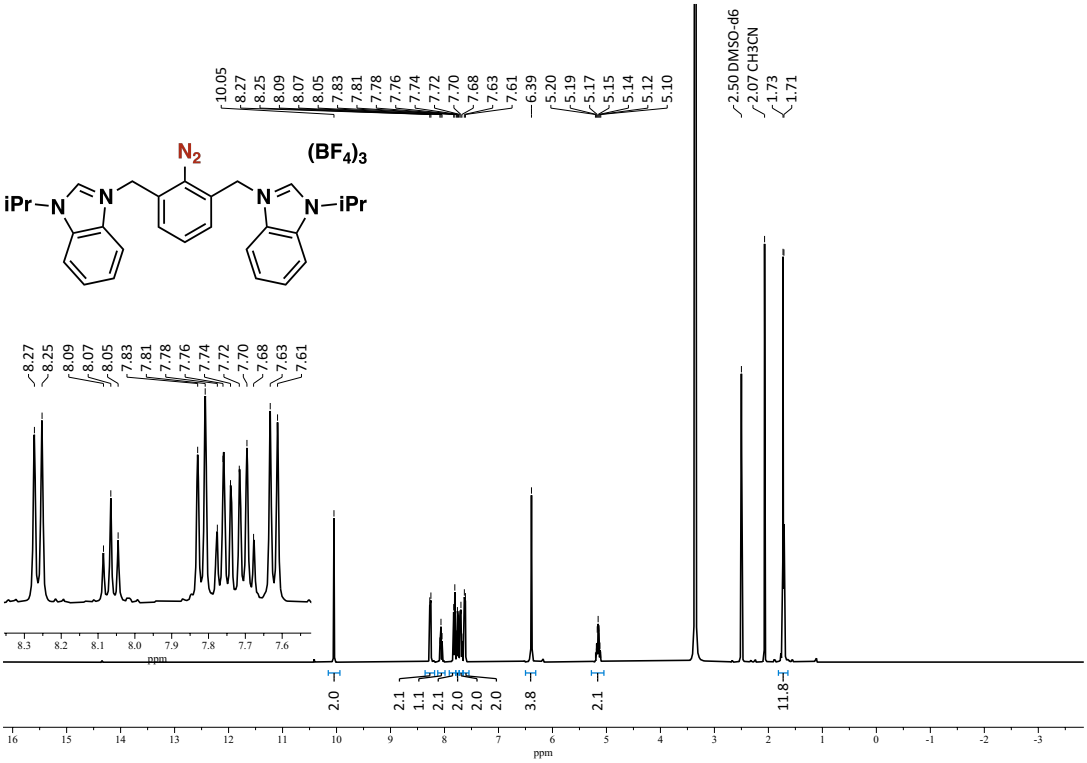

Figure S40. ^{1}H NMR (400MHz, 298K) of **5a** in DMSO–d_6

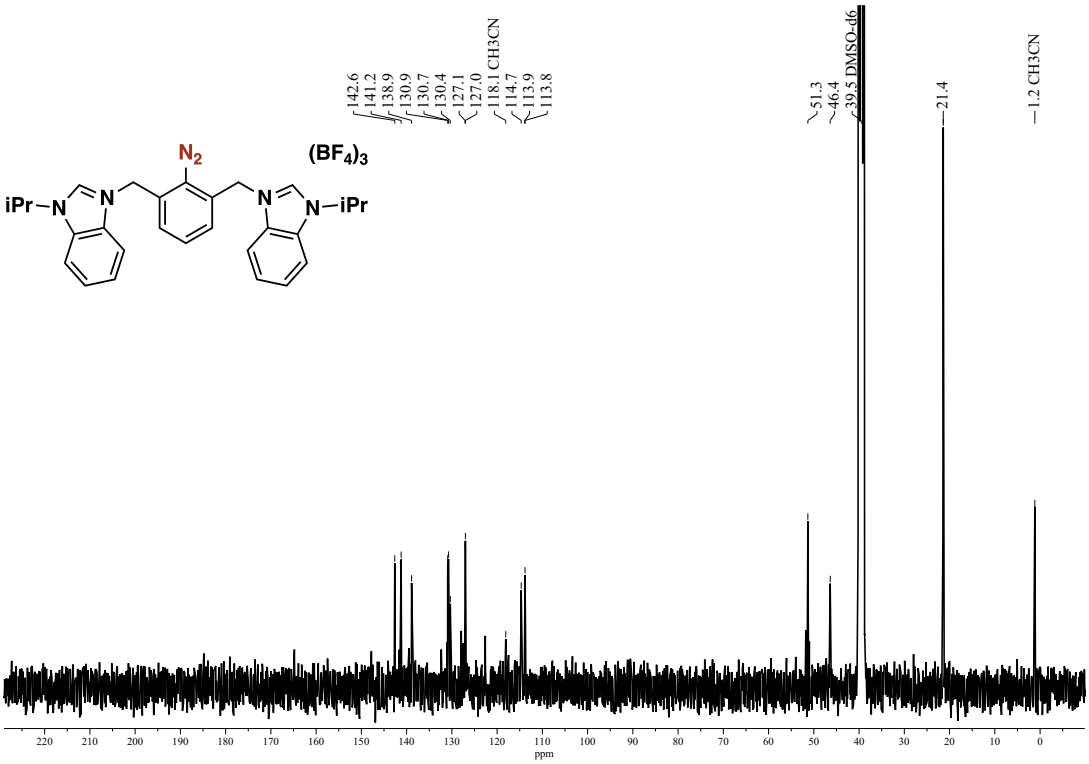

Figure S41. ^{13}C{^{1}H} NMR (101MHz, 298K) of **5a** in DMSO–d_6

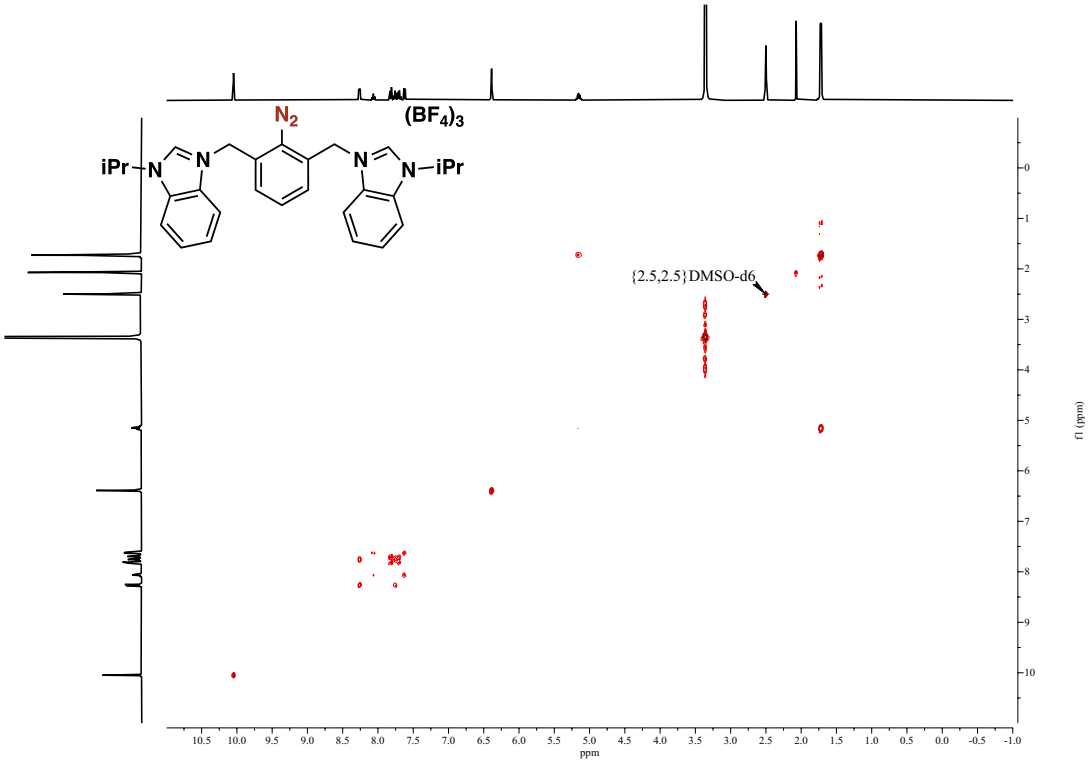

Figure S42. ^{1}H,^{1}H COSY NMR (400MHz, 298K) of **5a** in DMSO–d_6

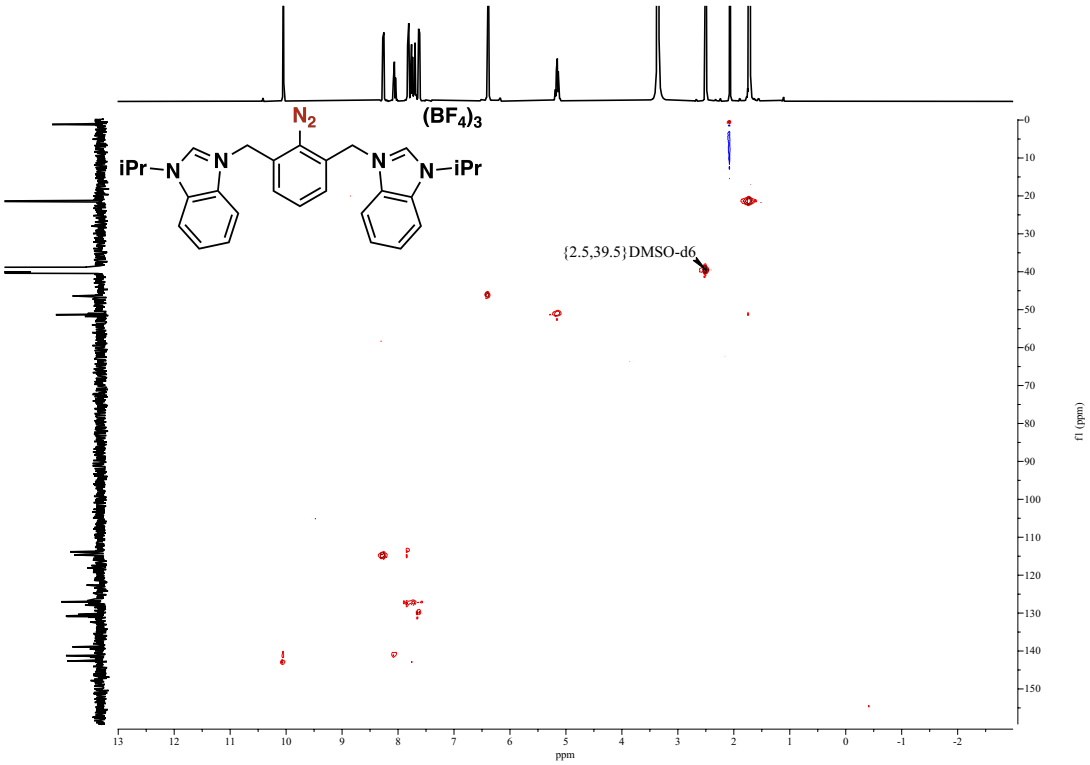

Figure S43. ^{1}H,^{13}C HSQC NMR (400MHz, 298K) of **5a** in DMSO–d_6

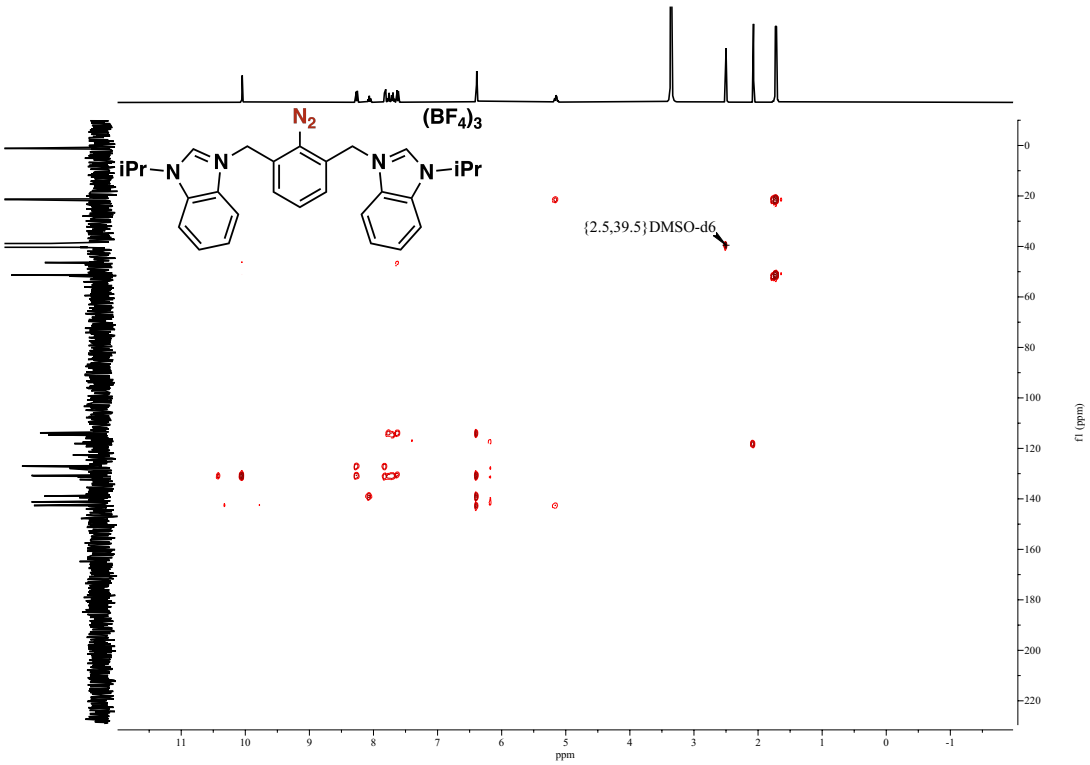

Figure S44. $^{1}H,^{13}C$ HMBC NMR (400MHz, 298K) of **5a** in DMSO–d_6

7.7 NMR spectra of compound 5b

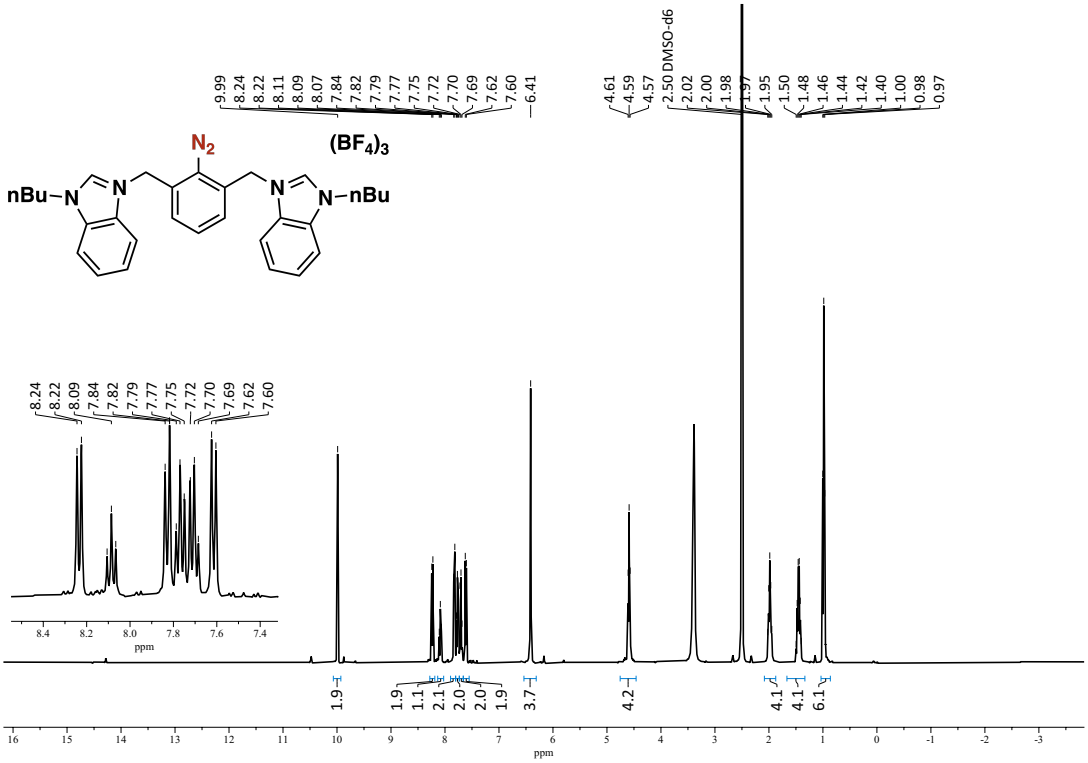

Figure S45. ^{1}H NMR (400MHz, 298K) of **5b** in DMSO–d_6

7.8 NMR spectra of complex 6a

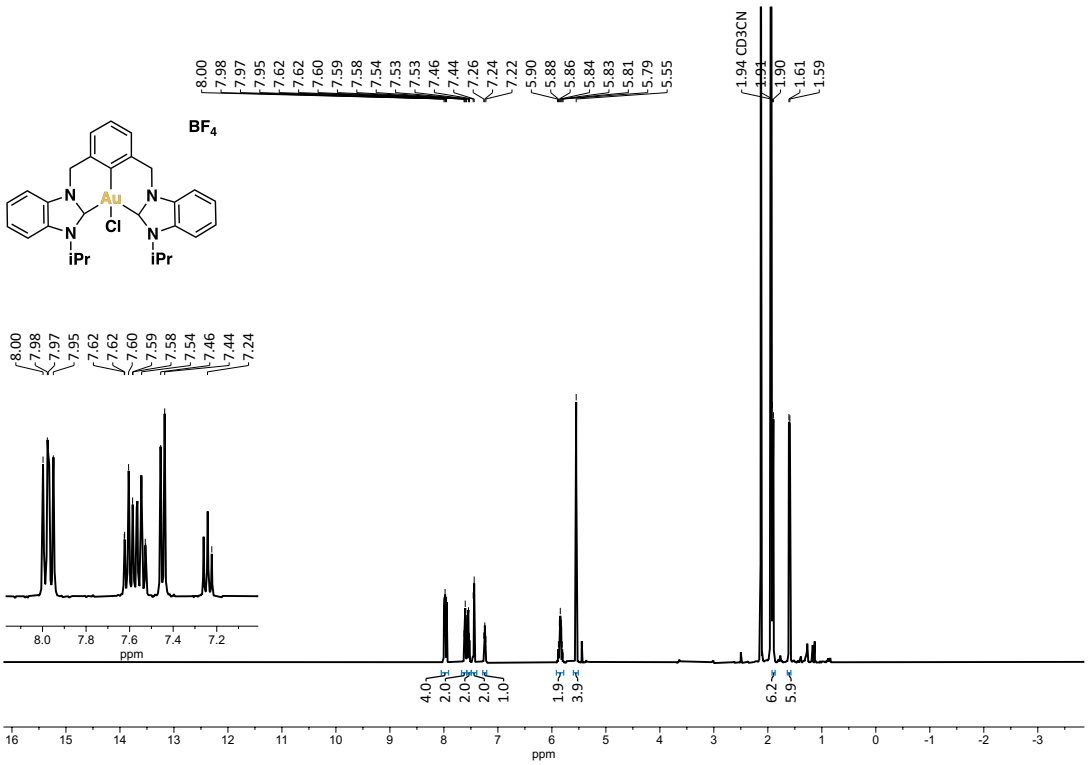

Figure S46. ^{1}H NMR (400MHz, 298K) of **6a** in CD_3CN

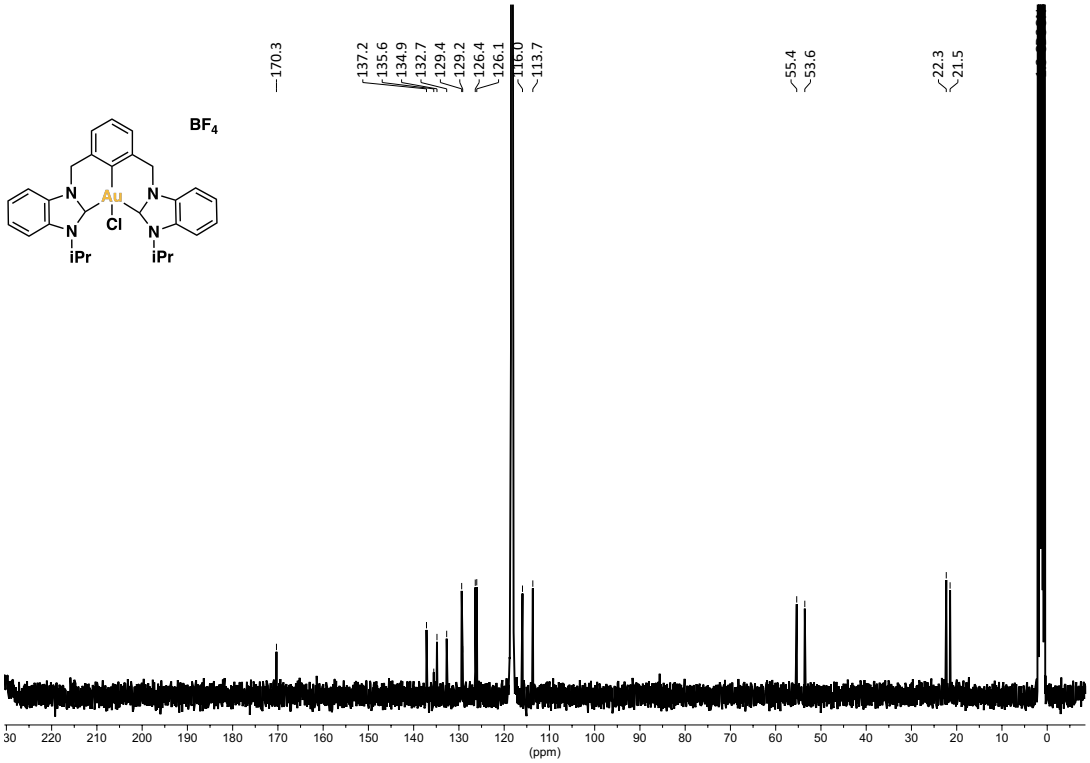

Figure S47. $^{13}C\{^{1}H\}$ NMR (101MHz, 298K) of **6a** in CD_3CN

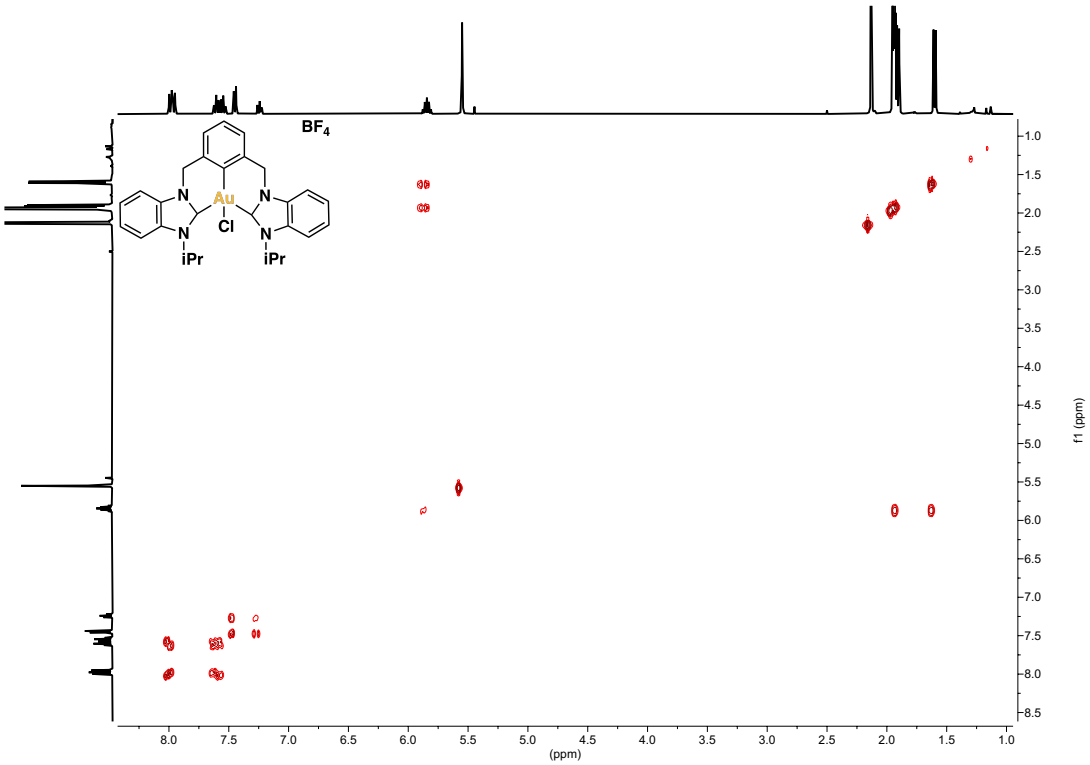

Figure S48. $^{1}H,^{1}H$ COSY NMR (400MHz, 298K) of **6a** in CD_3CN

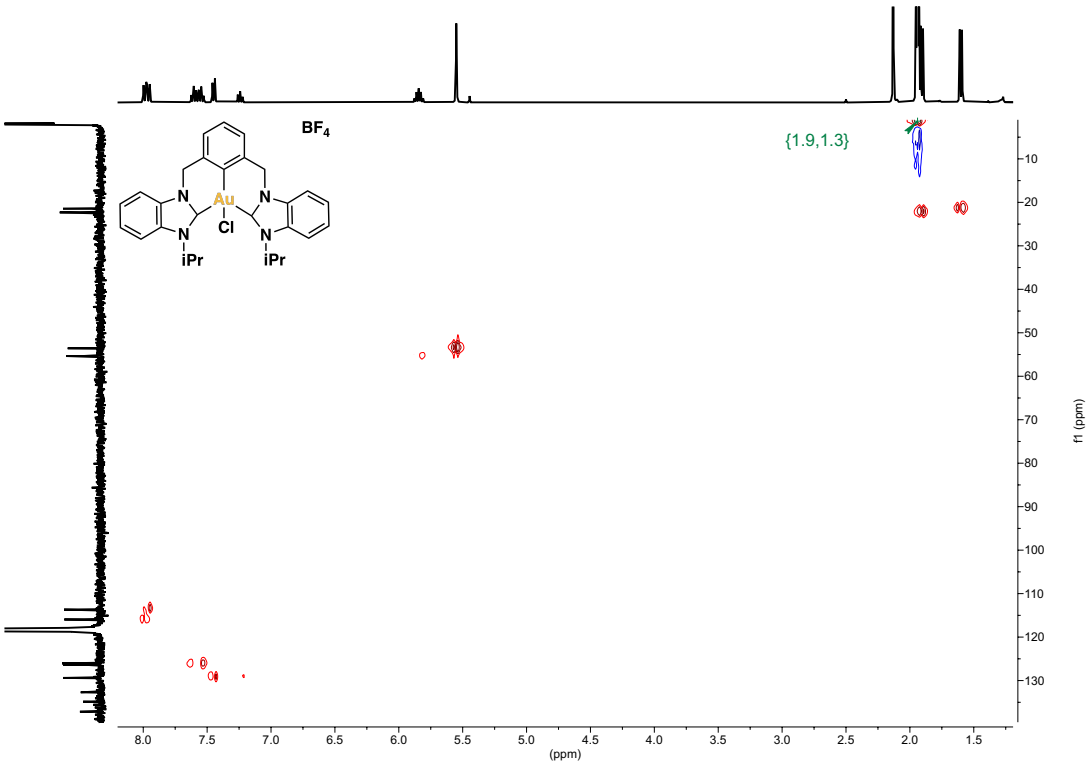

Figure S49. $^{1}H,^{13}C$ HSQC NMR (400MHz, 298K) of **6a** in CD_3CN

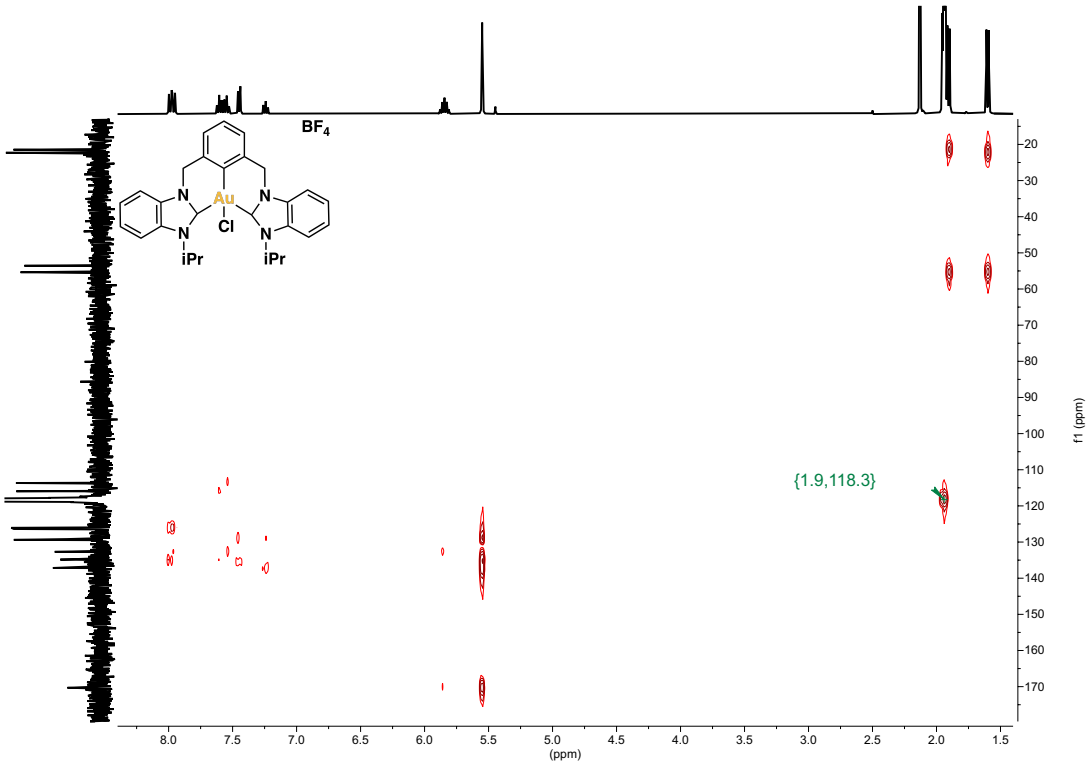

Figure S50. $^{1}H,^{13}C$ HMBC NMR (400MHz, 298K) of **6a** in CD_3CN

7.9 NMR spectra of complex 6b

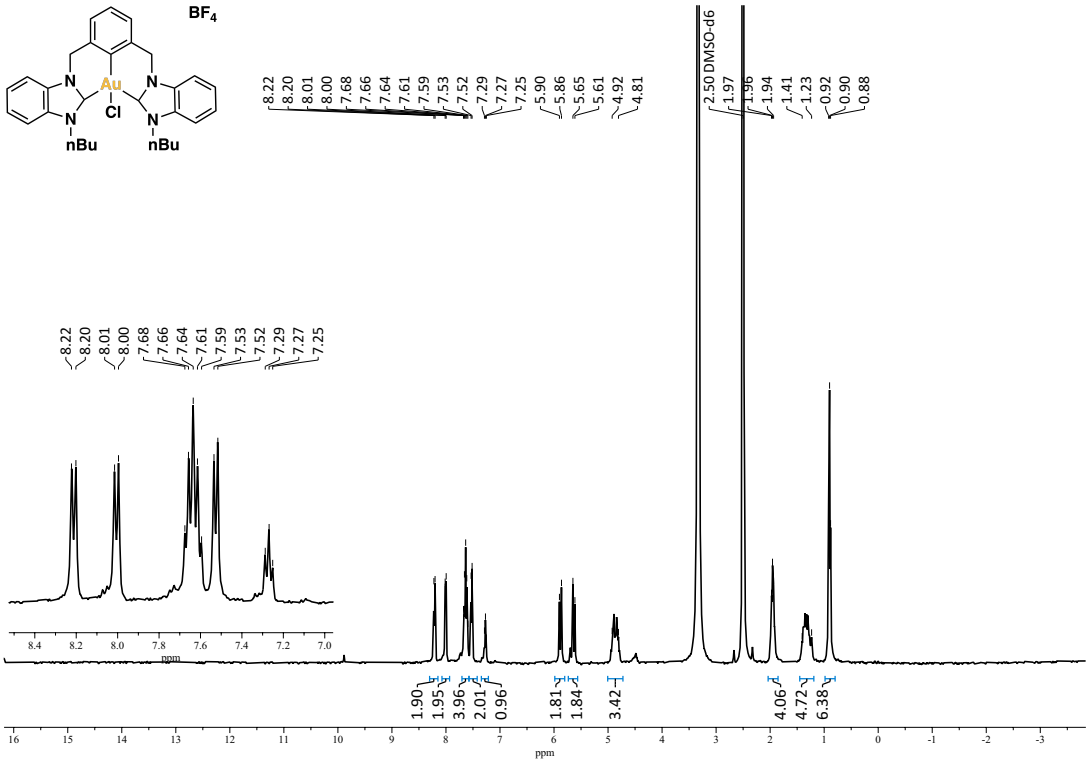

Figure S51. ^{1}H NMR (400MHz, 298K) of **6b** in DMSO–d_6

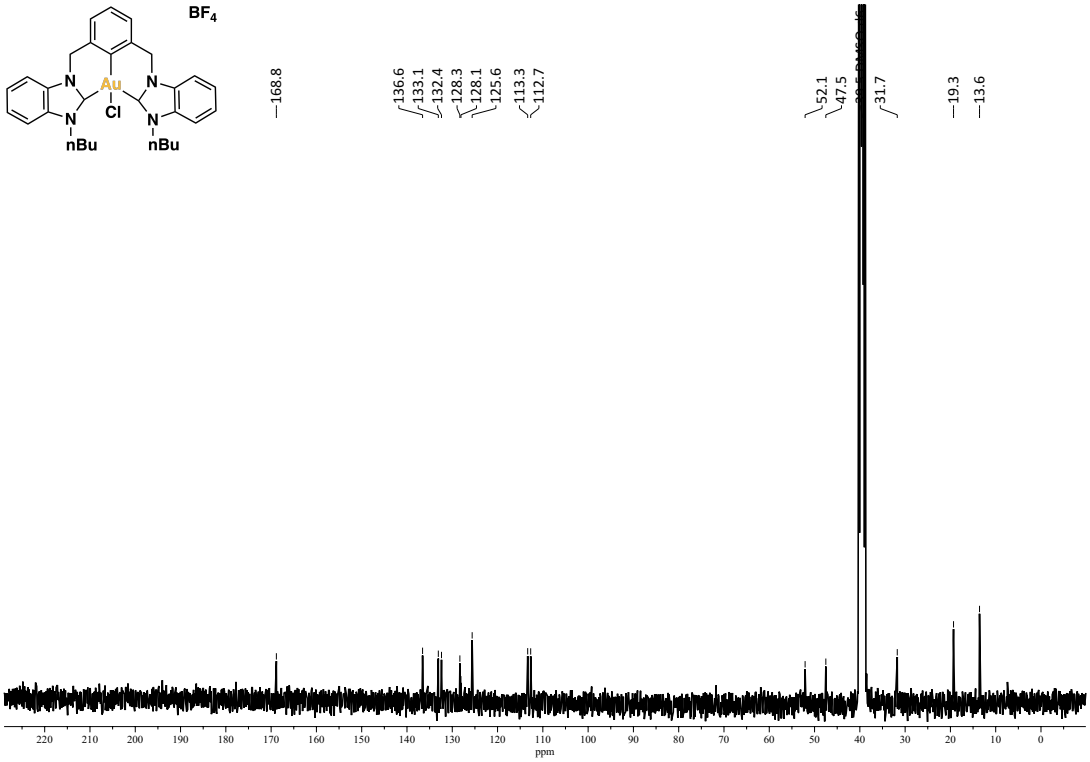

Figure S52. ^{13}C{^{1}H} NMR (101MHz, 298K) of **6b** in DMSO–d_6

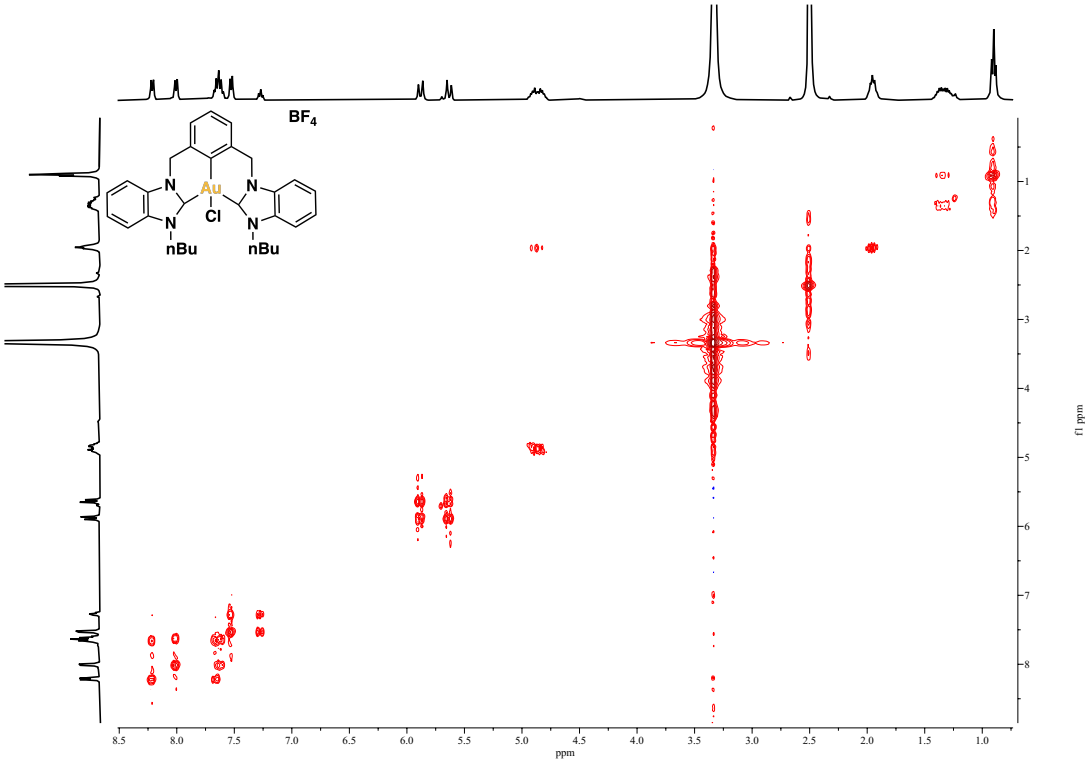

Figure S53. ^{1}H,^{1}H COSY NMR (400MHz, 298K) of **6b** in DMSO–d_6

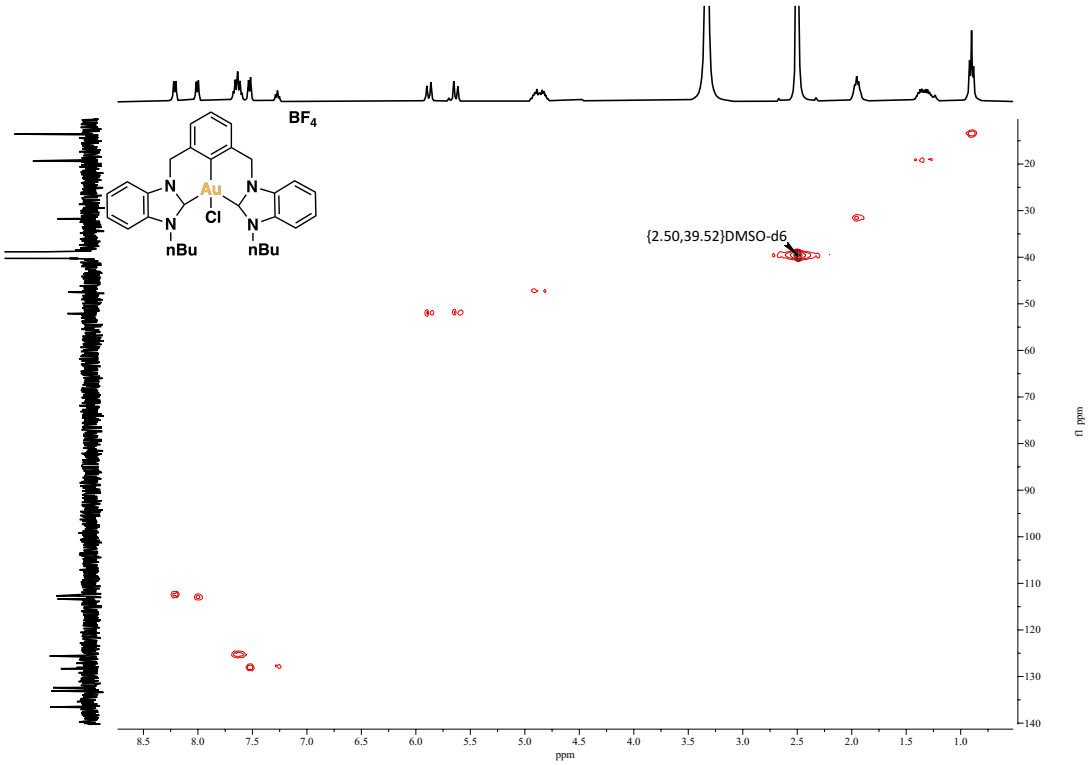

Figure S54. ^{1}H,^{13}C HSQC NMR (400MHz, 298K) of **6b** in DMSO–d_6

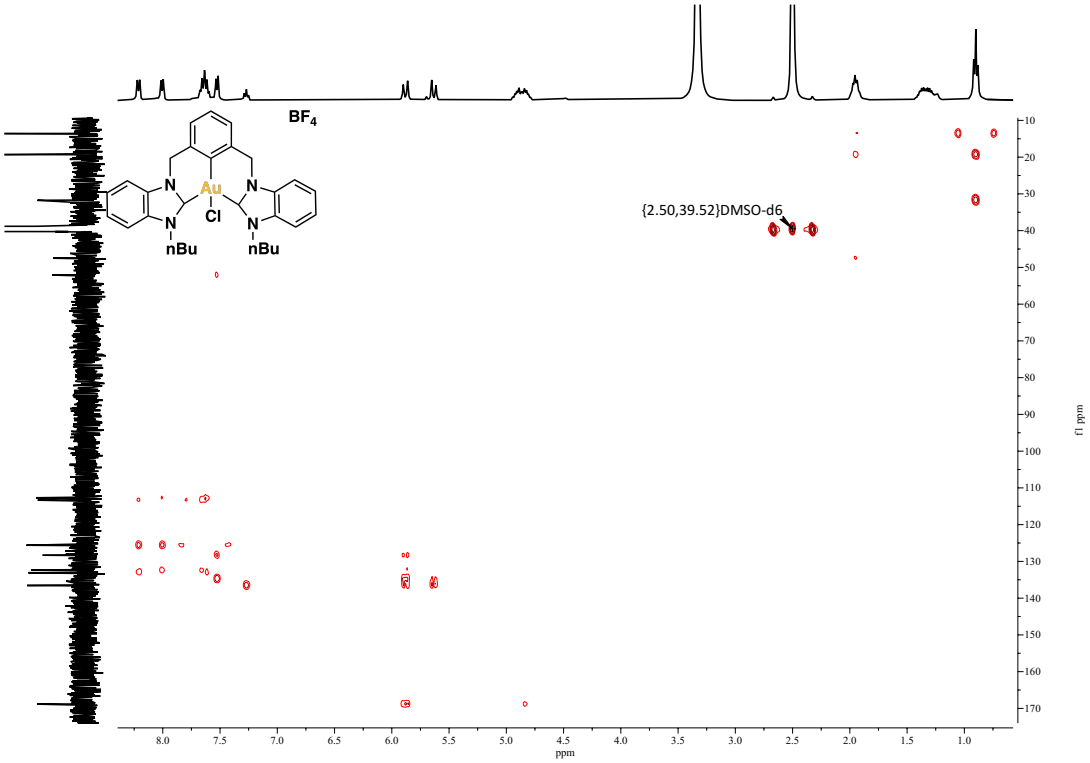

Figure S55. $^{1}H,^{13}C$ HMBC NMR (400MHz, 298K) of **6b** in DMSO–d_6

7.10 NMR spectra of complex 8a

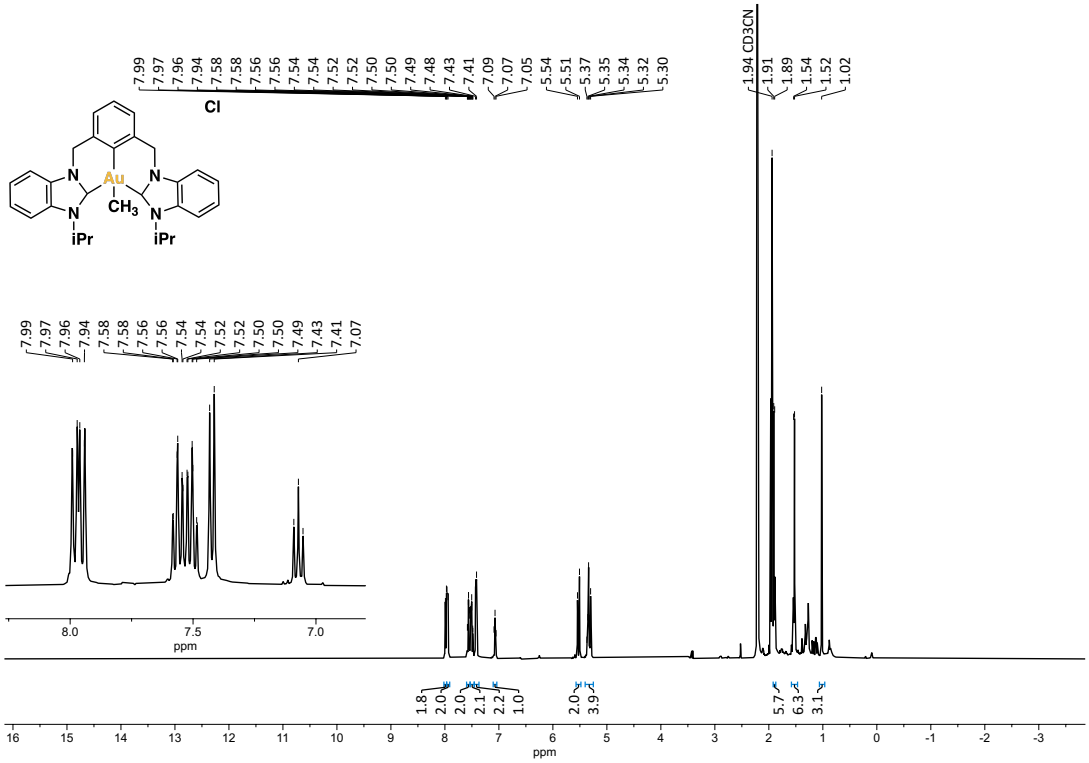

Figure S56. ^{1}H NMR (400MHz, 298K) of **8a** in CD_3CN

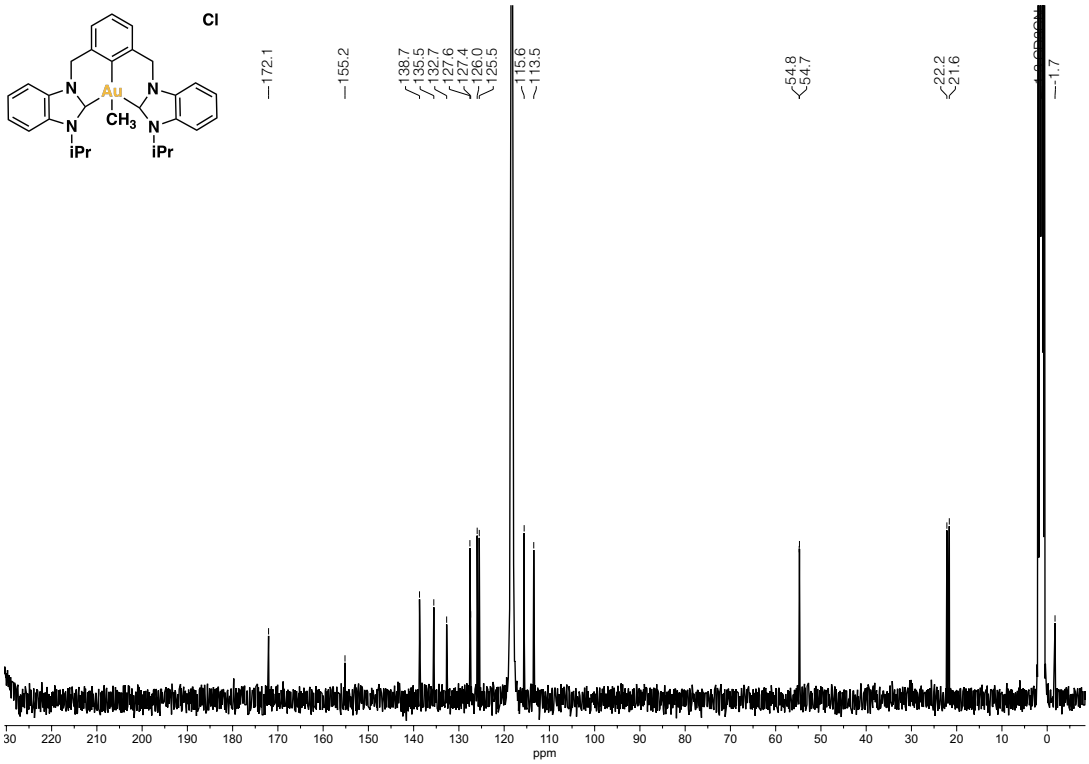

Figure S57. $^{13}C\{^{1}H\}$ NMR (101MHz, 298K) of **8a** in CD_3CN

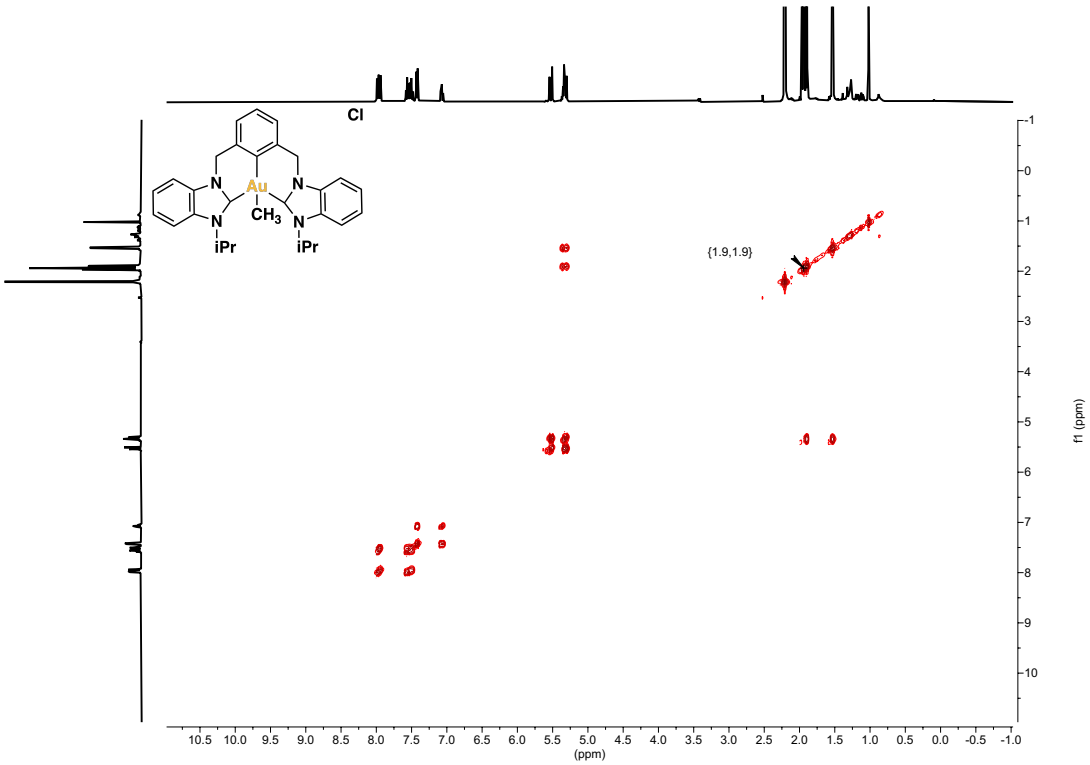

Figure S58. $^{1}H,^{1}H$ COSY NMR (400MHz, 298K) of **8a** in CD_3CN

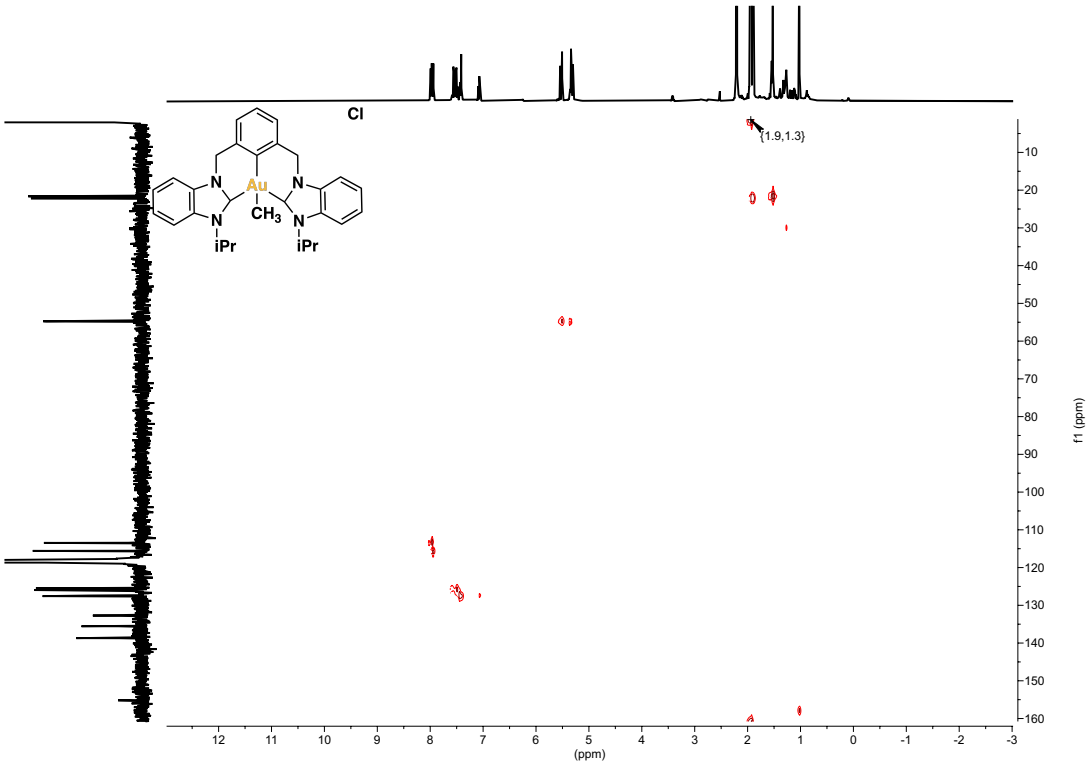

Figure S59. $^{1}H,^{13}C$ HSQC NMR (400MHz, 298K) of **8a** in CD_3CN

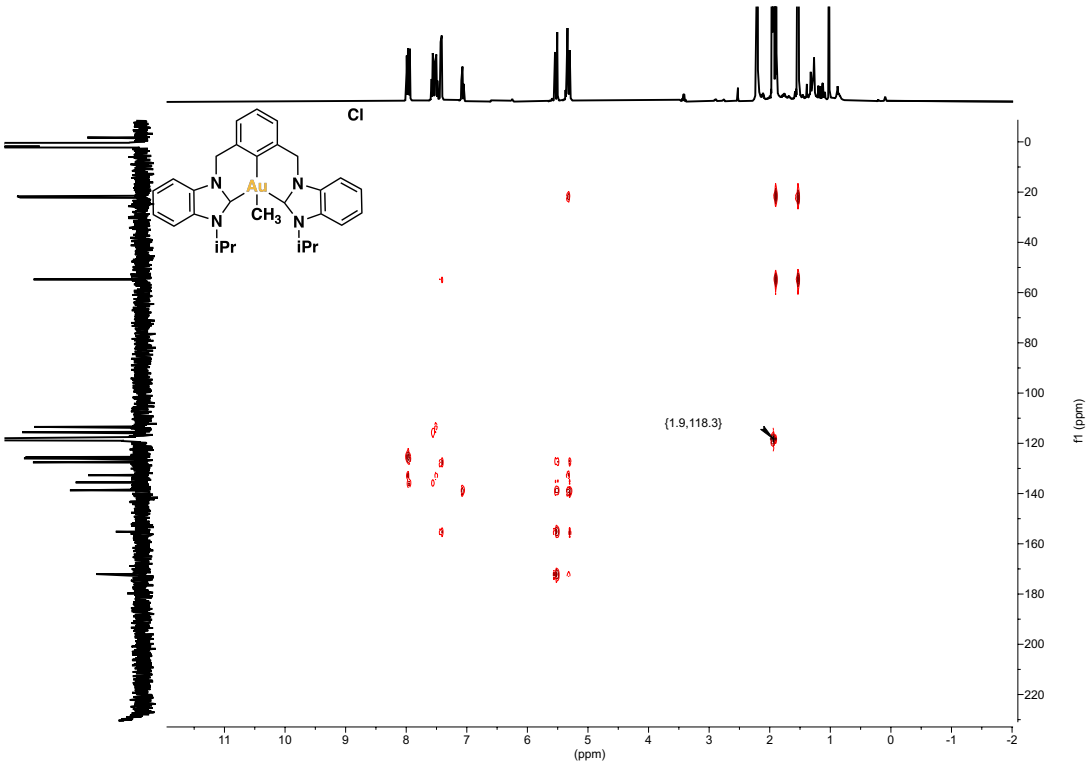

Figure S60. $^{1}H,^{13}C$ HMBC NMR (400MHz, 298K) of **8a** in CD_3CN

7.11 NMR spectra of complex 8b

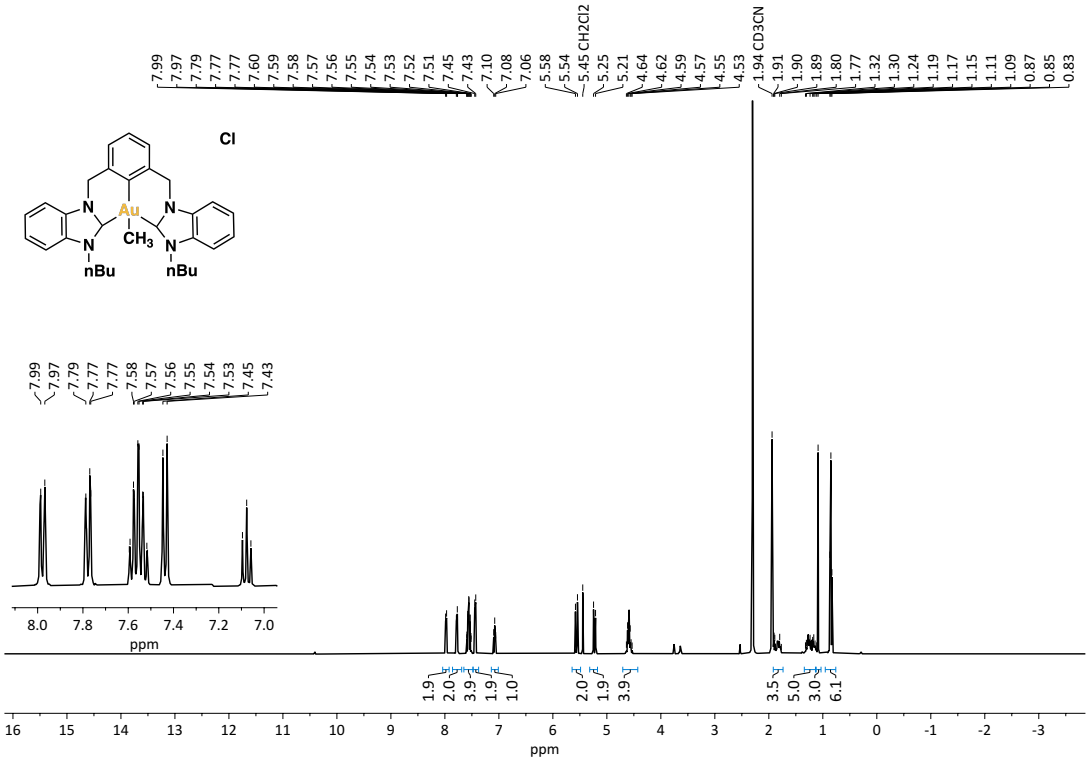

Figure S61. ^{1}H NMR (400MHz, 298K) of **8b** in CD_3CN

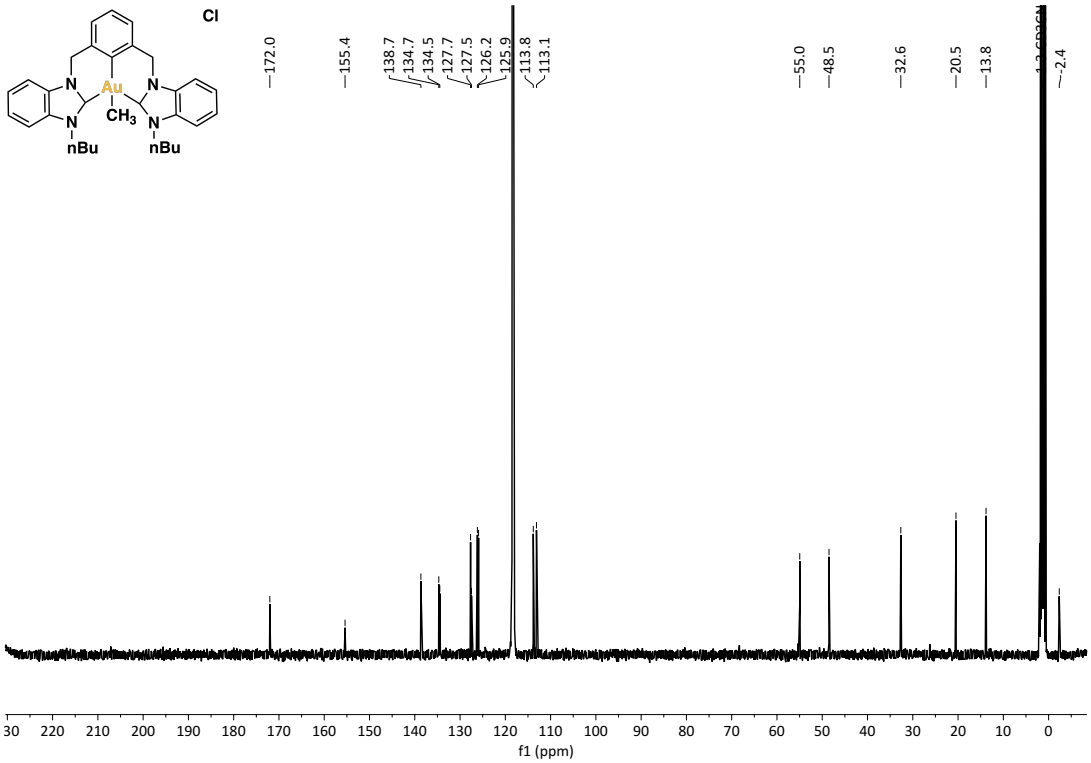

Figure S62. $^{13}C\{^{1}H\}$ NMR (101MHz, 298K) of **8b** in CD_3CN

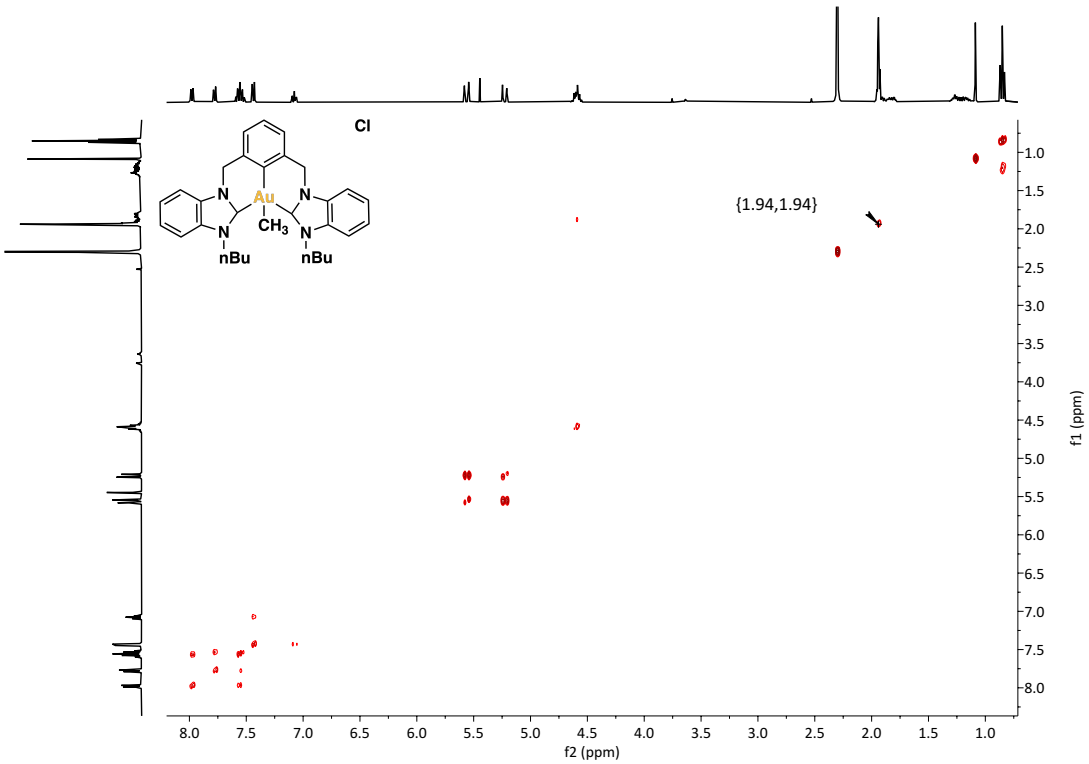

Figure S63. $^{1}H,^{1}H$ COSY NMR (400MHz, 298K) of **8b** in CD_3CN

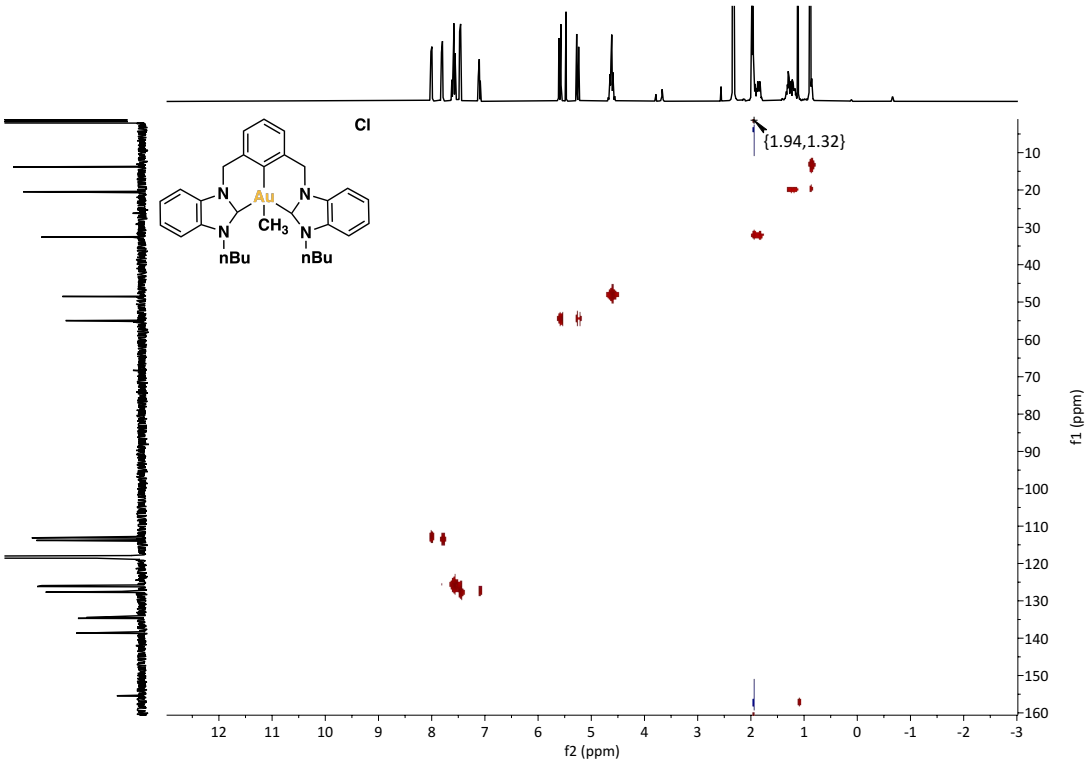

Figure S64. $^{1}H,^{13}C$ HSQC NMR (400MHz, 298K) of **8b** in CD_3CN

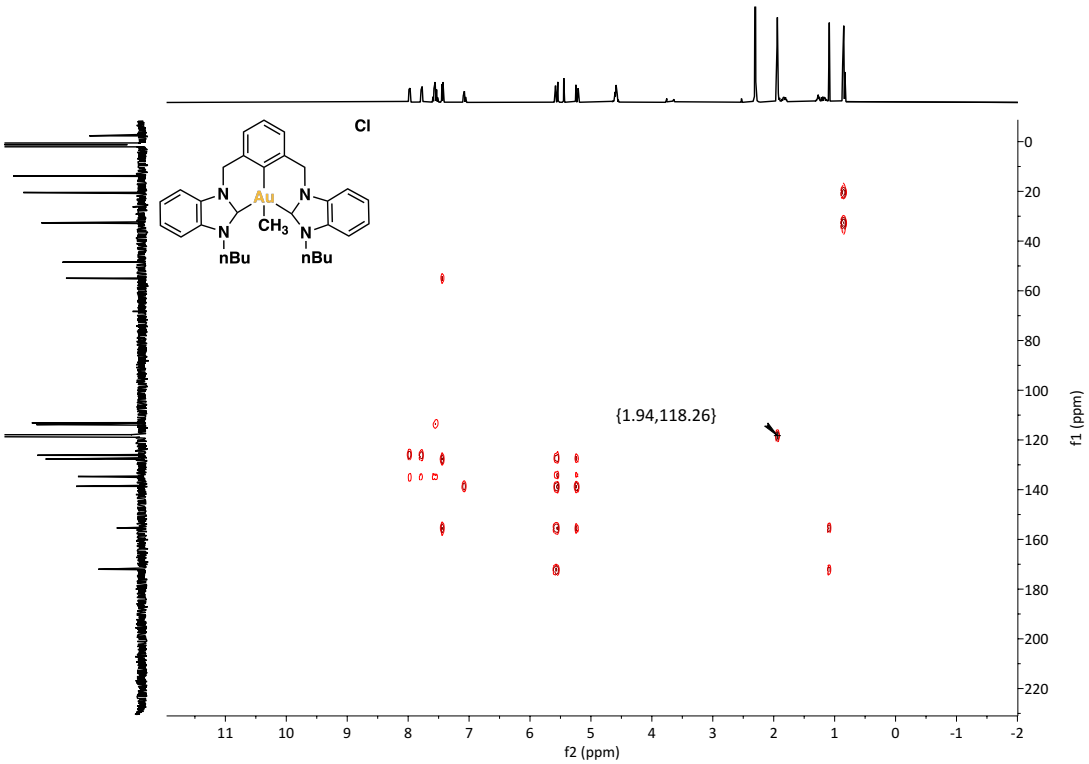

Figure S65. $^{1}H,^{13}C$ HMBC NMR (400MHz, 298K) of **8b** in CD_3CN

7.12 NMR spectra of complex 9a

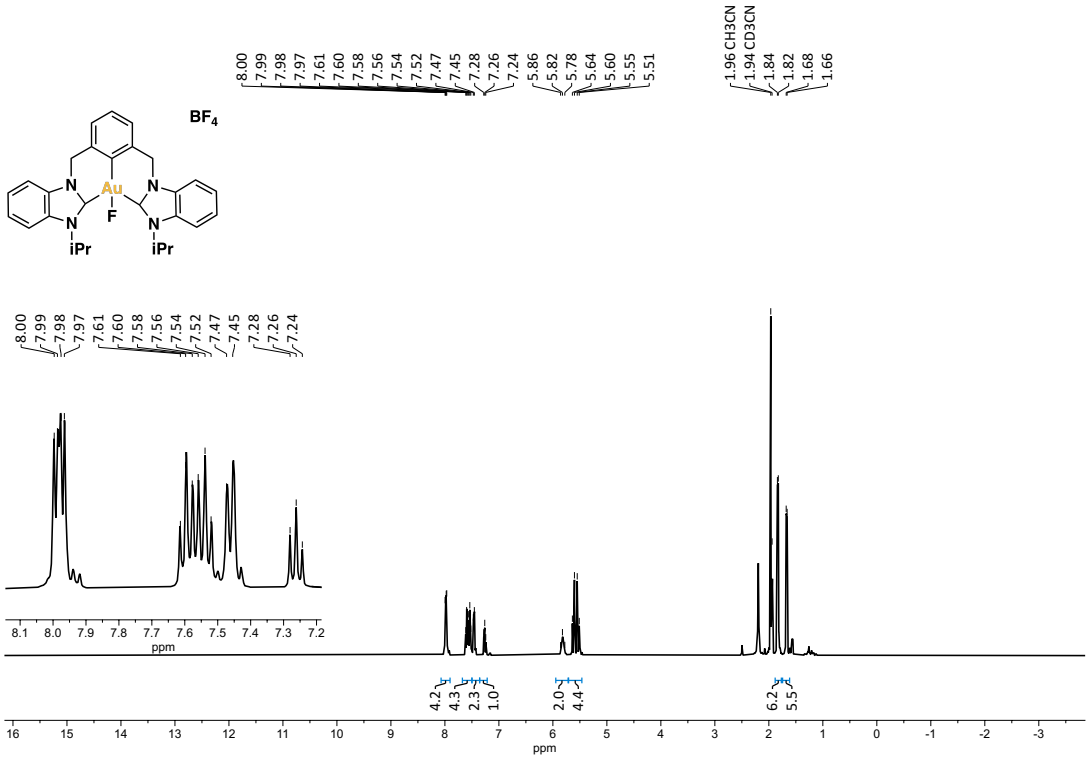

Figure S66. ^{1}H NMR (400MHz, 298K) of **9a** in CD_3CN

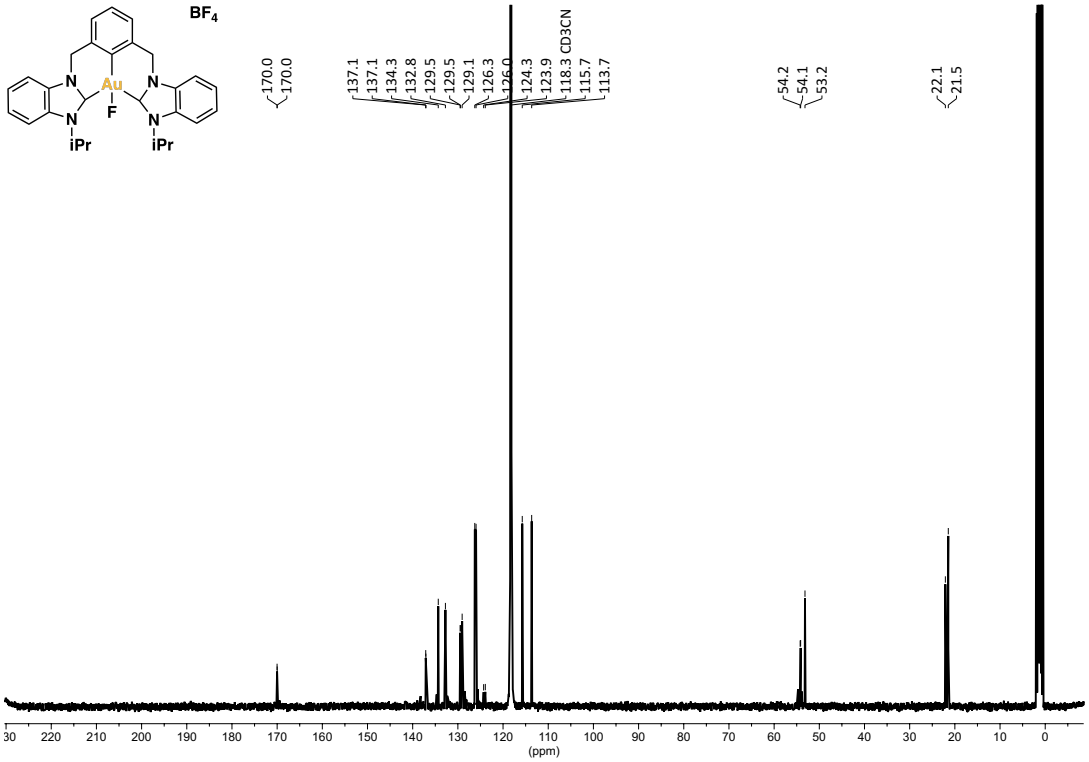

Figure S67. $^{13}C\{^{1}H\}$ NMR (101MHz, 298K) of **9a** in CD_3CN

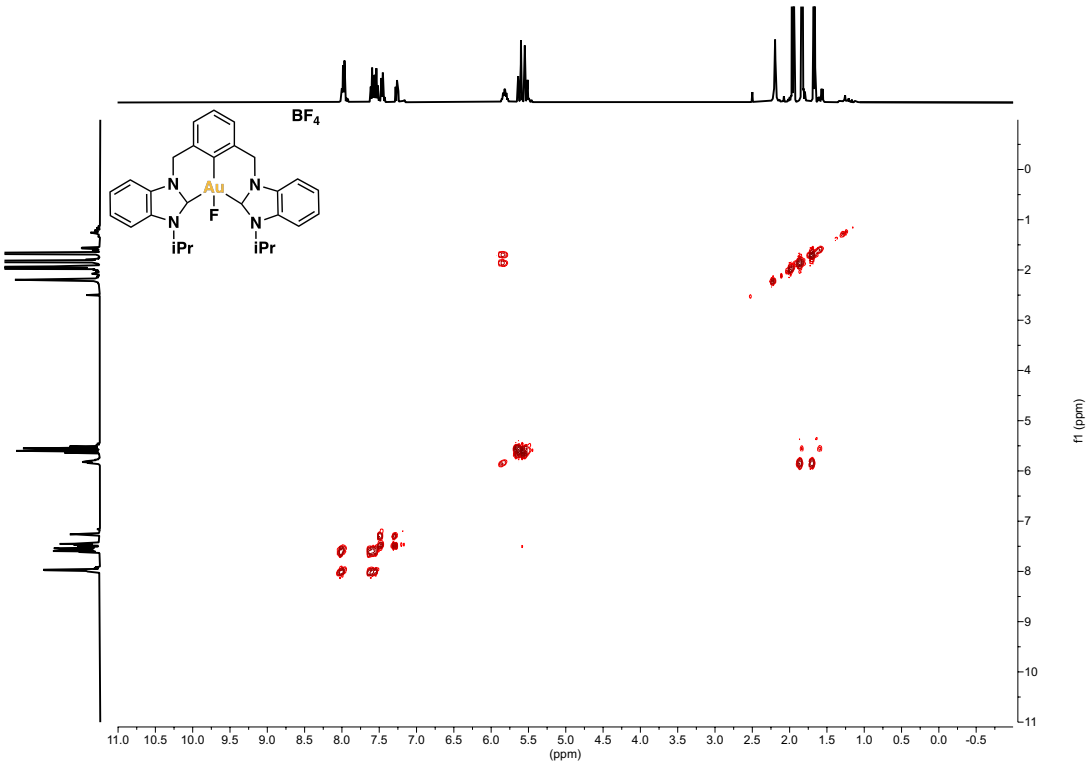

Figure S68. $^{1}H,^{1}H$ COSY NMR (400MHz, 298K) of **9a** in CD_3CN

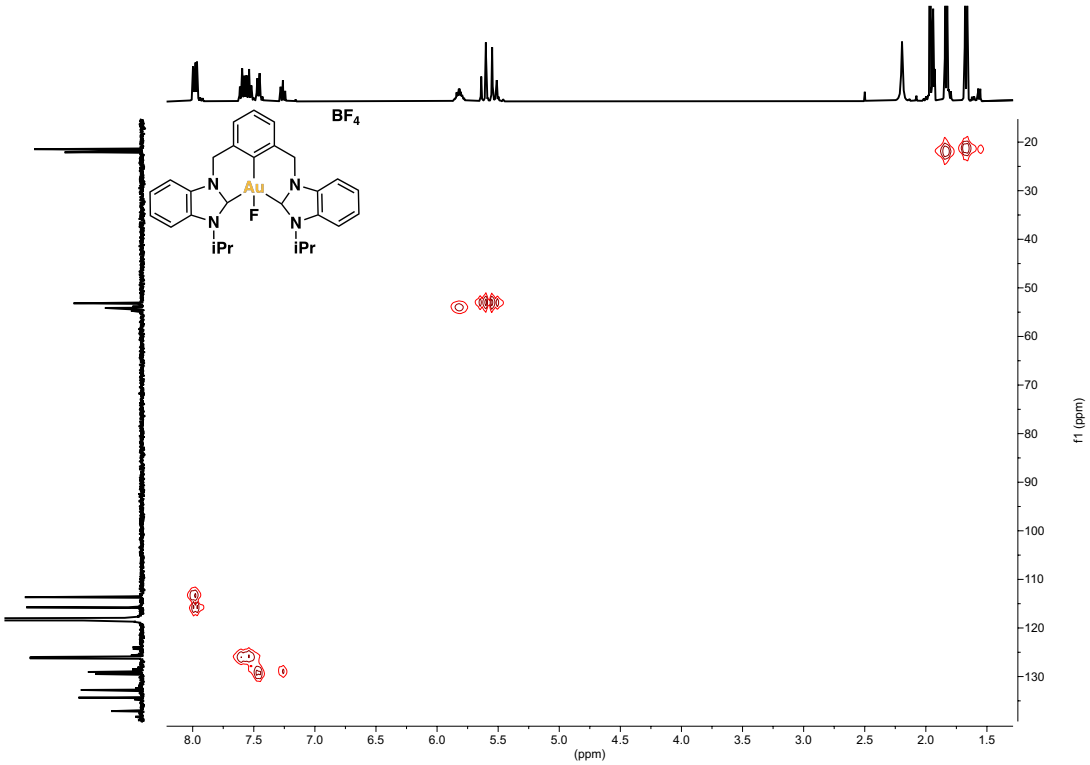

Figure S69. $^{1}H,^{13}C$ HSQC NMR (400MHz, 298K) of **9a** in CD_3CN

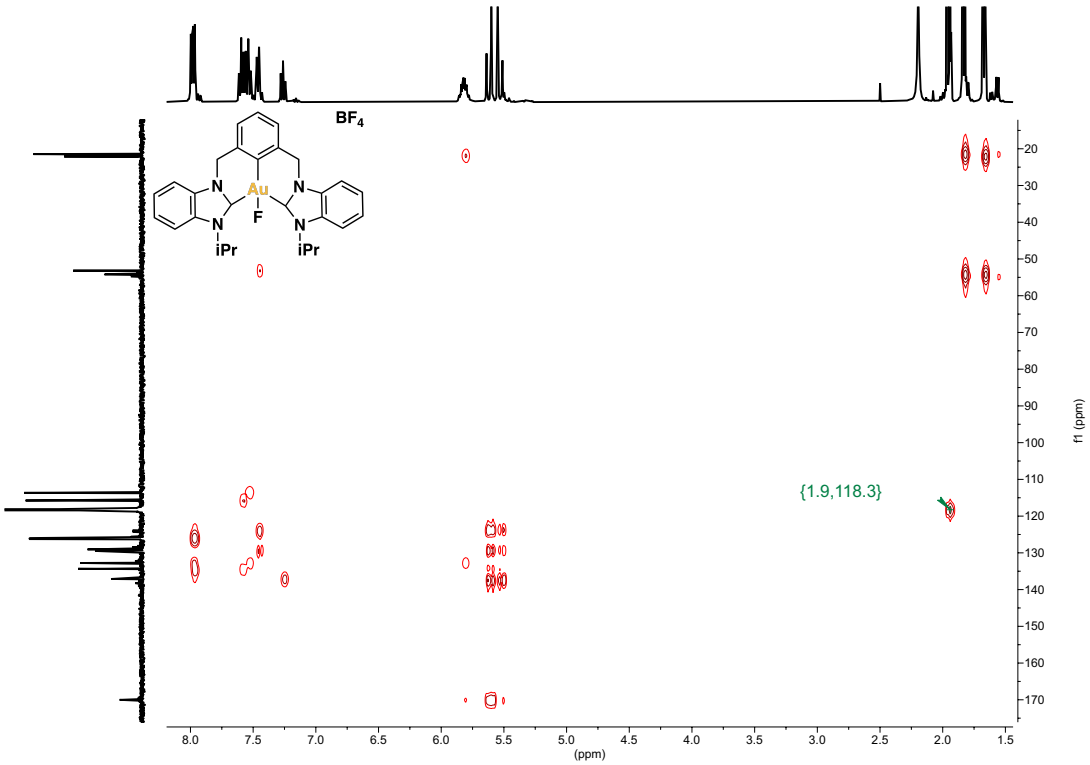

Figure S70. $^{1}H,^{13}C$ HMBC NMR (400MHz, 298K) of **9a** in CD_3CN

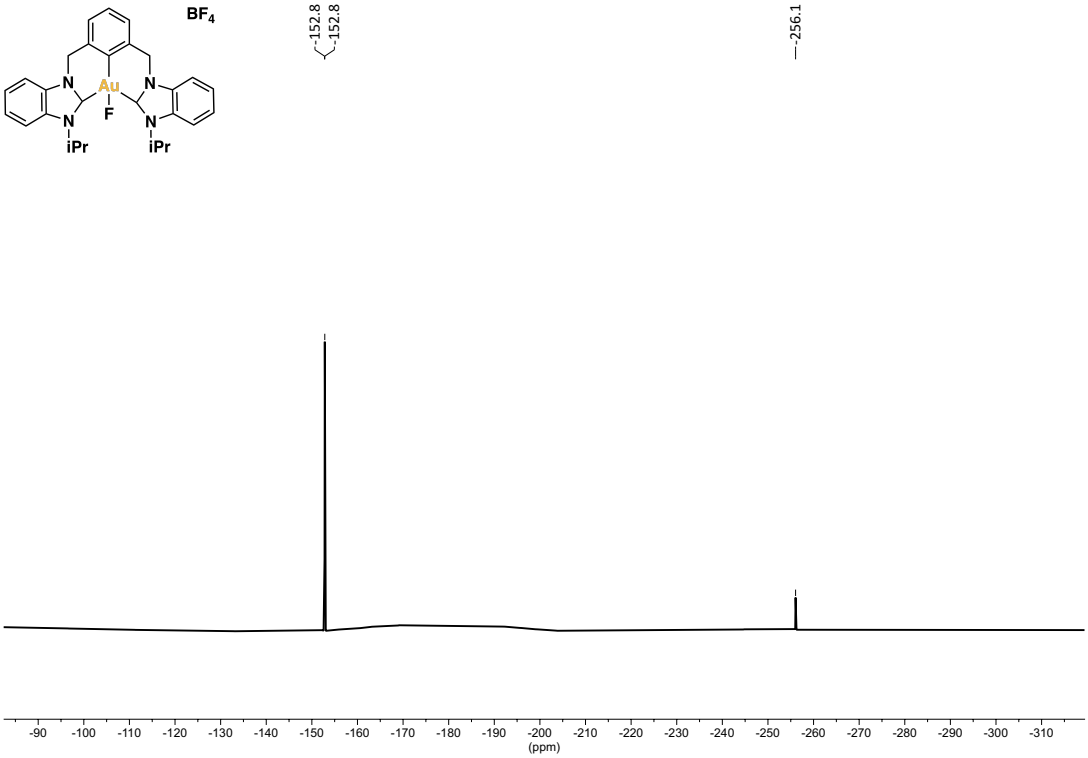

Figure S71. ^{19}F NMR (376MHz, 298K) of **9a** in CD_3CN

7.13 NMR spectra of complex 9b

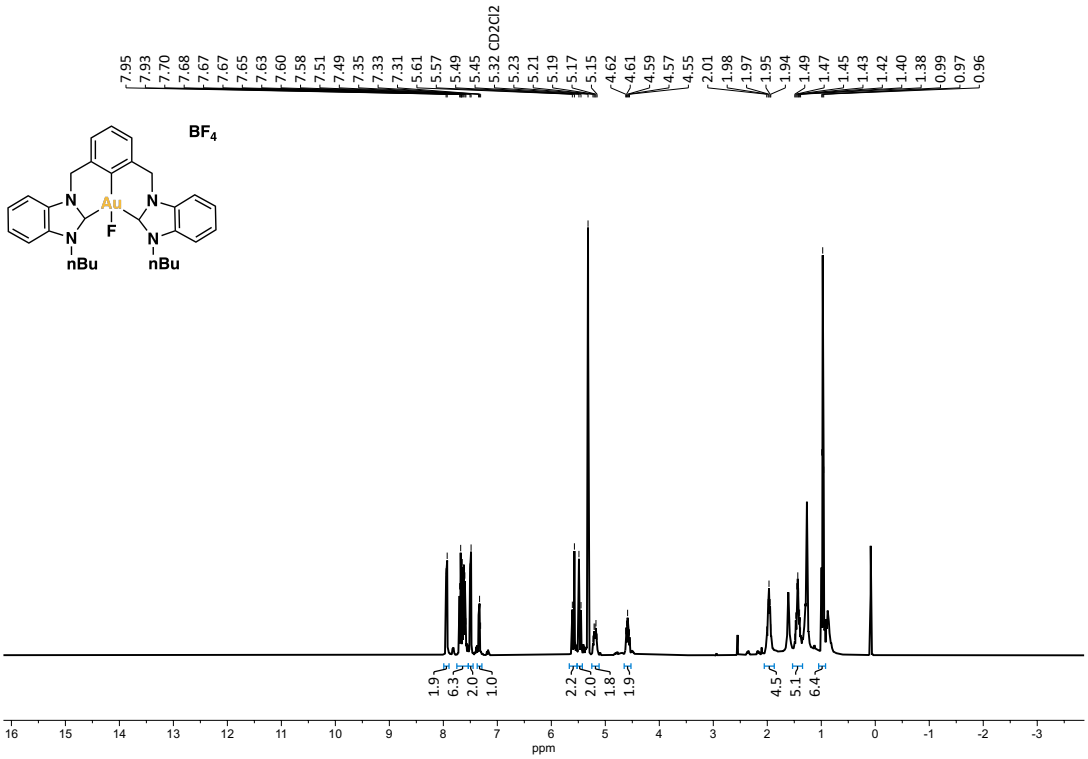

Figure S72. ^{1}H NMR (400MHz, 298K) of **9b** in CD_2Cl_2

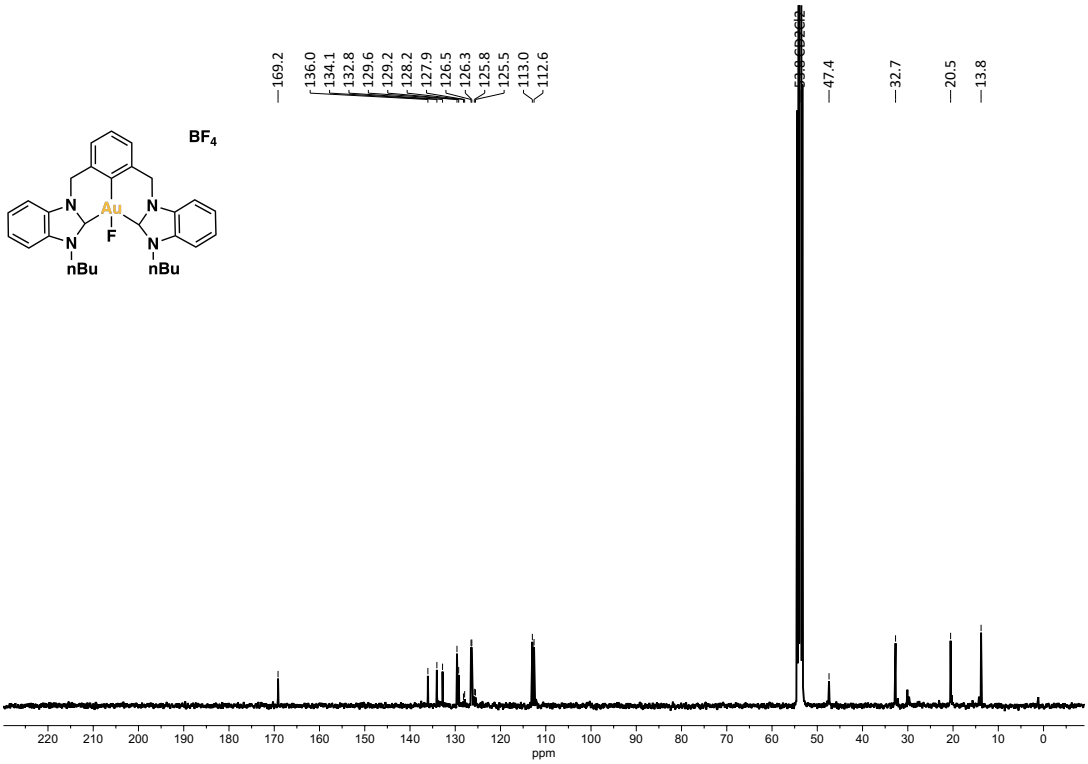

Figure S73. $^{13}C\{^{1}H\}$ NMR (101MHz, 298K) of **9b** in CD_2Cl_2

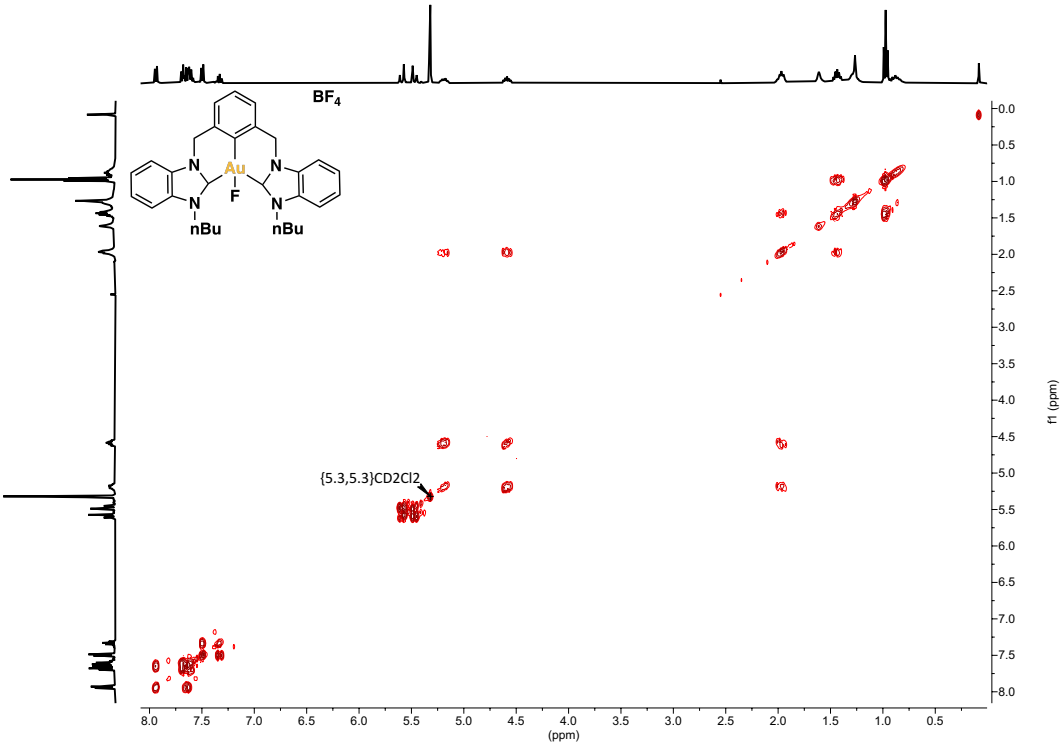

Figure S74. $^{1}H,^{1}H$ COSY NMR (400MHz, 298K) of **9b** in CD_2Cl_2

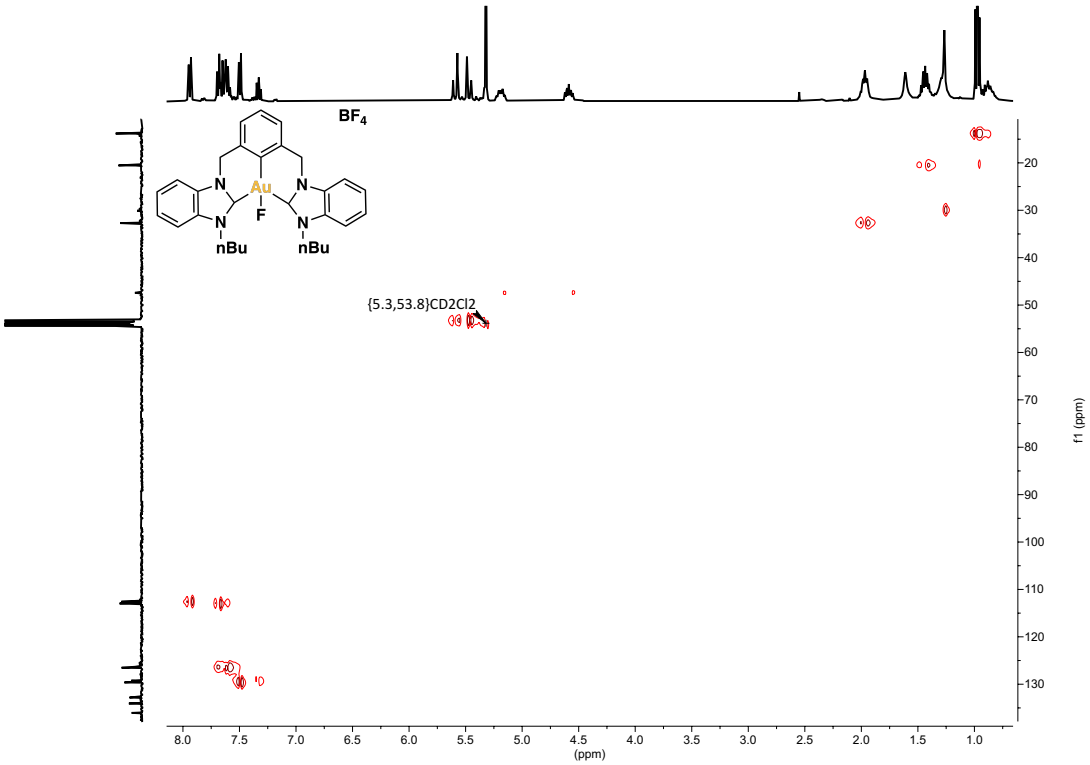

Figure S75. $^{1}H,^{13}C$ HSQC NMR (400MHz, 298K) of **9b** in CD_2Cl_2

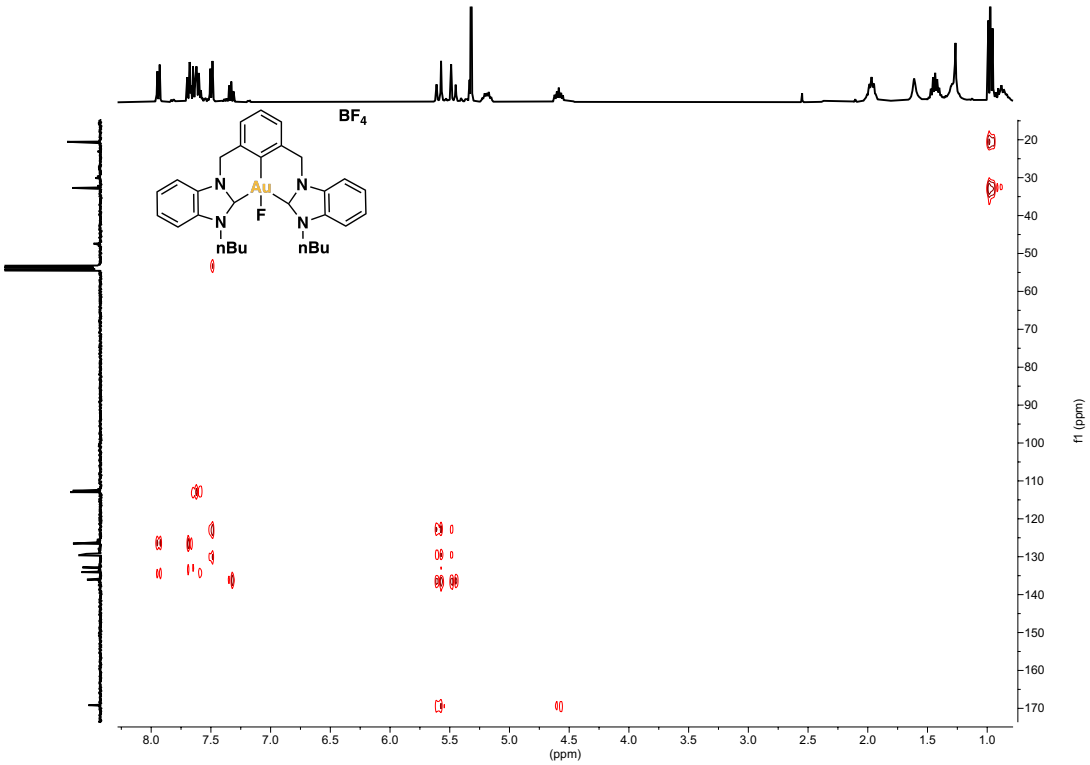

Figure S76. $^{1}H,^{13}C$ HMBC NMR (400MHz, 298K) of **9b** in CD_2Cl_2

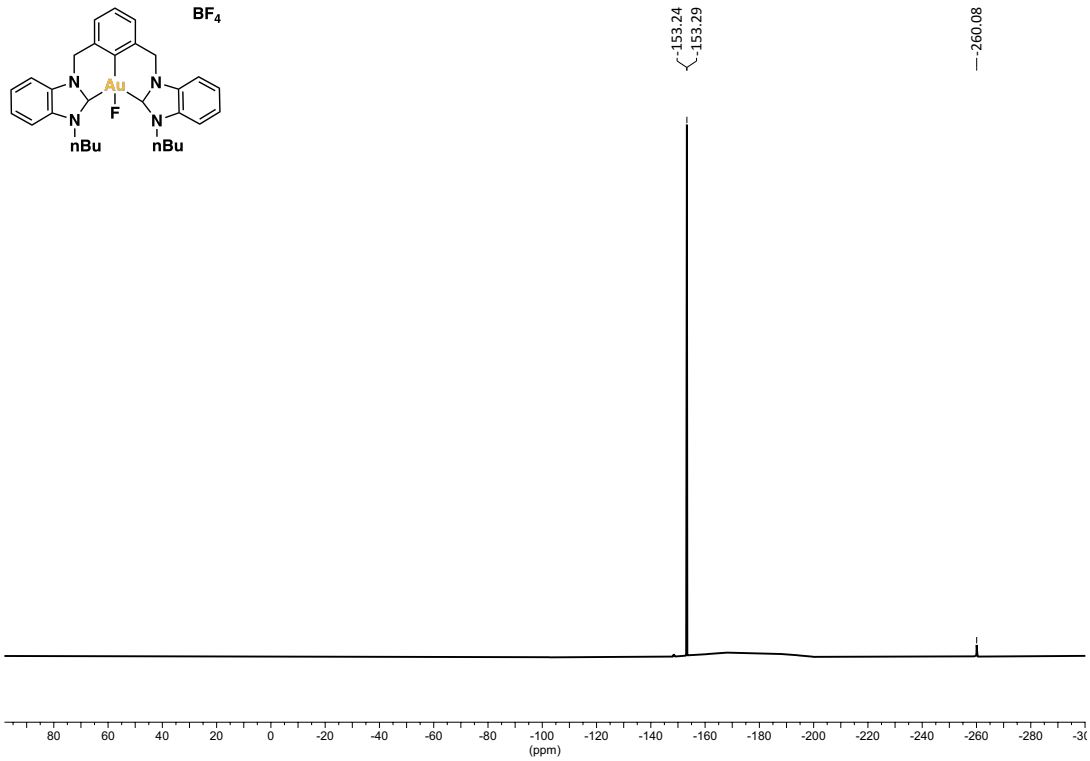

Figure S77. ^{19}F NMR (376MHz, 298K) of **9b** in CD_2Cl_2

7.14 NMR spectra of complex 10a

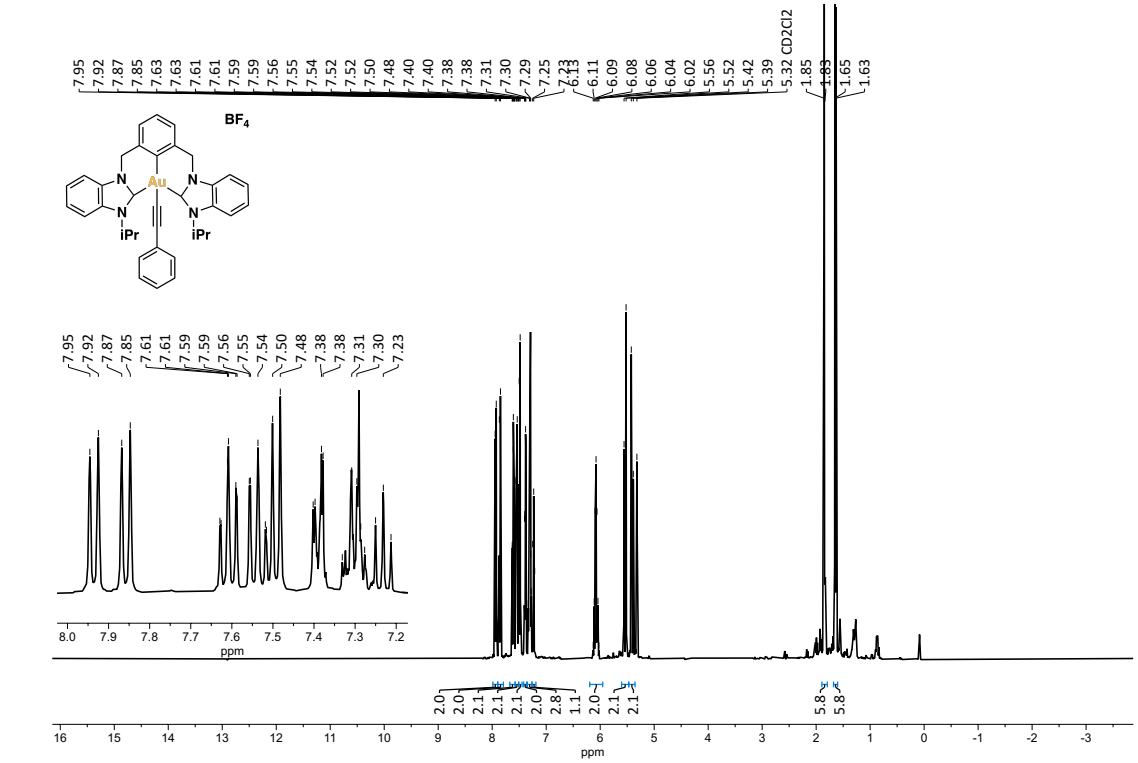

Figure S78. ^{1}H NMR (400MHz, 298K) of **10a** in CD_2Cl_2

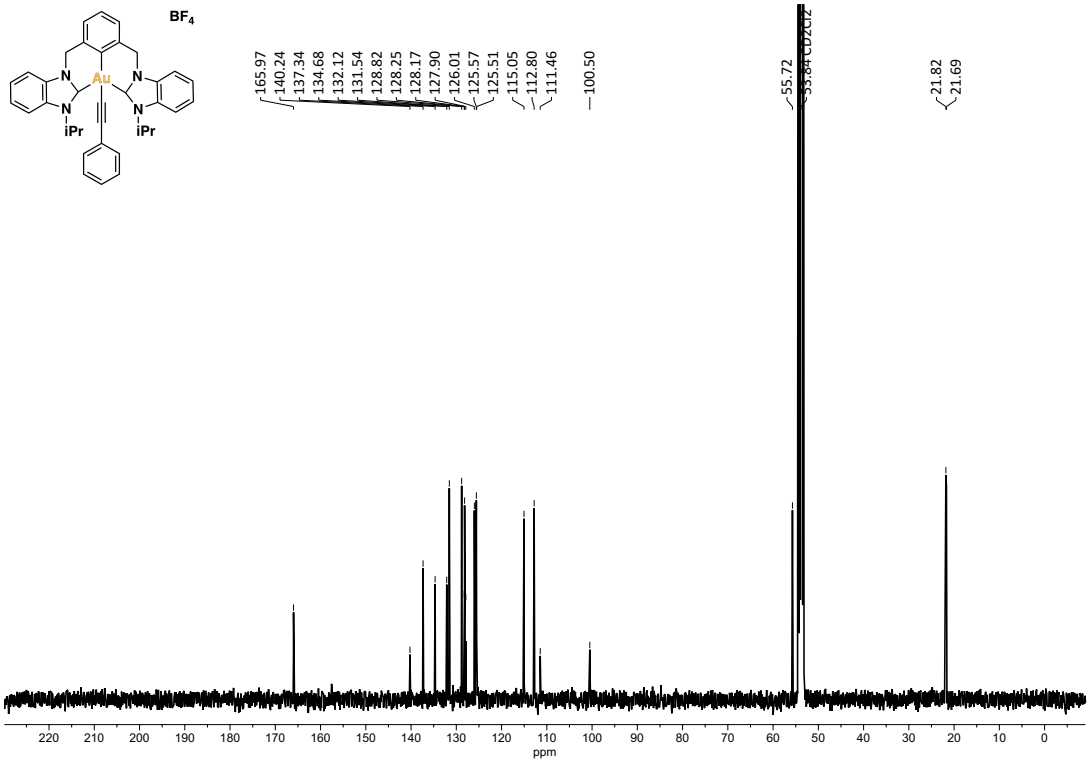

Figure S79. $^{13}C\{^{1}H\}$ NMR (101MHz, 298K) of **10a** in CD_2Cl_2

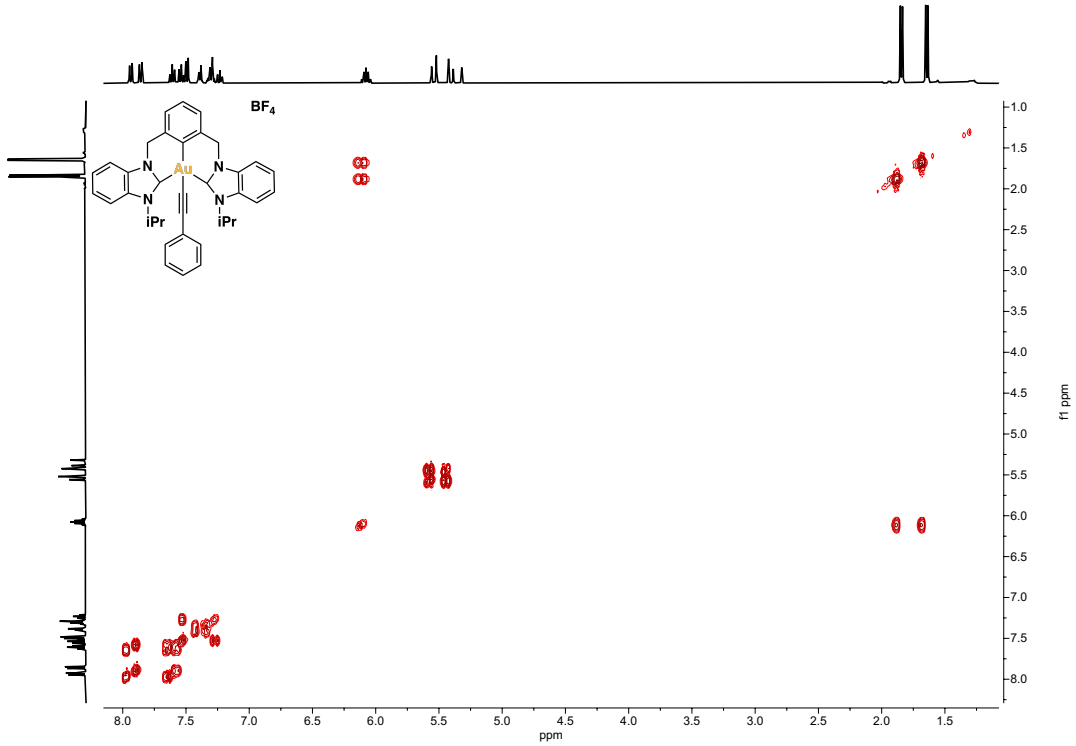

Figure S80. $^{1}H,^{1}H$ COSY NMR (400MHz, 298K) of **10a** in CD_2Cl_2

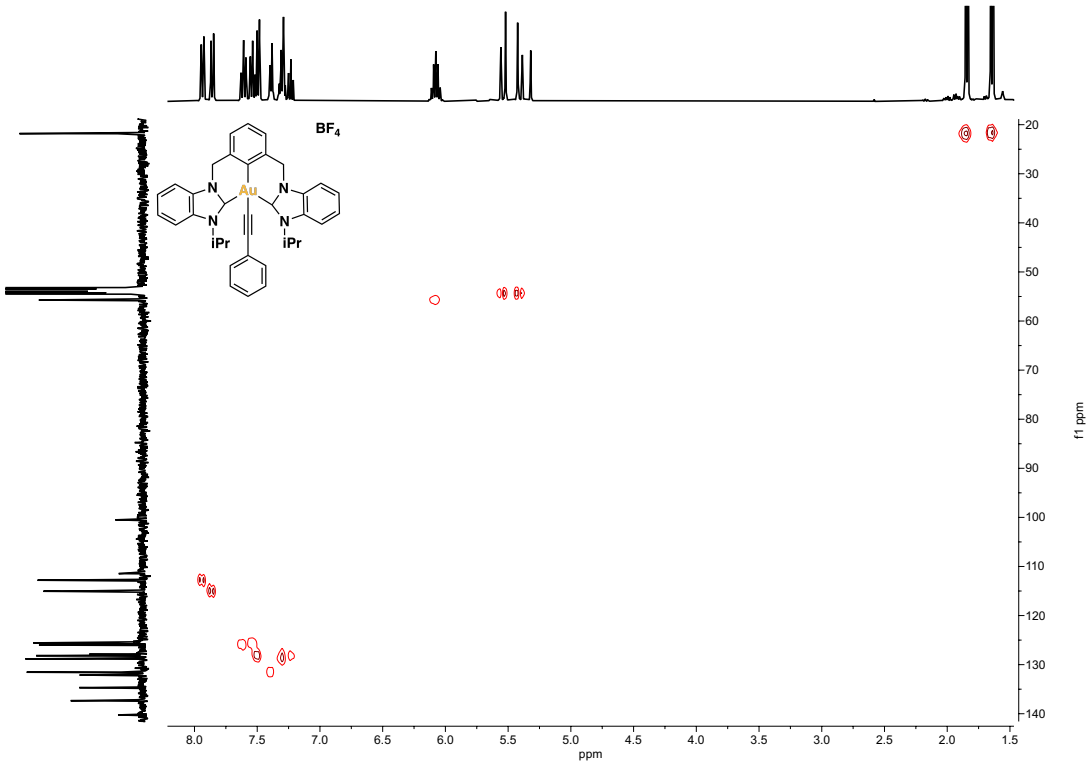

Figure S81. $^{1}H,^{13}C$ HSQC NMR (400MHz, 298K) of **10a** in CD_2Cl_2

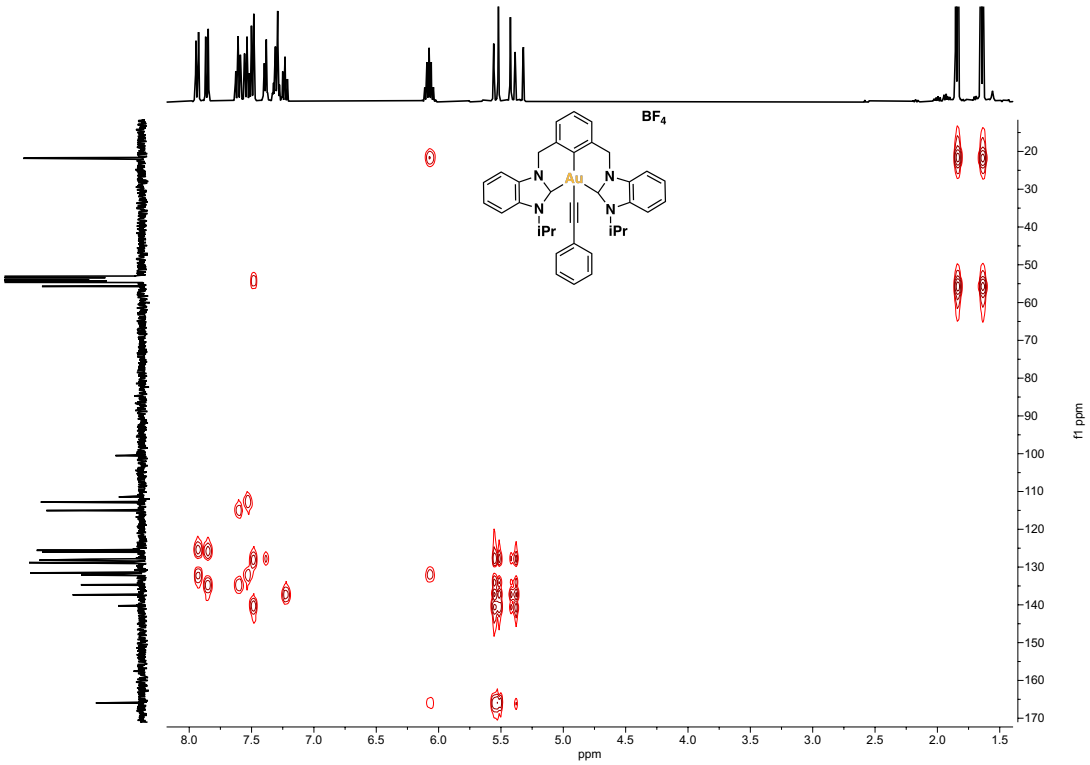

Figure S82. $^{1}H,^{13}C$ HMBC NMR (400MHz, 298K) of **10a** in CD_2Cl_2

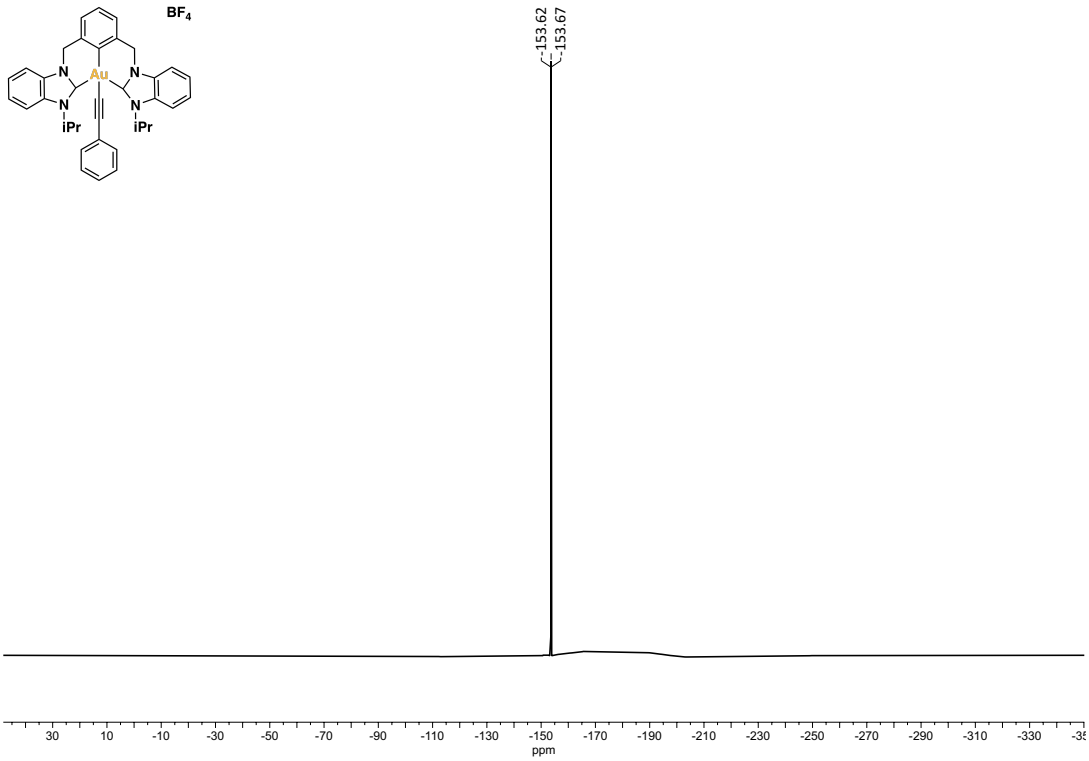

Figure S83. ^{19}F NMR (376MHz, 298K) of **10a** in CD_2Cl_2

7.15 NMR spectra of complex 10b

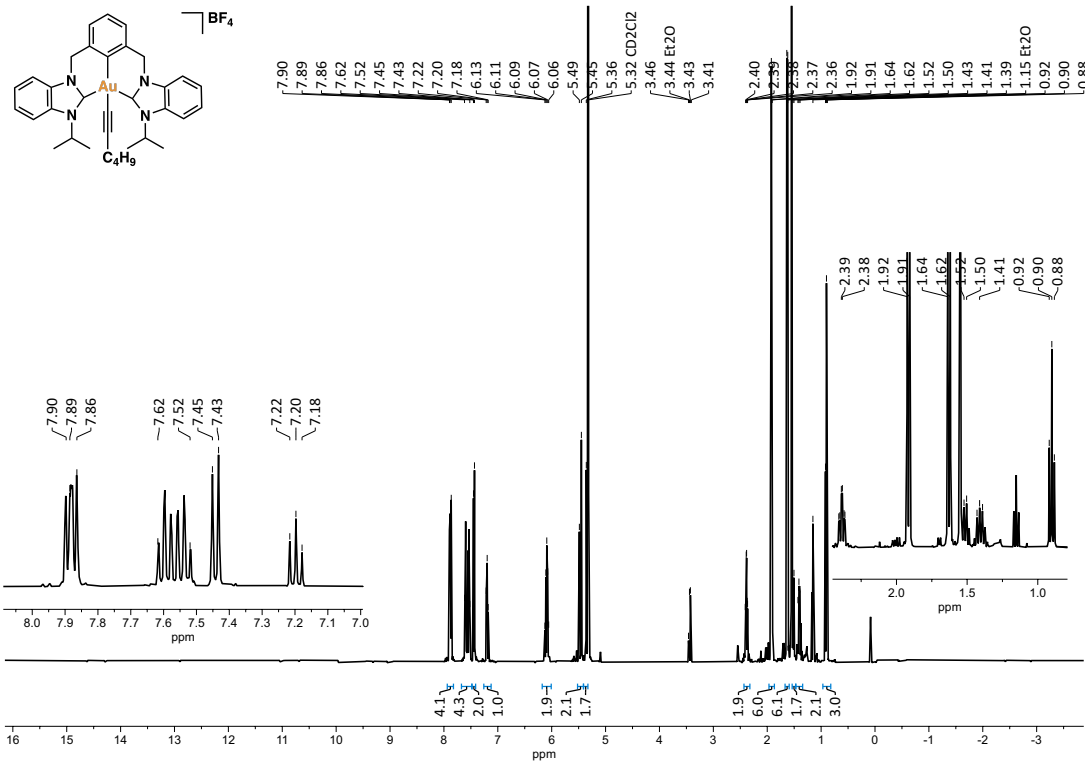

Figure S84. ^{1}H NMR (400MHz, 298K) of **10b** in CD_2Cl_2

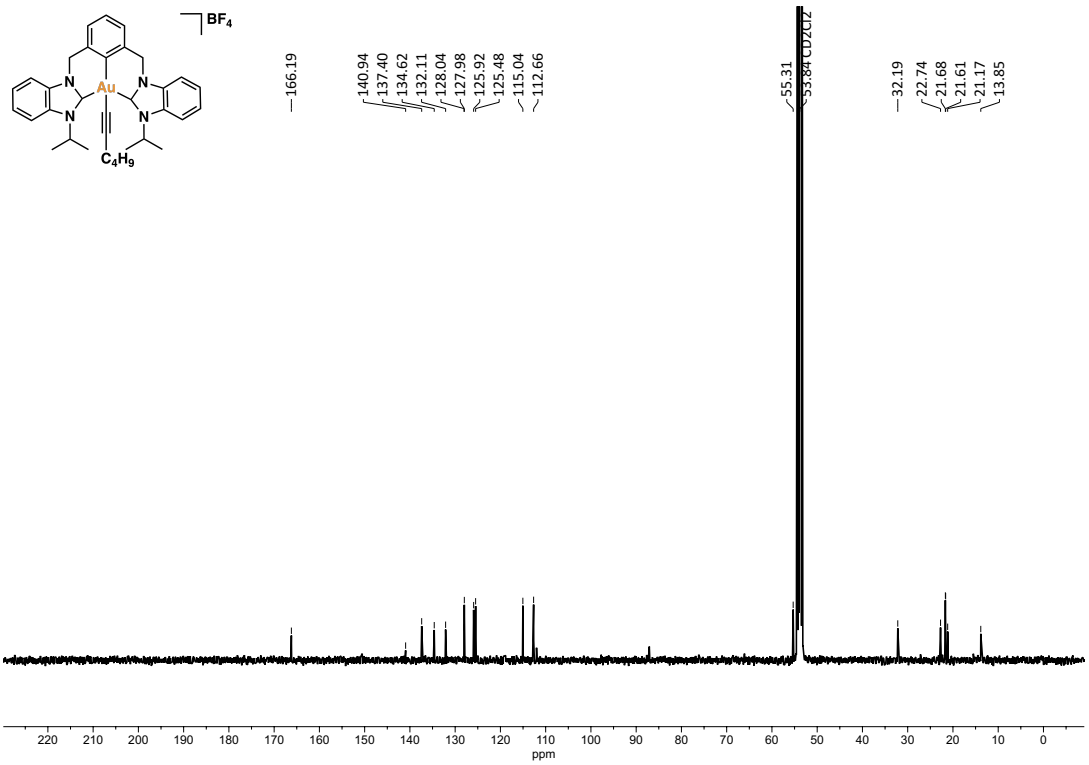

Figure S85. $^{13}C\{^{1}H\}$ NMR (101MHz, 298K) of **10b** in CD_2Cl_2

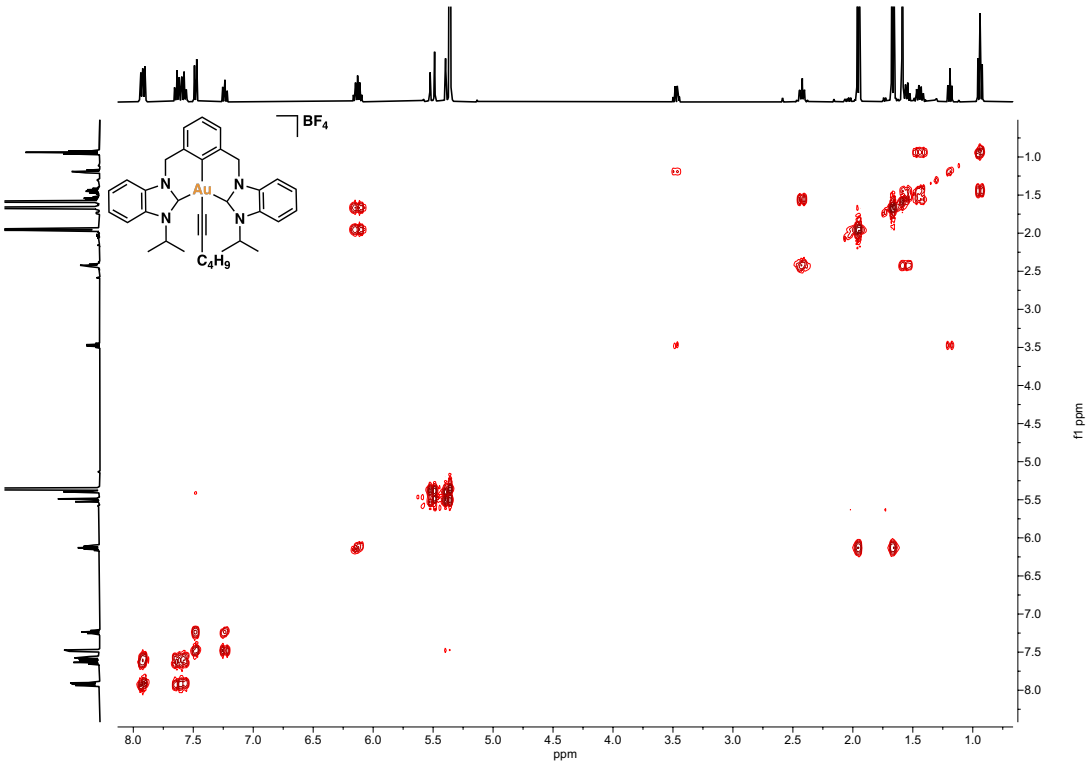

Figure S86. $^{1}H,^{1}H$ COSY NMR (400MHz, 298K) of **10b** in CD_2Cl_2

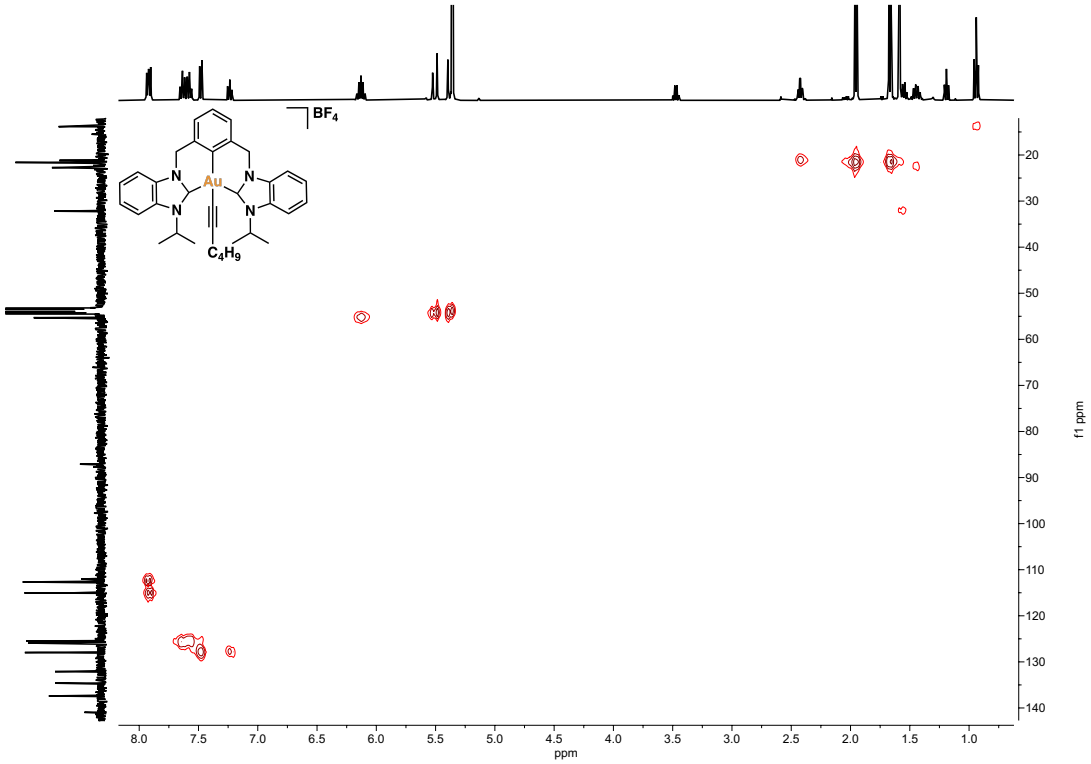

Figure S87. $^{1}H,^{13}C$ HSQC NMR (400MHz, 298K) of **10b** in CD_2Cl_2

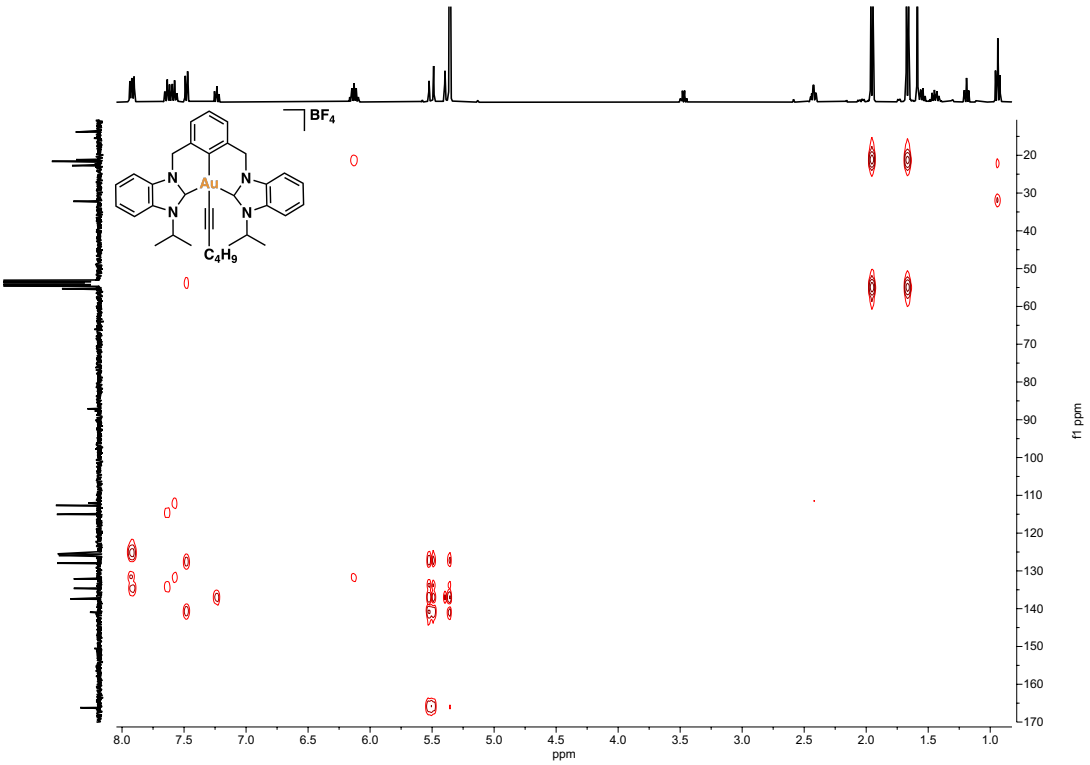

Figure S88. $^{1}H,^{13}C$ HMBC NMR (400MHz, 298K) of **10b** in CD_2Cl_2

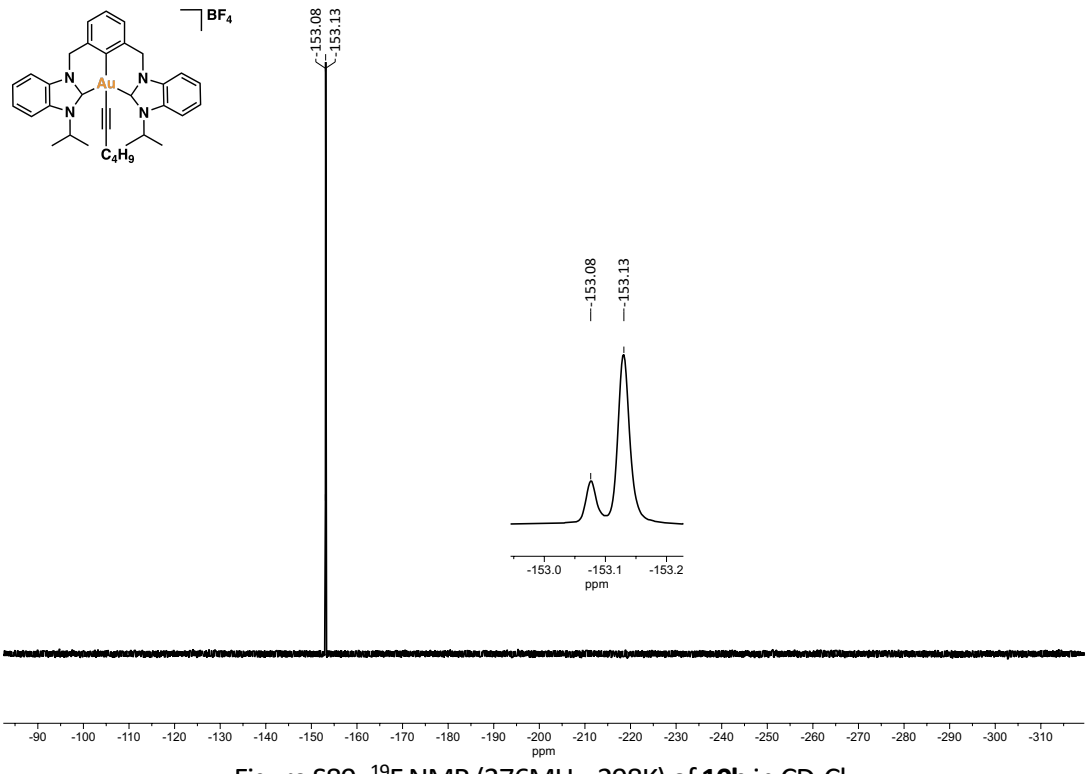

Figure S89. ^{19}F NMR (376MHz, 298K) of **10b** in CD_2Cl_2

7.16 NMR spectra of complex 11a

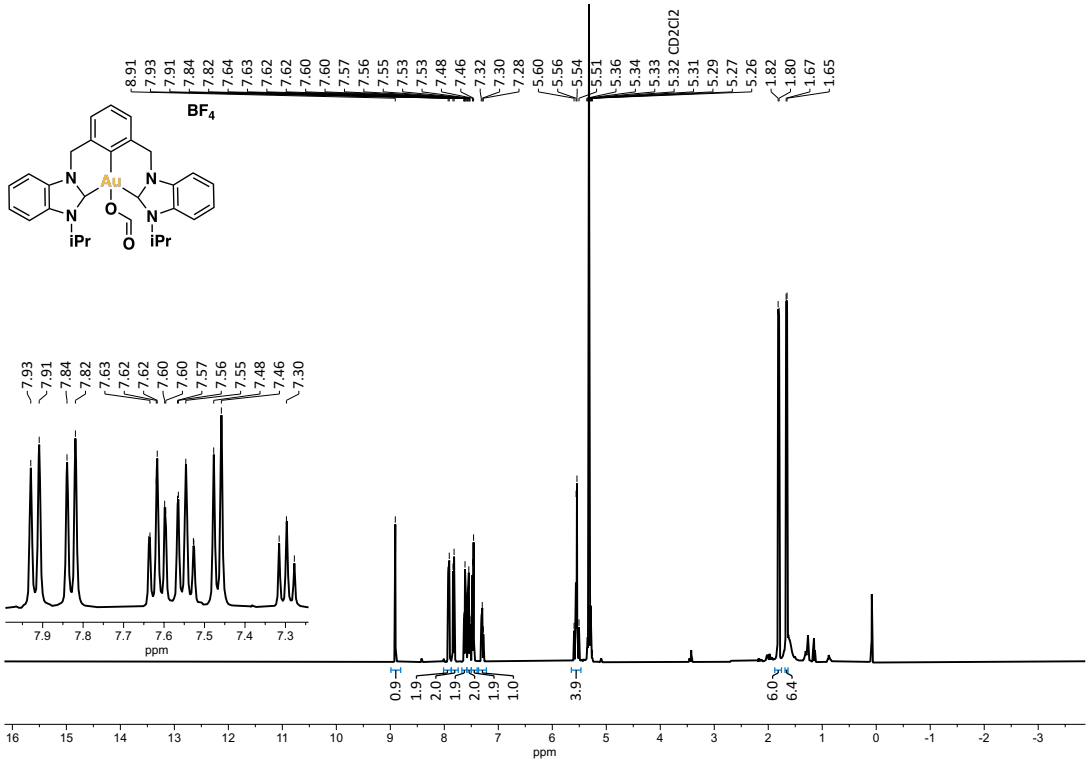

Figure S90. ^{1}H NMR (400MHz, 298K) of **11a** in CD_2Cl_2

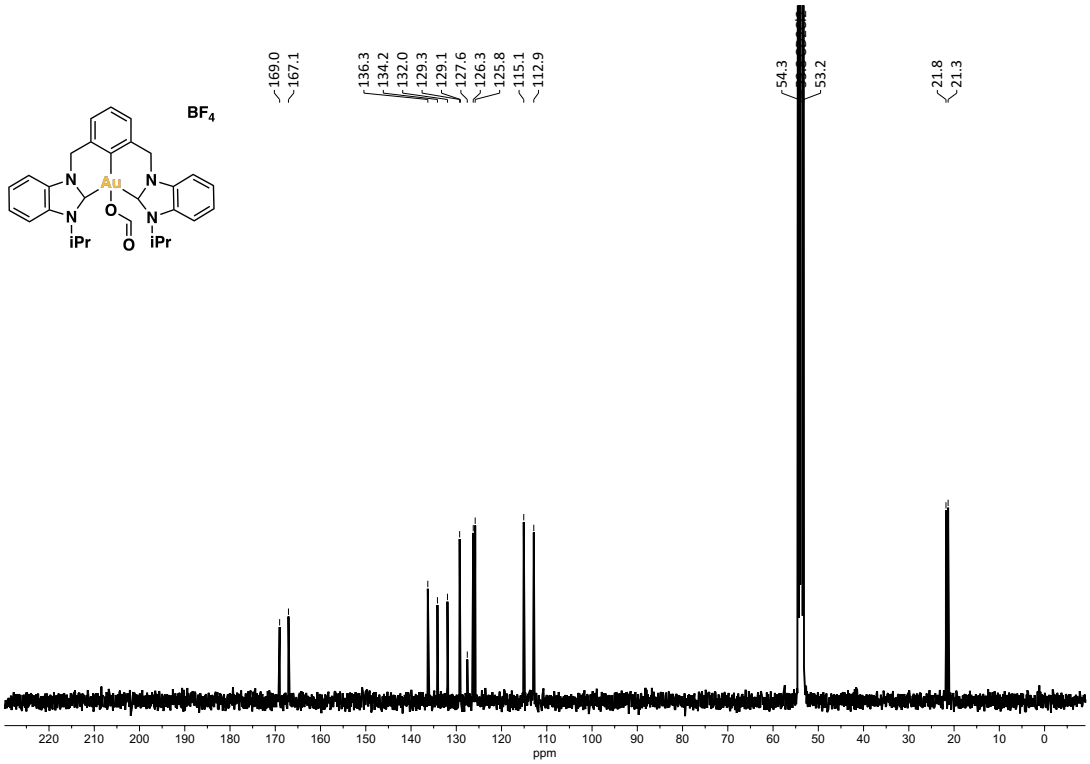

Figure S91. $^{13}C\{^{1}H\}$ NMR (101MHz, 298K) of **11a** in CD_2Cl_2

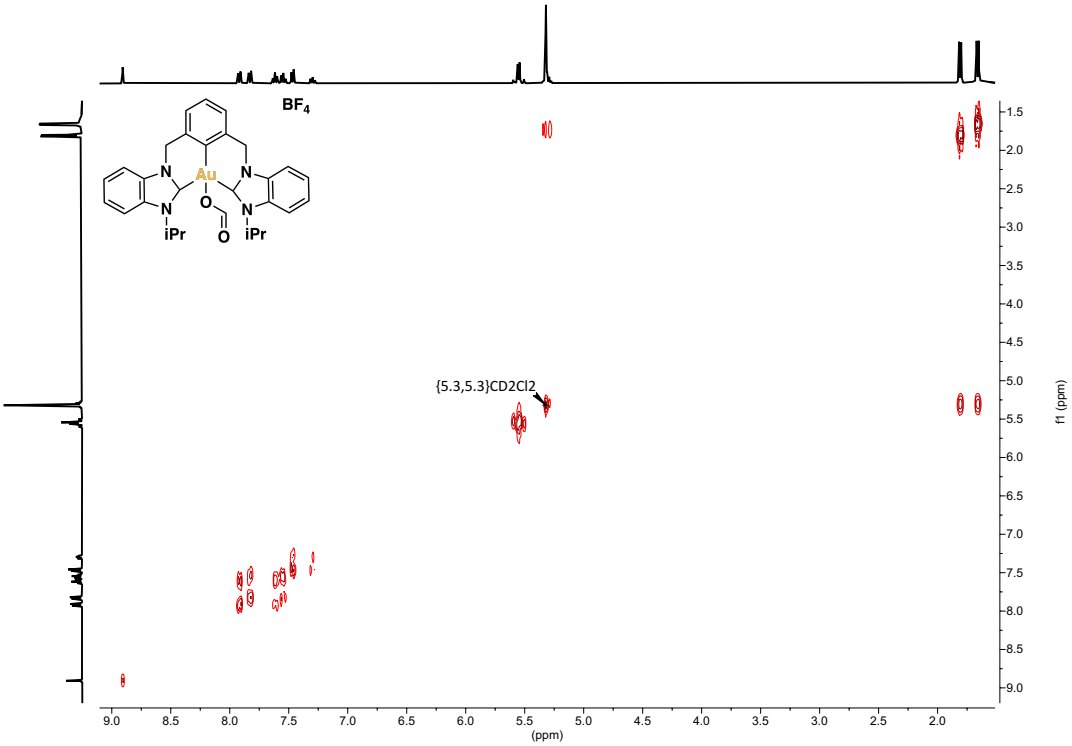

Figure S92. $^{1}H,^{1}H$ COSY NMR (400MHz, 298K) of **11a** in CD_2Cl_2

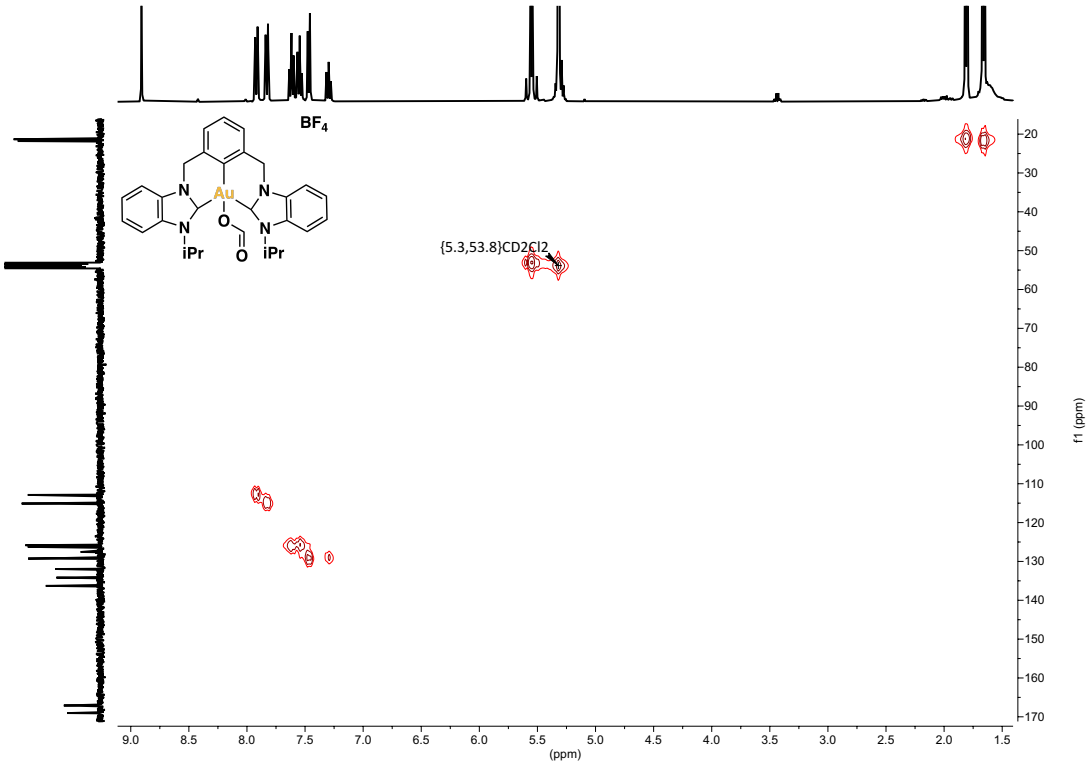

Figure S93. $^{1}H,^{13}C$ HSQC NMR (400MHz, 298K) of **11a** in CD_2Cl_2

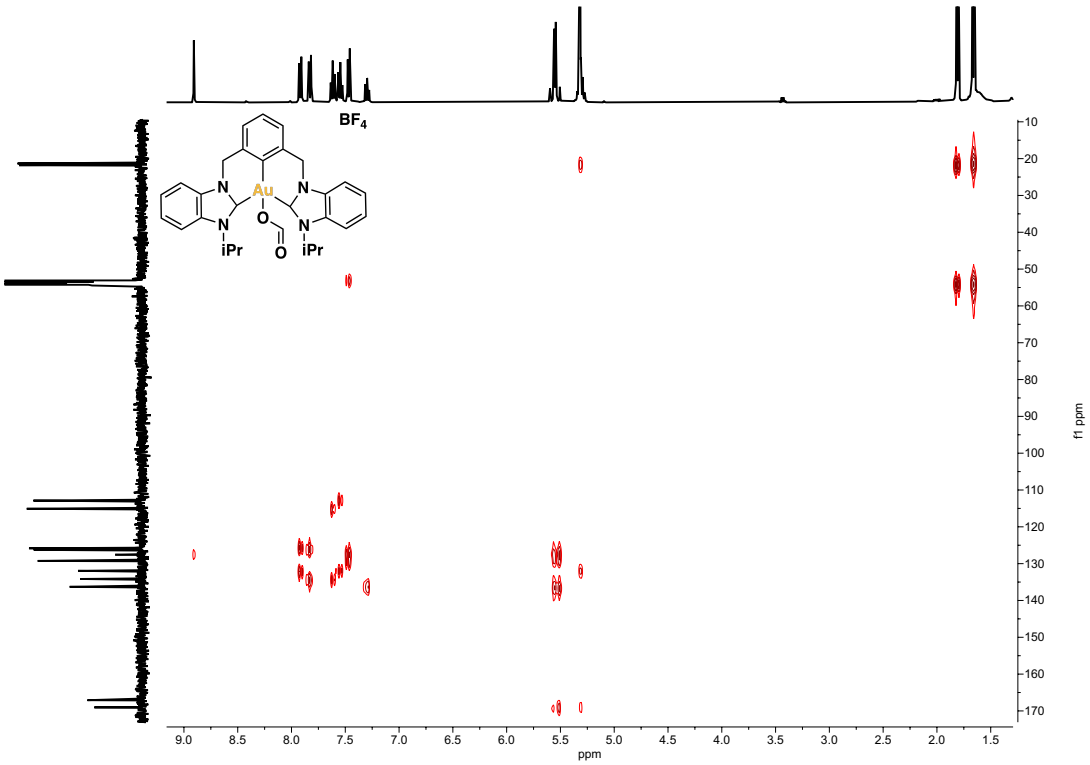

Figure S94. $^{1}H,^{13}C$ HMBC NMR (400MHz, 298K) of **11a** in CD_2Cl_2

7.17 NMR spectra of complex 12a

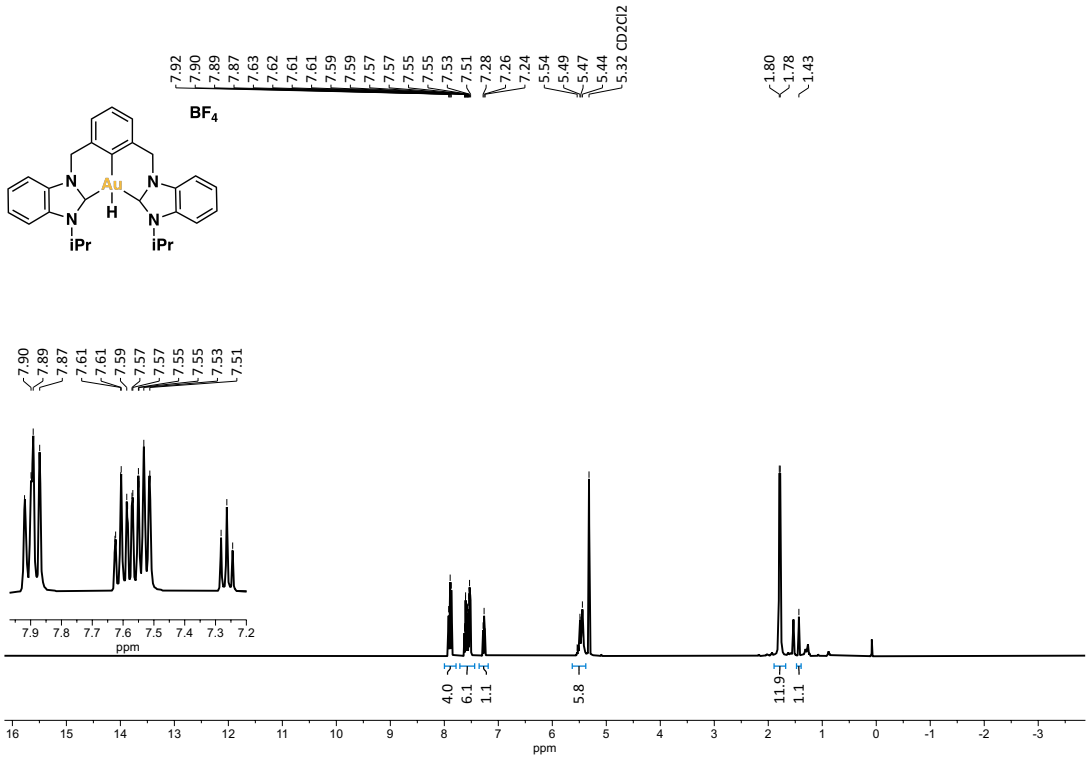

Figure S95. ^{1}H NMR (400MHz, 298K) of **12a** in CD_2Cl_2

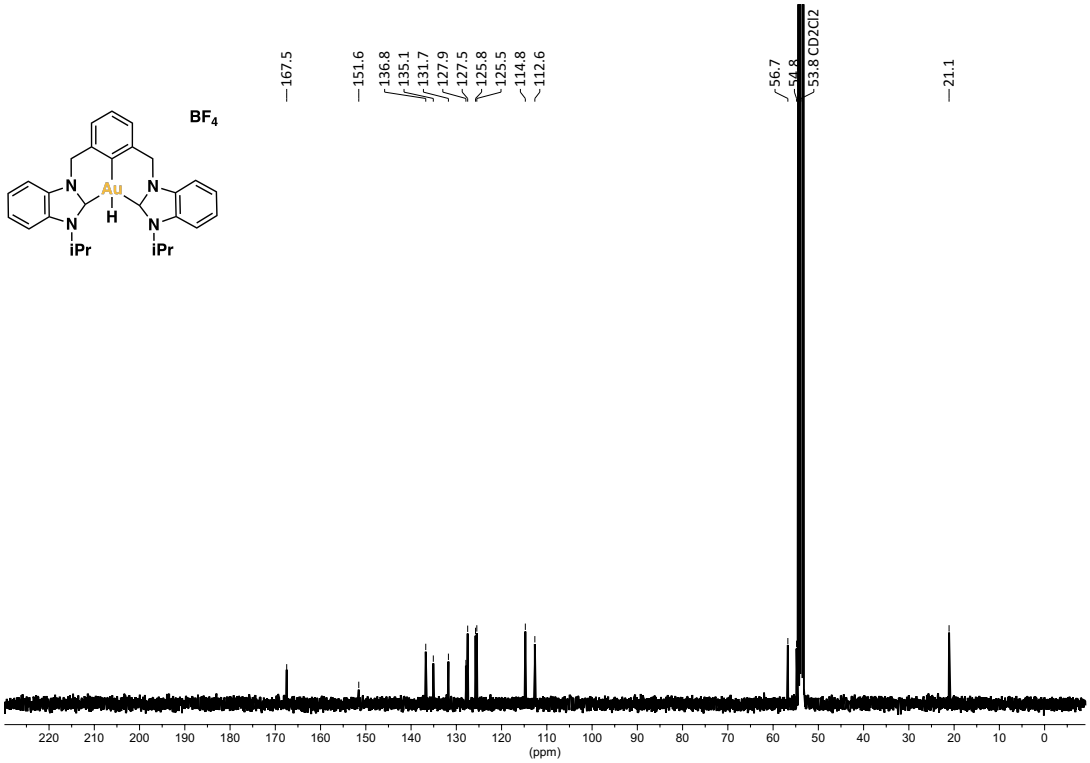

Figure S96. $^{13}C\{^{1}H\}$ NMR (101MHz, 298K) of **12a** in CD_2Cl_2

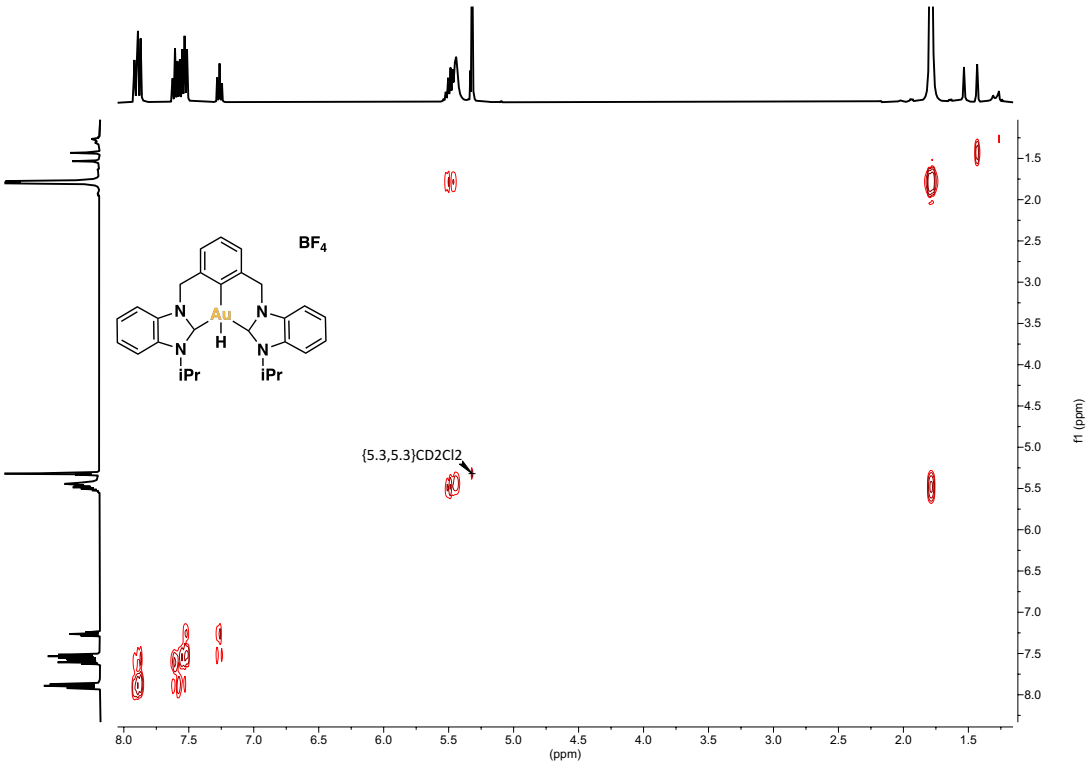

Figure S97. $^{1}H,^{1}H$ COSY NMR (400MHz, 298K) of **12a** in CD_2Cl_2

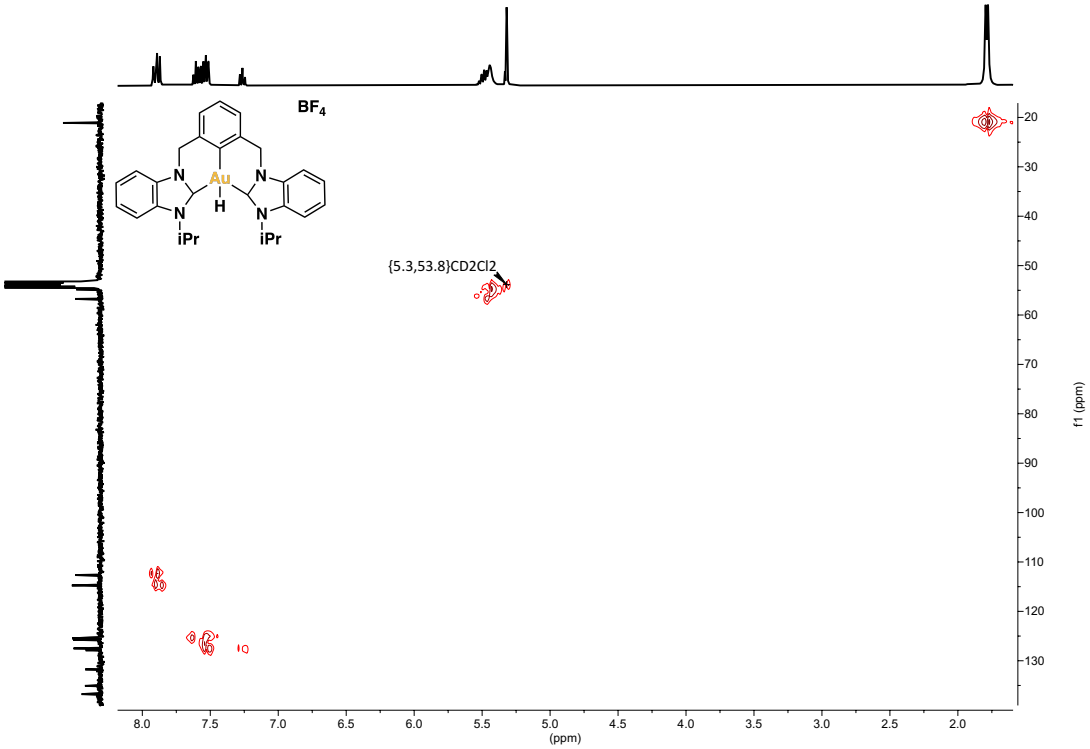

Figure S98. $^{1}H,^{13}C$ HSQC NMR (400MHz, 298K) of **12a** in CD_2Cl_2

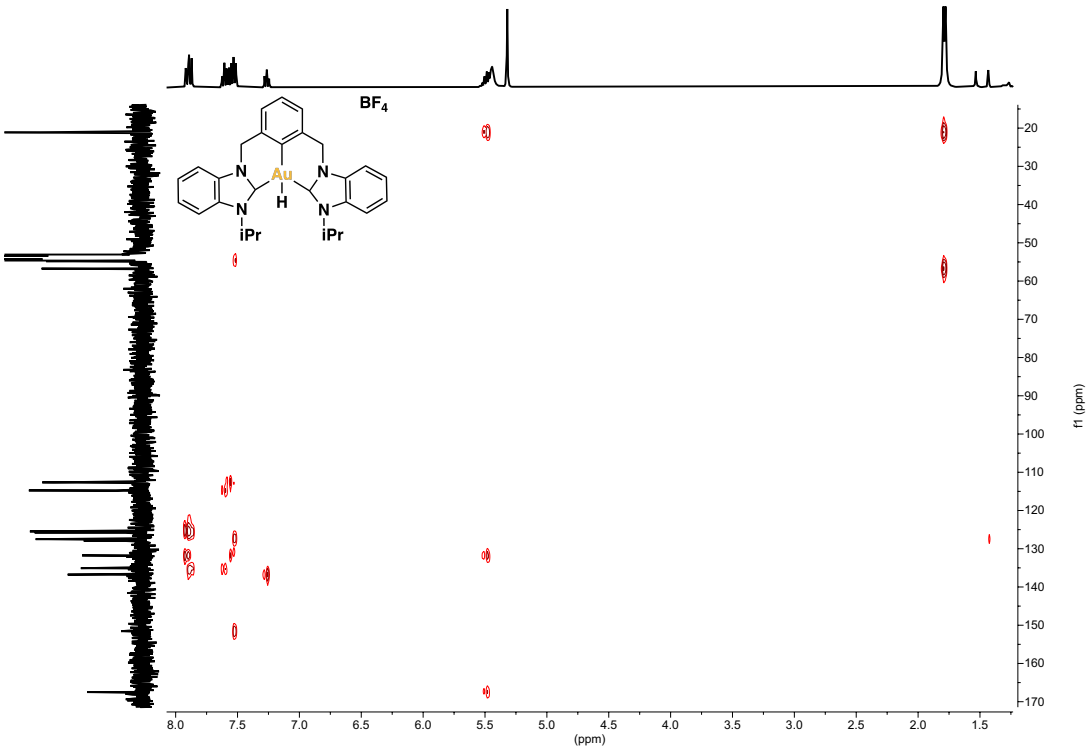

Figure S99. $^{1}H,^{13}C$ HMBC NMR (400MHz, 298K) of **12a** in CD_2Cl_2

7.18 NMR spectra of complex 13a

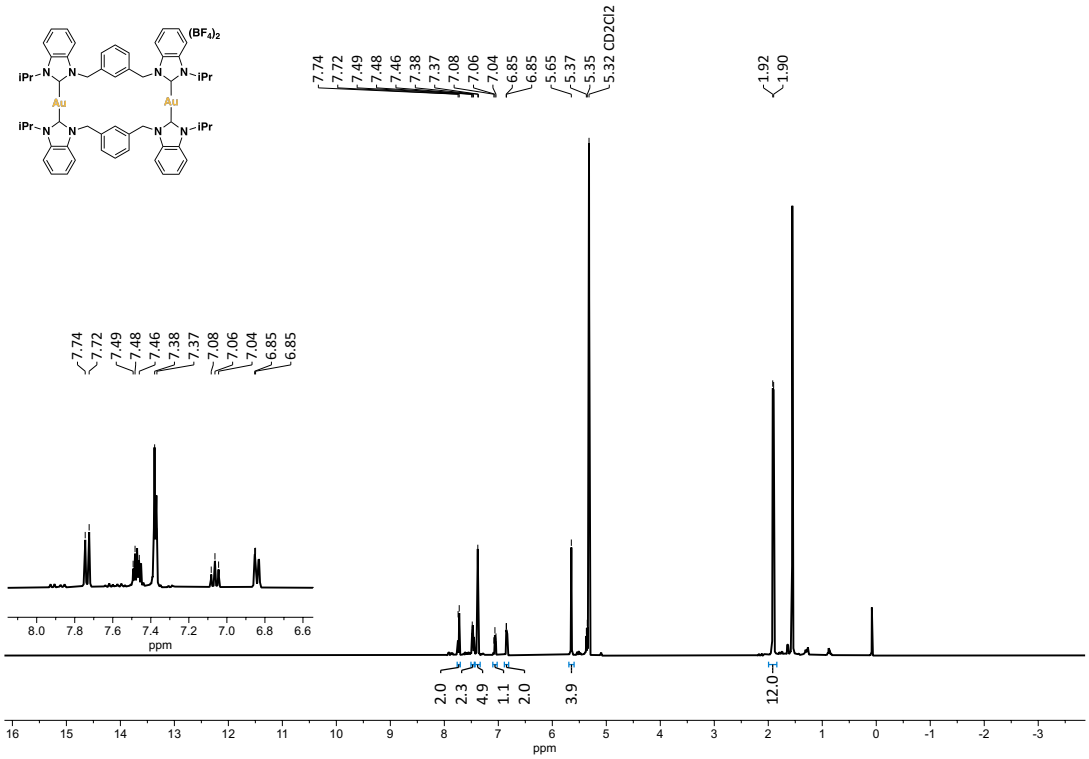

Figure S100. ^{1}H NMR (400MHz, 298K) of **13a** in CD_2Cl_2

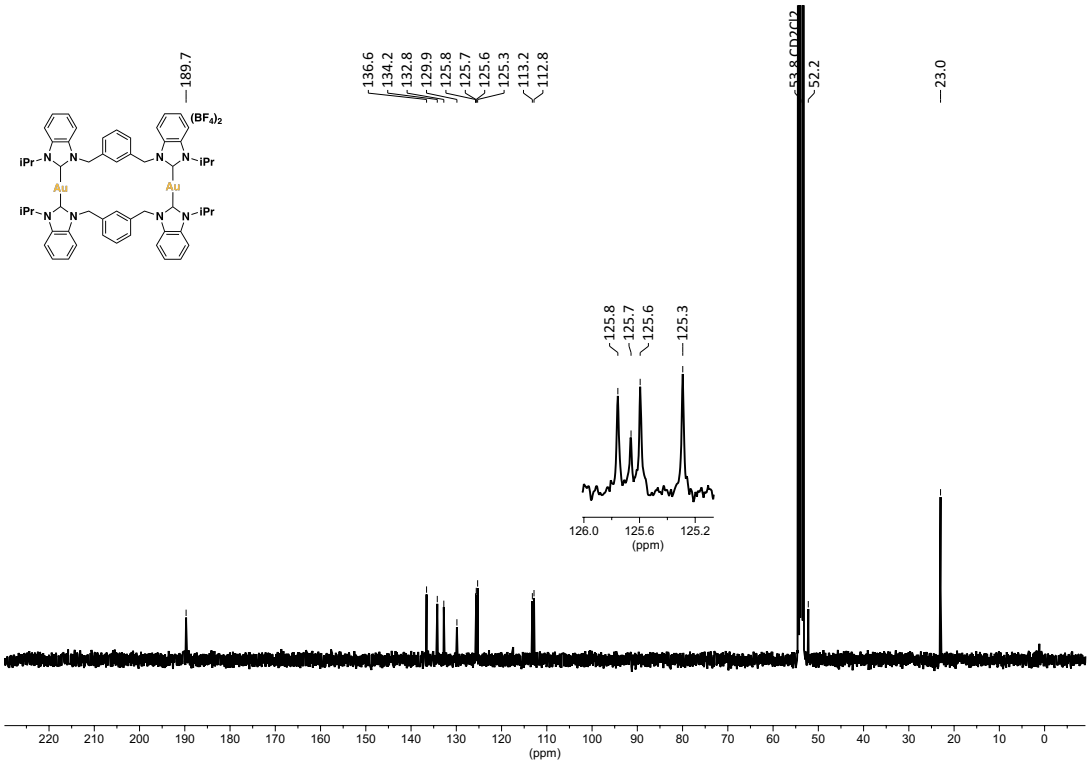

Figure S101. $^{13}C\{^{1}H\}$ NMR (101MHz, 298K) of **13a** in CD_2Cl_2

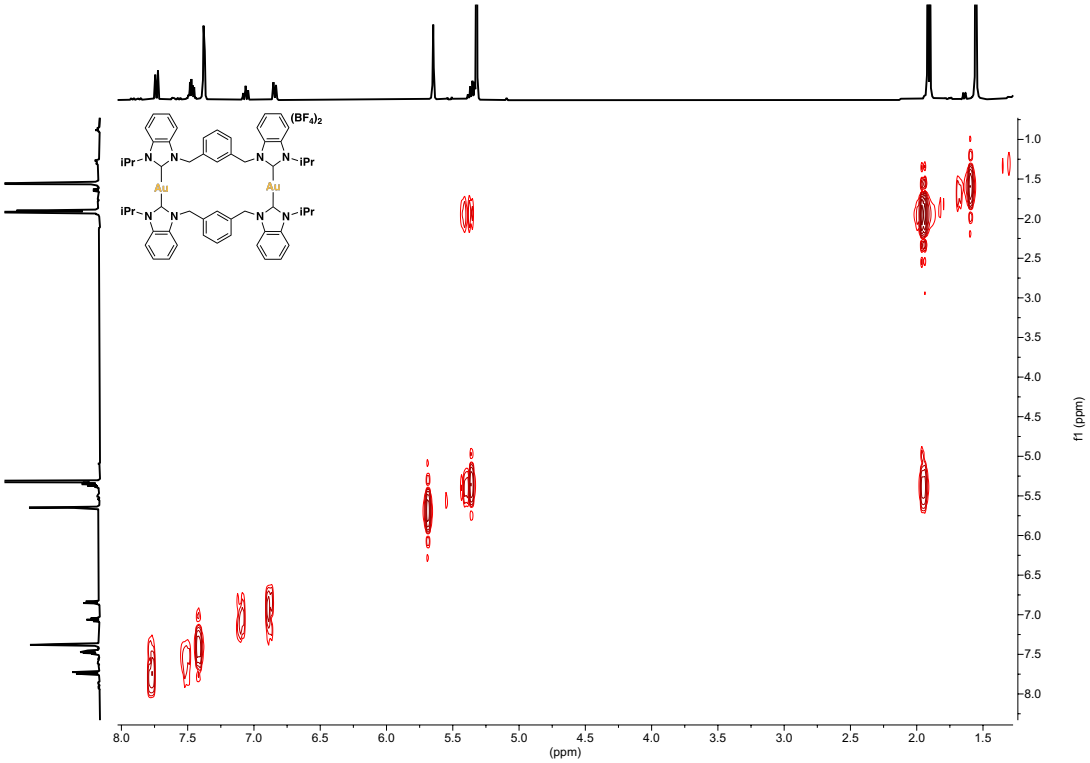

Figure S102. $^{1}H,^{1}H$ COSY NMR (400MHz, 298K) of **13a** in CD_2Cl_2

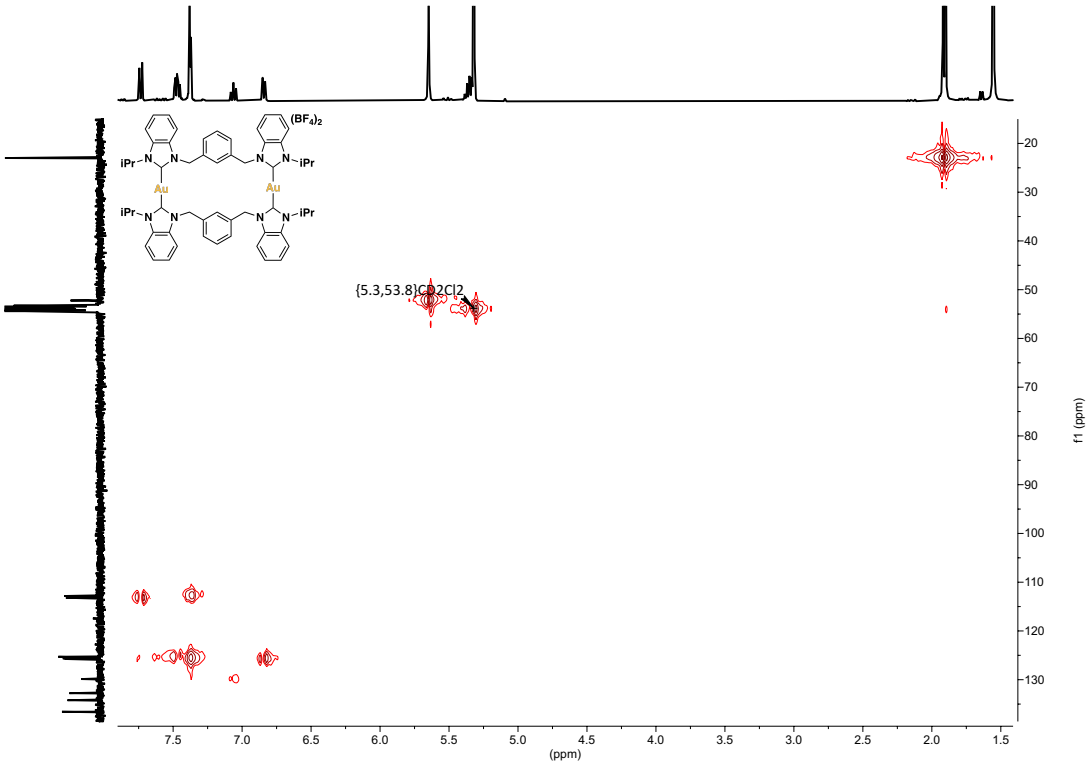

Figure S103. $^{1}H,^{13}C$ HSQC NMR (400MHz, 298K) of **13a** in CD_2Cl_2

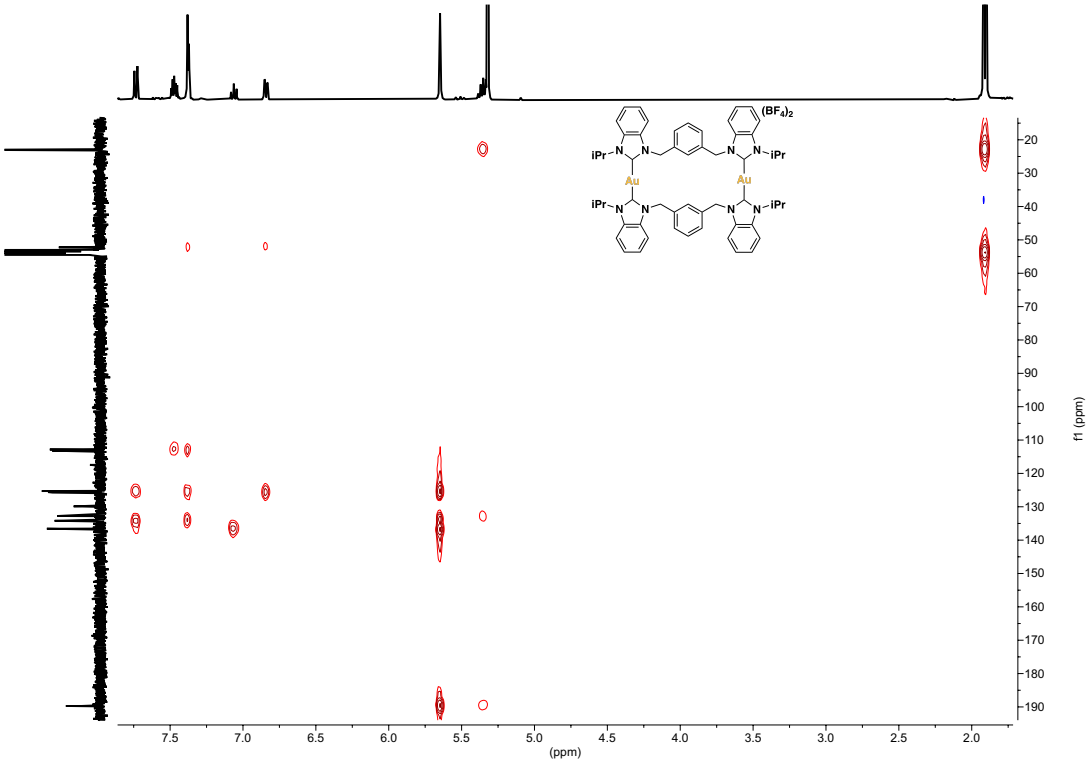

Figure S104. $^{1}H,^{13}C$ HMBC NMR (400MHz, 298K) of **13a** in CD_2Cl_2

8 X–Ray structures and crystallographic data

8.1 Compound 5b

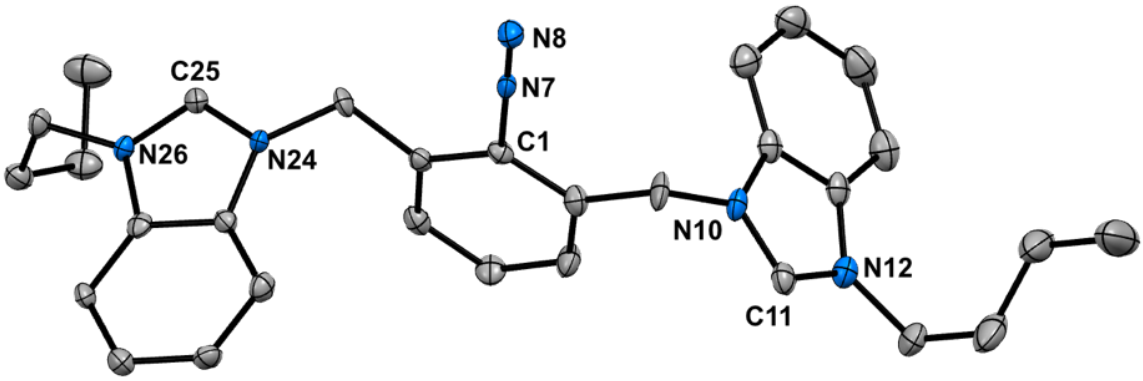

Figure S105. Crystal structure of **5b** (CCDC 2334006). Ellipsoids set at 50% probability; H atoms and BF_4 counterions were removed for clarity.

Table S1. Crystallographic parameters for compound **5b**

Chemical formula	$C_{62}H_{73}B_6F_{24}N_{13}$	
Formula weight	1521.19 g/mol	
Temperature	100(2) K	
Wavelength	0.71076 Å	
Crystal size	0.080 x 0.120 x 0.220 mm	
Crystal habit	colorless needle	
Crystal system	triclinic	
Space group	P –1	
Unit cell dimensions	a = 14.84(2) Å	α = 95.25(4)°
	b = 15.50(2) Å	β = 99.16(4)°
	c = 16.50(3) Å	γ = 108.37(3)°
Volume	3515.(9) $Å^3$	
Z	2	
Density (calculated)	1.438 g/cm^3	
Absorption coefficient	0.130 mm^{-1}	
F(000)	1564	

A colorless needle–like specimen of $C_{62}H_{73}B_6F_{24}N_{13}$, approximate dimensions 0.080 mm x 0.120 mm x 0.220 mm, was used for the X–ray crystallographic analysis. The X–ray intensity data were measured on a D8 QUEST ECO three–circle diffractometer system equipped with a Ceramic x–ray tube (Mo Kα, λ = 0.71076 Å) and a doubly curved silicon crystal Bruker Triumph monochromator. A total of 364 frames were collected. The total exposure time was 10.11 hours. The frames were integrated with the Bruker SAINT software package using

a narrow–frame algorithm. The integration of the data using a triclinic unit cell yielded a total of 33289 reflections to a maximum θ angle of 26.20° (0.80 Å resolution), of which 13648 were independent (average redundancy 2.439, completeness = 96.6%, R_{int} = 6.03%, R_{sig} = 10.16%) and 7491 (54.89%) were greater than 2σ(F^2). The final cell constants of a = 14.84(2) Å, b = 15.50(2) Å, c = 16.50(3) Å, α = 95.25(4)°, β = 99.16(4)°, γ = 108.37(3)°, volume = 3515.(9) $Å^3$, are based upon the refinement of the XYZ–centroids of 8974 reflections above 20 σ(I) with 5.775° < 2θ < 52.26°. Data were corrected for absorption effects using the Multi–Scan method (SADABS). The ratio of minimum to maximum apparent transmission was 0.818. The calculated minimum and maximum transmission coefficients (based on crystal size) are 0.6097 and 0.7453. The structure was solved and refined using the Bruker SHELXTL Software Package, using the space group P –1, with Z = 2 for the formula unit, $C_{62}H_{73}B_6F_{24}N_{13}$. The final anisotropic full–matrix least–squares refinement on F^2 with 959 variables converged at R1 = 6.68%, for the observed data and wR2 = 16.54% for all data. The goodness–of–fit was 1.019. The largest peak in the final difference electron density synthesis was 0.724 e–/$Å^3$ and the largest hole was –0.400 e–/$Å^3$ with an RMS deviation of 0.064 e–/Å3. On the basis of the final model, the calculated density was 1.438 g/cm^3 and F(000), 1564 e^-.

8.2 Compound 6a

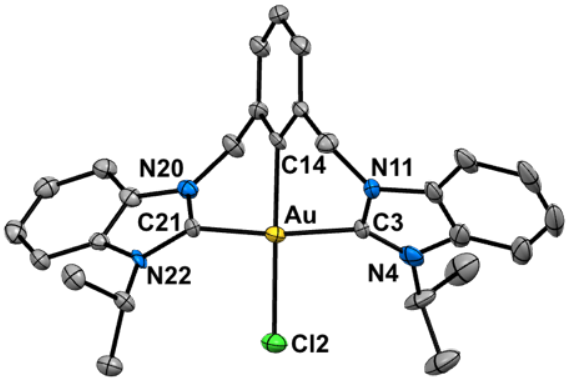

Figure S106. Crystal structure of **6a** (CCDC 2334008). Ellipsoids set at 50% probability; H atoms and BF_4 counterion were removed for clarity.

Table S2. Crystallographic parameters for compound **6a.**

Chemical formula	$C_{62}H_{70}Au_2B_2Cl_6F_8N_{10}O$	
Formula weight	1751.53 g/mol	
Temperature	100(2) K	
Wavelength	0.71073 Å	
Crystal size	0.040 x 0.090 x 0.160 mm	
Crystal habit	colorless plate	
Crystal system	monoclinic	
Space group	P 1 21/n 1	
Unit cell dimensions	a = 9.3865(19) Å	α = 90°
	b = 17.981(4) Å	β = 98.923(6)°
	c = 20.354(5) Å	γ = 90°
Volume	3393.7(13) $Å^3$	
Z	2	
Density (calculated)	1.714 g/cm^3	
Absorption coefficient	4.625 mm^{-1}	
F(000)	1724	

A colorless, plate–like specimen of $C_{62}H_{70}Au_2B_2Cl_6F_8N_{10}O$, approximate dimensions 0.040 mm x 0.090 mm x 0.160 mm, was used for the X–ray crystallographic analysis. The X–ray intensity data were measured on a D8 QUEST ECO three–circle diffractometer system equipped with a Ceramic x–ray tube (Mo Kα, λ = 0.71073 Å) and a doubly curved silicon crystal Bruker Triumph monochromator. A total of 501 frames were collected. The total exposure time was 1.39 hours. The frames were integrated with the Bruker SAINT software package using a narrow–frame algorithm. The integration of the data using a monoclinic unit cell yielded a total of 107683 reflections to a maximum θ angle of 28.33° (0.75 Å

resolution), of which 8436 were independent (average redundancy 12.765, completeness = 99.8%, R_{int} = 10.18%, R_{sig} = 4.52%) and 6907 (81.88%) were greater than $2\sigma(F^2)$. The final cell constants of a = 9.3865(19) Å, b = 17.981(4) Å, c = 20.354(5) Å, β = 98.923(6)°, volume = 3393.7(13) $Å^3$, are based upon the refinement of the XYZ–centroids of 9884 reflections above 20 σ(I) with 5.077° < 2θ < 56.19°. Data were corrected for absorption effects using the Multi–Scan method (SADABS). The ratio of minimum to maximum apparent transmission was 0.736. The calculated minimum and maximum transmission coefficients (based on crystal size) are 0.5250 and 0.8370. The structure was solved and refined using the Bruker SHELXTL Software Package, using the space group P 1 21/n 1, with Z = 2 for the formula unit, $C_{62}H_{70}Au_2B_2Cl_6F_8N_{10}O$. The final anisotropic full–matrix least–squares refinement on F^2 with 433 variables converged at R1 = 7.15%, for the observed data and wR2 = 14.88% for all data. The goodness–of–fit was 1.170. The largest peak in the final difference electron density synthesis was 1.993 $e^-/Å^3$ and the largest hole was –4.131e^- /$Å^3$with an RMS deviation of 0.222 $e^-/Å^3$. On the basis of the final model, the calculated density was1.714 g/cm^3 and F(000), 1724e^-.

8.3 Complex 6b

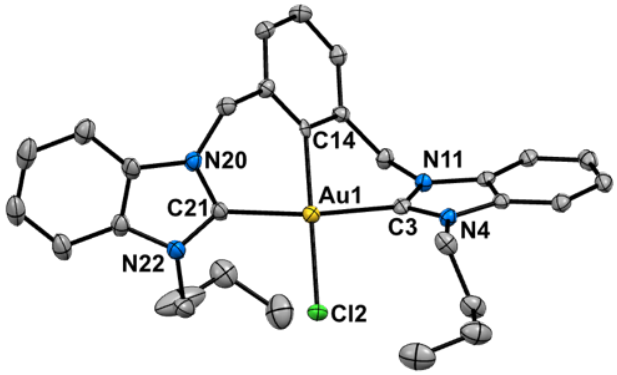

Figure S107. Crystal structure of **6b** (CCDC 2334007). Ellipsoids set at 50% probability; H atoms and BF_4 counterion were removed for clarity.

Table S3. Crystallographic parameters for compound **6b**

Chemical formula	$C_{31}H_{35}AuBCl_3F_4N_4O_0$	
Formula weight	853.75 g/mol	
Temperature	100(2) K	
Wavelength	0.71073 Å	
Crystal size	0.080 x 0.100 x 0.140 mm	
Crystal habit	yellow block	
Crystal system	triclinic	
Space group	P –1	
Unit cell dimensions	a = 10.0080(4) Å	α = 86.0800(10)°
	b = 10.3247(4) Å	β = 89.9980(10)°
	c = 16.4908(6) Å	γ = 69.3010(10)°
Volume	1589.73(11) $Å^3$	
Z	2	
Density (calculated)	1.784 g/cm^3	
Absorption coefficient	4.932 mm^{-1}	
F(000)	840	

A yellow block–like specimen of $C_{31}H_{35}AuBCl_3F_4N_4O_0$, approximate dimensions 0.080 mm x 0.100 mm x 0.140 mm, was used for the X–ray crystallographic analysis. The X–ray intensity data were measured on a D8 QUEST ECO three–circle diffractometer system equipped with a Ceramic x–ray tube (Mo Kα, λ = 0.71073 Å) and a doubly curved silicon crystal Bruker Triumph monochromator. A total of 1043 frames were collected. The total exposure time was 1.45 hours. The frames were integrated with the Bruker SAINT software package using a narrow–frame algorithm. The integration of the data using a triclinic unit cell yielded a total of 97134 reflections to a maximum θ angle of 27.62° (0.77 Å resolution), of which 7327

were independent (average redundancy 13.257, completeness = 99.2%, R_{int} = 7.59%, R_{sig} = 3.31%) and 6249 (85.29%) were greater than $2\sigma(F^2)$. The final cell constants of a = 10.0080(4) Å, b = 10.3247(4) Å, c = 16.4908(6) Å, α = 86.0800(10)°, β = 89.9980(10)°, γ = 69.3010(10)°, volume = 1589.73(11) $Å^3$, are based upon the refinement of the XYZ–centroids of 9982 reflections above 20 σ(I) with 5.558° < 2θ < 54.71°. Data were corrected for absorption effects using the Multi–Scan method (SADABS). The ratio of minimum to maximum apparent transmission was 0.821. The calculated minimum and maximum transmission coefficients (based on crystal size) are 0.5450 and 0.6940. The structure was solved and refined using the Bruker SHELXTL Software Package, using the space group P–1, with Z = 2 for the formula unit, $C_{31}H_{35}AuBCl_3F_4N_4O_0$. The final anisotropic full–matrix least–squares refinement on F^2 with 407 variables converged at R1 = 3.31%, for the observed data and wR2 = 8.18% for all data. The goodness–of–fit was 1.172. The largest peak in the final difference electron density synthesis was 4.965 $e^-/Å^3$ and the largest hole was –1.574 $e^-/Å^3$ with an RMS deviation of 0.168 $e^-/Å^3$. On the basis of the final model, the calculated density was 1.784 g/cm^3 and F(000), 840 e^-.

8.4 Complex 8a

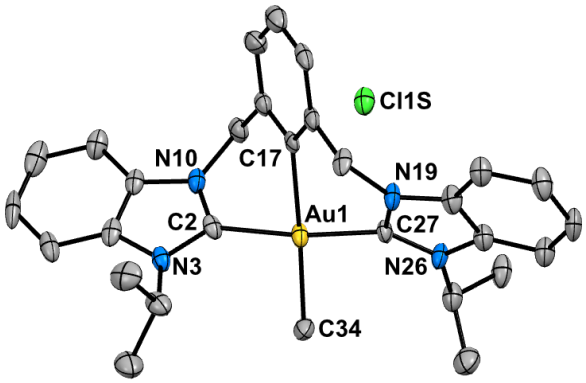

Figure S108. Crystal structure of **8a** (CCDC 2334012). Ellipsoids set at 50% probability; H atoms were removed for clarity.

Table S4. Crystallographic parameters for compound **8a**

Chemical formula	$C_{31}H_{35}AuClN_5O_0$	
Formula weight	710.05 g/mol	
Temperature	130(2) K	
Wavelength	0.71076 Å	
Crystal size	0.050 x 0.120 x 0.130 mm	
Crystal habit	colorless prism	
Crystal system	triclinic	
Space group	P –1	
Unit cell dimensions	a = 9.2394(4) Å	α = 82.772(3)°
	b = 13.0032(7) Å	β = 84.032(3)°
	c = 13.1246(7) Å	γ = 85.266(3)°
Volume	1551.95(14) $Å^3$	
Z	2	
Density (calculated)	1.519 g/cm^3	
Absorption coefficient	4.853 mm^{-1}	
F(000)	704	

A colorless, prism–like specimen of $C_{31}H_{35}AuClN_5O_0$, approximate dimensions 0.050 mm x 0.120 mm x 0.130 mm, was used for the X–ray crystallographic analysis. The X–ray intensity data were measured on a D8 QUEST ECO three–circle diffractometer system equipped with a Ceramic x–ray tube (Mo Kα, λ = 0.71076 Å) and a doubly curved silicon crystal Bruker Triumph monochromator. A total of 504 frames were collected. The total exposure time was 0.70 hours. The frames were integrated with the Bruker SAINT software package using a narrow–frame algorithm. The integration of the data using a triclinic unit cell yielded a total of 56526 reflections to a maximum θ angle of 27.69° (0.76 Å resolution), of which 7206

were independent (average redundancy 7.844, completeness = 99.4%, R_{int} = 11.49%, R_{sig} = 5.97%) and 5973 (82.89%) were greater than $2\sigma(F^2)$. The final cell constants of a = 9.2394(4) Å, b = 13.0032(7) Å, c = 13.1246(7) Å, α = 82.772(3)°, β = 84.032(3)°, γ = 85.266(3)°, volume = 1551.95(14) $Å^3$, are based upon the refinement of the XYZ–centroids of 9071 reflections above 20 σ(I) with 5.271° < 2θ < 54.78°. Data were corrected for absorption effects using the Multi–Scan method (SADABS). The ratio of minimum to maximum apparent transmission was 0.704. The calculated minimum and maximum transmission coefficients (based on crystal size) are 0.5710 and 0.7930. The structure was solved and refined using the Bruker SHELXTL Software Package, using the space group P–1, with Z = 2 for the formula unit, $C_{31}H_{35}AuClN_5O_0$. The final anisotropic full–matrix least–squares refinement on F^2 with 349 variables converged at R1 = 6.34%, for the observed data and wR2 = 16.94% for all data. The goodness–of–fit was 1.136. The largest peak in the final difference electron density synthesis was 8.413 $e^-/Å^3$ and the largest hole was –2.003 $e^-/Å^3$ with an RMS deviation of 0.260 $e^-/Å^3$. On the basis of the final model, the calculated density was 1.519 g/cm^3 and F(000), 704 e^-.

8.5 Complex 8b

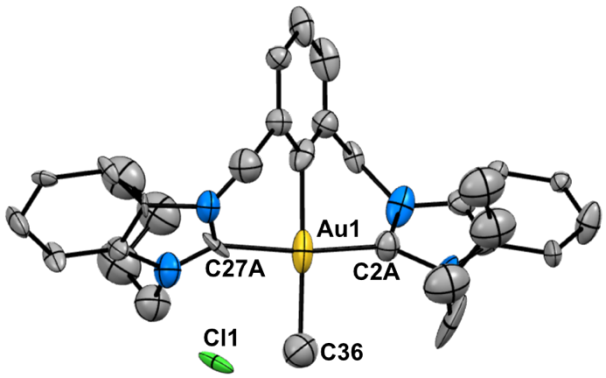

Figure S109. Crystal structure of **8b** (CCDC 2334004). Ellipsoids set at 50% probability; H atoms and BF_4 counterions were removed for clarity.

Table S5. Crystallographic parameters for compound **8b**

Chemical formula	$C_{31}H_{35}AuClN_4$	
Formula weight	696.04 g/mol	
Temperature	100(2) K	
Wavelength	0.71073 Å	
Crystal size	0.060 x 0.080 x 0.300 mm	
Crystal habit	colorless needle	
Crystal system	trigonal	
Space group	P 31	
Unit cell dimensions	a = 18.1457(11) Å	α = 90°
	b = 18.1457(11) Å	β = 90°
	c = 10.1390(9) Å	γ = 120°
Volume	2891.2(4) $Å^3$	
Z	3	
Density (calculated)	1.199 g/cm^3	
Absorption coefficient	3.905 mm^{-1}	
F(000)	1035	

A colorless, needle–like specimen of $C_{31}H_{35}AuClN_4$, approximate dimensions 0.060 mm x 0.080 mm x 0.300 mm, was used for the X–ray crystallographic analysis. The X–ray intensity data were measured on a D8 QUEST ECO three–circle diffractometer system equipped with a Ceramic x–ray tube (Mo Kα, λ = 0.71073 Å) and a doubly curved silicon crystal Bruker Triumph monochromator. A total of 1986 frames were collected. The total exposure time was 2.06 hours. The frames were integrated with the Bruker SAINT software package using a narrow–frame algorithm. The integration of the data using a trigonal unit cell yielded a total of 21282 reflections to a maximum θ angle of 23.83° (0.88 Å resolution), of which 5955

were independent (average redundancy 3.574, completeness = 99.9%, R_{int} = 7.87%, R_{sig} = 9.01%) and 4312 (72.41%) were greater than $2\sigma(F^2)$. The final cell constants of a = 18.1457(11) Å, b = 18.1457(11) Å, c = 10.1390(9) Å, volume = 2891.2(4) $Å^3$, are based upon the refinement of the XYZ–centroids of 4839reflections above 20 σ(I) with 6.026° < 2θ < 45.91°. The ratio of minimum to maximum apparent transmission was 0.705. The calculated minimum and maximum transmission coefficients (based on crystal size) are 0.3870 and 0.7990. The structure was solved and refined using the Bruker SHELXTL Software Package, using the space group P 31, with Z = 3 for the formula unit, $C_{31}H_{35}AuClN_4$. The final anisotropic full–matrix least–squares refinement on F^2 with 270 variables converged at R1 = 7.86%, for the observed data and wR2 = 20.95% for all data. The goodness–of–fit was 1.057. The largest peak in the final difference electron density synthesis was 1.367 $e^-/Å^3$and the largest hole was –0.882 $e^-/Å^3$ with an RMS deviation of 0.173 $e^-/Å^3$. On the basis of the final model, the calculated density was 1.199 g/cm^3 and F(000),1035 e^-.

8.6 Complex 9a

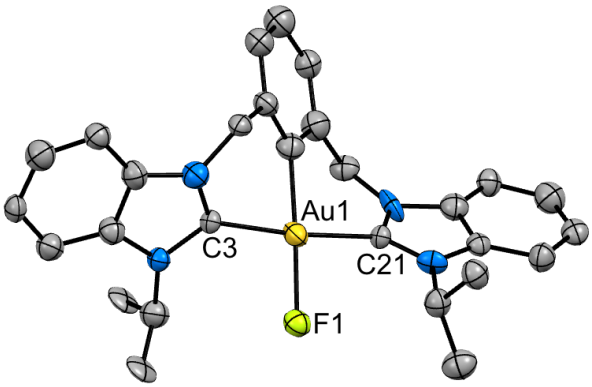

Figure S110. Crystal structure of **9a** (CCDC 2334005). Ellipsoids set at 50% probability; H atoms and BF_4 counterions were removed for clarity.

Table S6. Crystallographic parameters for compound **9a**

Chemical formula	$C_{57}H_{60}Au_2B_2Cl_2F_{10}N_8$	
Formula weight	1533.58 g/mol	
Temperature	100(2) K	
Wavelength	0.71073 Å	
Crystal size	0.010 x 0.050 x 0.190 mm	
Crystal habit	colorless needle	
Crystal system	monoclinic	
Space group	P 1 21/c 1	
Unit cell dimensions	a = 19.539(8) Å	α = 90°
	b = 10.181(4) Å	β = 97.270(10)°
	c = 28.551(11) Å	γ = 90°
Volume	5634.(4) $Å^3$	
Z	4	
Density (calculated)	1.808 g/cm^3	
Absorption coefficient	5.377 mm^{-1}	
F(000)	3000	

A colorless, needle–like specimen of $C_{57}H_{60}Au_2B_2Cl_2F_{10}N_8$, approximate dimensions 0.010 mm x 0.050 mm x 0.190 mm, was used for the X–ray crystallographic analysis. The X–ray intensity data were measured on a D8 QUEST ECO three–circle diffractometer system equipped with a Ceramic x–ray tube (Mo Kα, λ = 0.71073 Å) and a doubly curved silicon crystal Bruker Triumph monochromator. A total of 216 frames were collected. The total exposure time was 7.20 hours. The frames were integrated with the Bruker SAINT software package using a narrow–frame algorithm. The integration of the data using a monoclinic unit cell yielded a total of 48771 reflections to a maximum θ angle of 23.38° (0.90 Å

resolution), of which 8159 were independent (average redundancy 5.978, completeness = 99.2%, R_{int} = 27.72%, R_{sig} = 15.33%) and 4970 (60.91%) were greater than $2\sigma(F^2)$. The final cell constants of a = 19.539(8) Å, b = 10.181(4) Å, c = 28.551(11) Å, β = 97.270(10)°, volume = 5634.(4) $Å^3$, are based upon the refinement of the XYZ–centroids of 4066 reflections above 20 σ(I) with 4.928° < 2θ < 46.03°. Data were corrected for absorption effects using the Multi–Scan method (SADABS). The ratio of minimum to maximum apparent transmission was 0.450. The calculated minimum and maximum transmission coefficients (based on crystal size) are 0.4280 and 0.9480. The structure was solved and refined using the Bruker SHELXTL Software Package, using the space group P 1 21/c 1, with Z = 4 for the formula unit, $C_{57}H_{60}Au_2B_2Cl_2F_{10}N_8$. The final anisotropic full–matrix least–squares refinement on F^2 with 702 variables converged at R1 = 11.75%, for the observed data and wR2 = 28.76% for all data. The goodness–of–fit was 1.140. The largest peak in the final difference electron density synthesis was 1.863 $e^-/Å^3$ and the largest hole was –3.594 $e^-/Å^3$ with an RMS deviation of 0.300 $e^-/Å^3$. On the basis of the final model, the calculated density was 1.808 g/cm^3 and F(000), 3000 e^-.

8.7 Complex 9b

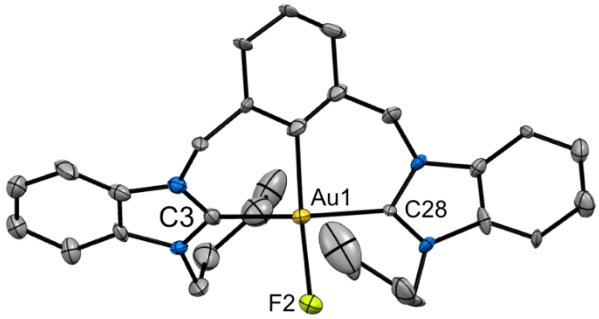

Figure S111. Crystal structure of **9b** (CCDC 2334010). Ellipsoids set at 50% probability; H atoms and BF_4 counterions were removed for clarity.

Table S7. Crystallographic parameters for compound **9b**

Chemical formula	$C_{31}H_{35}AuBCl_2F_5N_4$	
Formula weight	837.30 g/mol	
Temperature	100(2) K	
Wavelength	0.71073 Å	
Crystal size	0.040 x 0.080 x 0.300 mm	
Crystal habit	colorless needle	
Crystal system	orthorhombic	
Space group	P n a 21	
Unit cell dimensions	a = 19.7358(14) Å	α = 90°
	b = 17.0365(14) Å	β = 90°
	c = 18.6880(14) Å	γ = 90°
Volume	6283.4(8) $Å^3$	
Z	8	
Density (calculated)	1.770 g/cm^3	
Absorption coefficient	4.912 mm^{-1}	
F(000)	3296	

A colorless, needle–like specimen of $C_{31}H_{35}AuBCl_2F_5N_4$, approximate dimensions 0.040 mm x 0.080 mm x 0.300 mm, was used for the X–ray crystallographic analysis. The X–ray intensity data were measured on a D8 QUEST ECO three–circle diffractometer system equipped with a Ceramic x–ray tube (Mo Kα, λ = 0.71073 Å) and a doubly curved silicon crystal Bruker Triumph monochromator. A total of 604 frames were collected. The total exposure time was 1.23 hours. The frames were integrated with the Bruker SAINT software package using a narrow–frame algorithm. The integration of the data using an orthorhombic unit cell yielded a total of 153731 reflections to a maximum θ angle of 27.51°

(0.77 Å resolution), of which 14419 were independent (average redundancy 10.662, completeness = 99.8%, R_{int} = 16.82%, R_{sig}= 7.45%) and 10602 (73.53%) were greater than $2\sigma(F^2)$. The final cell constants of a = 19.7358(14) Å, b = 17.0365(14) Å, c = 18.6880(14) Å, volume = 6283.4(8) $Å^3$, are based upon the refinement of the XYZ–centroids of 9983 reflections above 20 σ(I) with 5.245° < 2θ < 53.29°. Data were corrected for absorption effects using the Multi–Scan method (SADABS). The ratio of minimum to maximum apparent transmission was 0.601. The calculated minimum and maximum transmission coefficients (based on crystal size) are 0.3200 and 0.8280. The structure was solved and refined using the Bruker SHELXTL Software Package, using the space group P n a 21, with Z = 8 for the formula unit, $C_{31}H_{35}AuBCl_2F_5N_4$. The final anisotropic full–matrix least–squares refinement on F^2 with 788 variables converged at R1 = 5.37%, for the observed data and wR2 = 10.78% for all data. The goodness–of–fit was 1.085. The largest peak in the final difference electron density synthesis was 1.708 $e^-/Å^3$ and the largest hole was –3.399 $e^-/Å^3$ with an RMS deviation of 0.194 $e^-/Å^3$. On the basis of the final model, the calculated density was 1.770 g/cm^3 and F(000), 3296 e^-.

8.8 Complex 10a

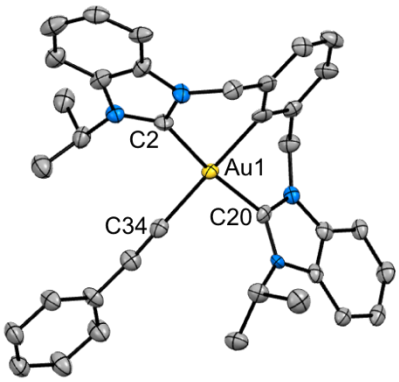

Figure S112. Crystal structure of **10a** (CCDC 2334013). Ellipsoids set at 50% probability; H atoms and BF_4 counterions were removed for clarity.

Table S8. Crystallographic parameters for compound **10a**

Chemical formula	$C_{37}H_{36}AuBCl_2F_4N_4$	
Formula weight	891.37 g/mol	
Temperature	100(2) K	
Wavelength	0.71073 Å	
Crystal size	0.050 x 0.130 x 0.300 mm	
Crystal habit	colorless plate	
Crystal system	triclinic	
Space group	P –1	
Unit cell dimensions	a = 9.5527(12) Å	α = 77.893(3)°
	b = 13.7464(17) Å	β = 80.575(3)°
	c = 14.2095(15) Å	γ = 80.828(3)°
Volume	1784.6(4) $Å^3$	
Z	2	
Density (calculated)	1.659 g/cm^3	
Absorption coefficient	4.325 mm^{-1}	
F(000)	880	

A colorless, plate–like specimen of $C_{37}H_{36}AuBCl_2F_4N_4$, approximate dimensions 0.050 mm x 0.130 mm x 0.300 mm, was used for the X–ray crystallographic analysis. The X–ray intensity data were measured on a D8 QUEST ECO three–circle diffractometer system equipped with a Ceramic x–ray tube (Mo Kα, λ = 0.71073 Å) and a doubly curved silicon crystal Bruker Triumph monochromator. A total of 583 frames were collected. The total exposure time was 3.24 hours. The frames were integrated with the Bruker SAINT software package using a narrow–frame algorithm. The integration of the data using a triclinic unit cell yielded a total of 54188 reflections to a maximum θ angle of 26.48° (0.80 Å resolution), of which 7338

were independent (average redundancy 7.385, completeness = 99.5%, R_{int} = 15.30%, R_{sig} = 8.79%) and 5967 (81.32%) were greater than $2\sigma(F^2)$. The final cell constants of a = 9.5527(12) Å, b = 13.7464(17) Å, c = 14.2095(15) Å, α = 77.893(3)°, β = 80.575(3)°, γ = 80.828(3)°, volume = 1784.6(4) $Å^3$, are based upon the refinement of the XYZ–centroids of 5770 reflections above 20 σ(I) with 6.114° < 2θ < 52.49°. Data were corrected for absorption effects using the Multi–Scan method (SADABS). The ratio of minimum to maximum apparent transmission was 0.770. The calculated minimum and maximum transmission coefficients (based on crystal size) are 0.3570 and 0.8130. The structure was solved and refined using the Bruker SHELXTL Software Package, using the space group P –1, with Z = 2 for the formula unit, $C_{37}H_{36}AuBCl_2F_4N_4$. The final anisotropic full–matrix least–squares refinement on F^2 with 491 variables converged at R1 = 6.31%, for the observed data and wR2 = 12.77% for all data. The goodness–of–fit was 1.066. The largest peak in the final difference electron density synthesis was 1.721 $e^-/Å^3$ and the largest hole was –3.241 $e^-/Å^3$ with an RMS deviation of 0.204 $e^-/Å^3$. On the basis of the final model, the calculated density was 1.659 g/cm^3 and F(000), 880 e^-.

8.9 Complex 11a

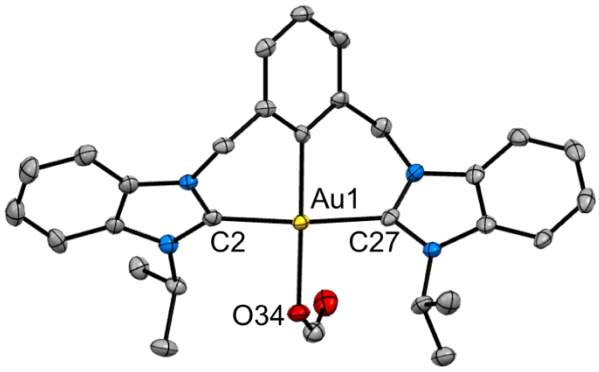

Figure S113. Crystal structure of **11a** (CCDC 2334009). Ellipsoids set at 50% probability; H atoms and BF_4 counterions were removed for clarity.

Table S9. Crystallographic parameters for compound **11a**

Chemical formula	$C_{29}H_{30}AuBF_4N_4O_2$	
Formula weight	750.34 g/mol	
Temperature	100(2) K	
Wavelength	0.71073 Å	
Crystal size	0.060 x 0.080 x 0.220 mm	
Crystal habit	colorless prism	
Crystal system	monoclinic	
Space group	P 1 21/n 1	
Unit cell dimensions	a = 13.4261(12) Å	α = 90°
	b = 12.5589(9) Å	β = 90.397(3)°
	c = 16.0123(13) Å	γ = 90°
Volume	2699.9(4) $Å^3$	
Z	4	
Density (calculated)	1.846 g/cm^3	
Absorption coefficient	5.513 mm^{-1}	
F(000)	1472	

A colorless, prism–like specimen of $C_{29}H_{30}AuBF_4N_4O_2$, approximate dimensions 0.060 mm x 0.080 mm x 0.220 mm, was used for the X–ray crystallographic analysis. The X–ray intensity data were measured on a D8 QUEST ECO three–circle diffractometer system equipped with a Ceramic x–ray tube (Mo Kα, λ = 0.71073 Å) and a doubly curved silicon crystal Bruker Triumph monochromator. A total of 704 frames were collected. The total exposure time was 0.59 hours. The frames were integrated with the Bruker SAINT software package using a narrow–frame algorithm. The integration of the data using a monoclinic unit cell yielded a total of 129169 reflections to a maximum θ angle of 27.59° (0.77 Å resolution), of which

6241 were independent (average redundancy 20.697, completeness = 99.7%, R_{int} = 13.70%, R_{sig} = 4.53%) and 4746 (76.05%) were greater than $2\sigma(F^2)$. The final cell constants of a = 13.4261(12) Å, b = 12.5589(9) Å, c = 16.0123(13) Å, β = 90.397(3)°, volume = 2699.9(4) $Å^3$, are based upon the refinement of the XYZ–centroids of 9992 reflections above 20 σ(I) with 5.088° < 2θ < 54.31°. Data were corrected for absorption effects using the Multi–Scan method (SADABS). The ratio of minimum to maximum apparent transmission was 0.745. The calculated minimum and maximum transmission coefficients (based on crystal size) are 0.3770 and 0.7330. The structure was solved and refined using the Bruker SHELXTL Software Package, using the space group P 1 21/n 1, with Z = 4 for the formula unit, $C_{29}H_{30}AuBF_4N_4O_2$. The final anisotropic full–matrix least–squares refinement on F^2 with 374 variables converged at R1 = 3.03%, for the observed data and wR2 = 6.46% for all data. The goodness–of–fit was 1.047. The largest peak in the final difference electron density synthesis was 0.963 $e^-/Å^3$ and the largest hole was –1.229 $e^-/Å^3$ with an RMS deviation of 0.156 $e^-/Å^3$. On the basis of the final model, the calculated density was 1.846 g/cm^3 and F(000), 1472 e^-.

8.10 Complex 12a

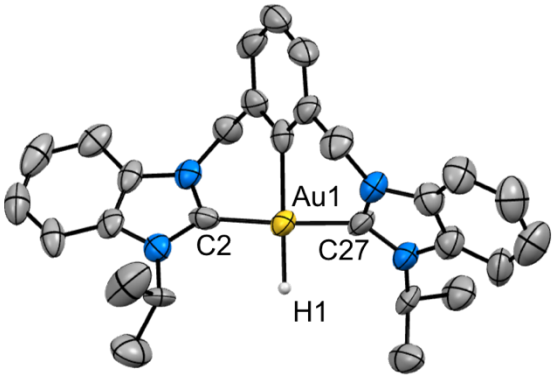

Figure S114. Crystal structure of **12a** (CCDC 2334011). Ellipsoids set at 50% probability; H atoms and BF_4 counterions were removed for clarity.

Table S10. Crystallographic parameters for compound **12a**

Chemical formula	$C_{28}H_{30}AuBF_4N_4$	
Formula weight	706.33 g/mol	
Temperature	307(2) K	
Wavelength	0.71073 Å	
Crystal size	0.040 x 0.070 x 0.130 mm	
Crystal habit	colorless block	
Crystal system	triclinic	
Space group	P –1	
Unit cell dimensions	a = 9.2528(6) Å	α = 90.162(2)°
	b = 16.3004(10) Å	β = 95.521(3)°
	c = 18.1706(10) Å	γ = 95.260(3)°
Volume	2716.2(3) $Å^3$	
Z	4	
Density (calculated)	1.727 g/cm^3	
Absorption coefficient	5.468 mm^{-1}	
F(000)	1384	

A colorless, block–like specimen of $C_{28}H_{30}AuBF_4N_4$, approximate dimensions 0.040 mm x 0.070 mm x 0.130 mm, was used for the X–ray crystallographic analysis. The X–ray intensity data were measured on a D8 QUEST ECO three–circle diffractometer system equipped with a Ceramic x–ray tube (Mo Kα, λ = 0.71073 Å) and a doubly curved silicon crystal Bruker Triumph monochromator. A total of 703 frames were collected. The total exposure time was 1.95 hours. The frames were integrated with the Bruker SAINT software package using a narrow–frame algorithm. The integration of the data using a triclinic unit cell yielded a total of 71663 reflections to a maximum θ angle of 23.50° (0.89 Å resolution), of which 8026

were independent (average redundancy 8.929, completeness = 99.8%, R_{int} = 10.82%, R_{sig} = 5.45%) and 5706 (71.09%) were greater than $2\sigma(F^2)$. The final cell constants of a = 9.2528(6) Å, b = 16.3004(10) Å, c = 18.1706(10) Å, α = 90.162(2)°, β = 95.521(3)°, γ = 95.260(3)°, volume = 2716.2(3) $Å^3$, are based upon the refinement of the XYZ–centroids of 9281 reflections above 20 σ(I) with 5.019° < 2θ < 53.88°. Data were corrected for absorption effects using the Multi–Scan method (SADABS). The ratio of minimum to maximum apparent transmission was 0.785. The calculated minimum and maximum transmission coefficients (based on crystal size) are 0.5370 and 0.8110. The structure was solved and refined using the Bruker SHELXTL Software Package, using the space group P –1, with Z = 4 for the formula unit, $C_{28}H_{30}AuBF_4N_4$. The final anisotropic full–matrix least–squares refinement on F^2 with 679 variables converged at R1 = 6.30%, for the observed data and wR2 = 13.46% for all data. The goodness–of–fit was 1.127. The largest peak in the final difference electron density synthesis was 1.758 $e^-/Å^3$and the largest hole was –1.364 $e^-/Å^3$ with an RMS deviation of 0.148 $e^-/Å^3$. On the basis of the final model, the calculated density was 1.727 g/cm^3 and F(000), 1384 e^-.

8.11 Complex 13a

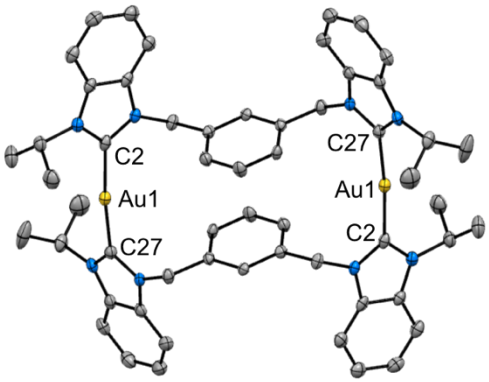

Figure S115. Crystal structure of **13a** (CCDC 2334014). Ellipsoids set at 50% probability; H atoms and BF_4 counterions were removed for clarity.

Table S11. Crystallographic parameters for compound **13a**

Chemical formula	$C_{62}H_{72}Au_2B_2Cl_{12}F_8N_8$	
Formula weight	1922.22 g/mol	
Temperature	100(2) K	
Wavelength	0.71073 Å	
Crystal size	0.050 x 0.120 x 0.240 mm	
Crystal habit	colorless plate	
Crystal system	triclinic	
Space group	P –1	
Unit cell dimensions	a = 10.5400(13) Å	α = 87.440(4)°
	b = 13.2869(19) Å	β = 88.406(4)°
	c = 13.5269(18) Å	γ = 74.202(4)°
Volume	1820.7(4) $Å^3$	
Z	1	
Density (calculated)	1.753 g/cm^3	
Absorption coefficient	4.530 mm^{-1}	
F(000)	944	

A colorless, plate–like specimen of $C_{62}H_{72}Au_2B_2Cl_{12}F_8N_8$, approximate dimensions 0.050 mm x 0.120 mm x 0.240 mm, was used for the X–ray crystallographic analysis. The X–ray intensity data were measured on a D8 QUEST ECO three–circle diffractometer system equipped with a Ceramic x–ray tube (Mo Kα, λ = 0.71073 Å) and a doubly curved silicon crystal Bruker Triumph monochromator. A total of 647 frames were collected. The total exposure time was 0.54 hours. The frames were integrated with the Bruker SAINT software package using a narrow–frame algorithm. The integration of the data using a triclinic unit cell yielded a total of 81153 reflections to a maximum θ angle of 28.38° (0.75 Å resolution),

of which 9086 were independent (average redundancy 8.932, completeness = 99.6%, R_{int} = 7.20%, R_{sig} = 4.18%) and 7751 (85.31%) were greater than $2\sigma(F^2)$. The final cell constants of a = 10.5400(13) Å, b = 13.2869(19) Å, c = 13.5269(18) Å, α = 87.440(4)°, β = 88.406(4)°, γ = 74.202(4)°, volume = 1820.7(4) $Å^3$, are based upon the refinement of the XYZ–centroids of 9765 reflections above 20 σ(I) with 5.225° < 2θ < 56.34°. Data were corrected for absorption effects using the Multi–Scan method (SADABS). The ratio of minimum to maximum apparent transmission was 0.699. The calculated minimum and maximum transmission coefficients (based on crystal size) are 0.4090 and 0.8050. The structure was solved and refined using the Bruker SHELXTL Software Package, using the space group P –1, with Z = 1 for the formula unit, $C_{62}H_{72}Au_2B_2Cl_{12}F_8N_8$. The final anisotropic full–matrix least–squares refinement on F^2 with 442 variables converged at R1 = 4.17%, for the observed data and wR2 = 10.25% for all data. The goodness–of–fit was 1.059. The largest peak in the final difference electron density synthesis was 2.072 $e^-/Å^3$ and the largest hole was –2.660 $e^-/Å^3$ with an RMS deviation of 0.171 $e^-/Å^3$. On the basis of the final model, the calculated density was 1.753 g/cm^3 and F(000), 944 e^-.

9 Effective Fragment Orbitals (EFOs) of the pincer ligands

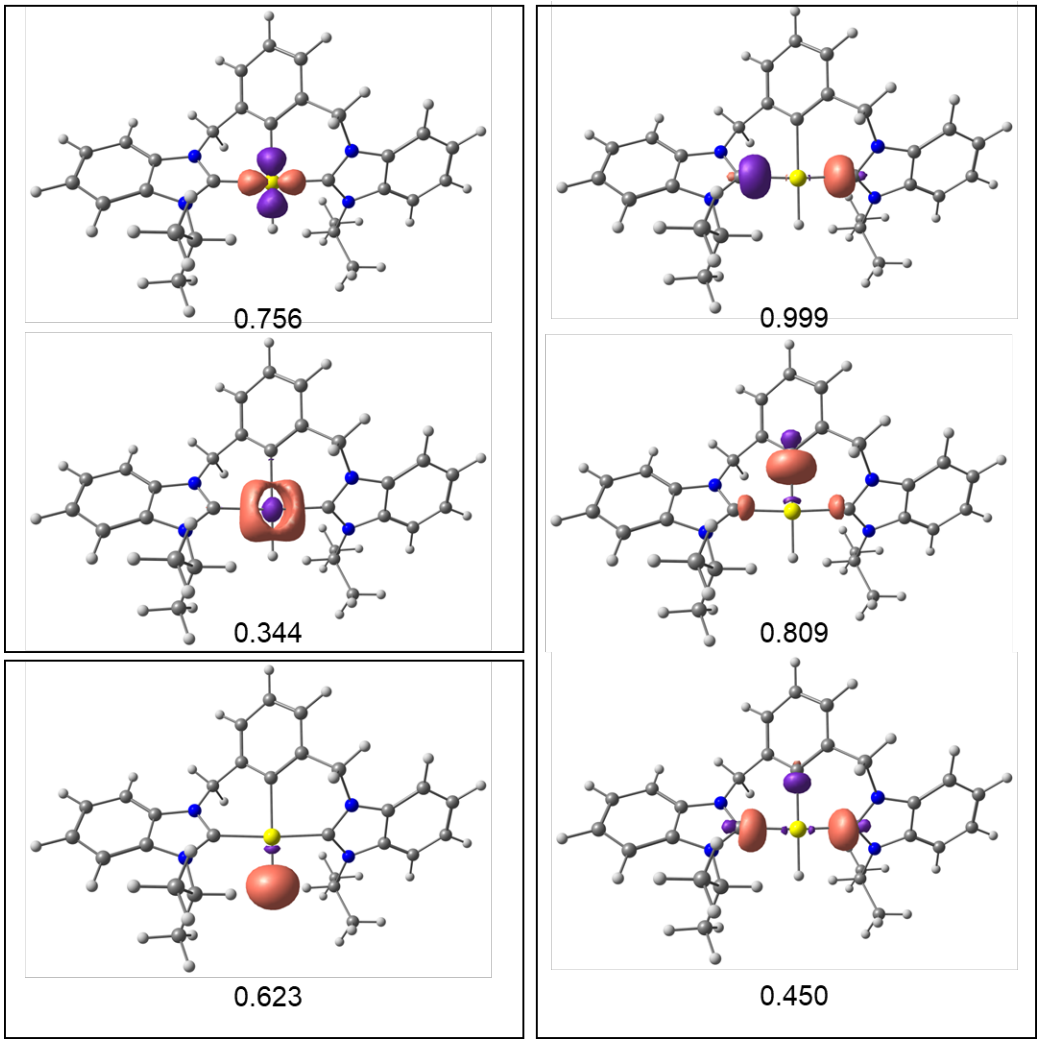

Figure S116. Most relevant EFOs and (spin) occupations of Au, H and pincer ligand for **12a**. Isocontour set to 0.1.

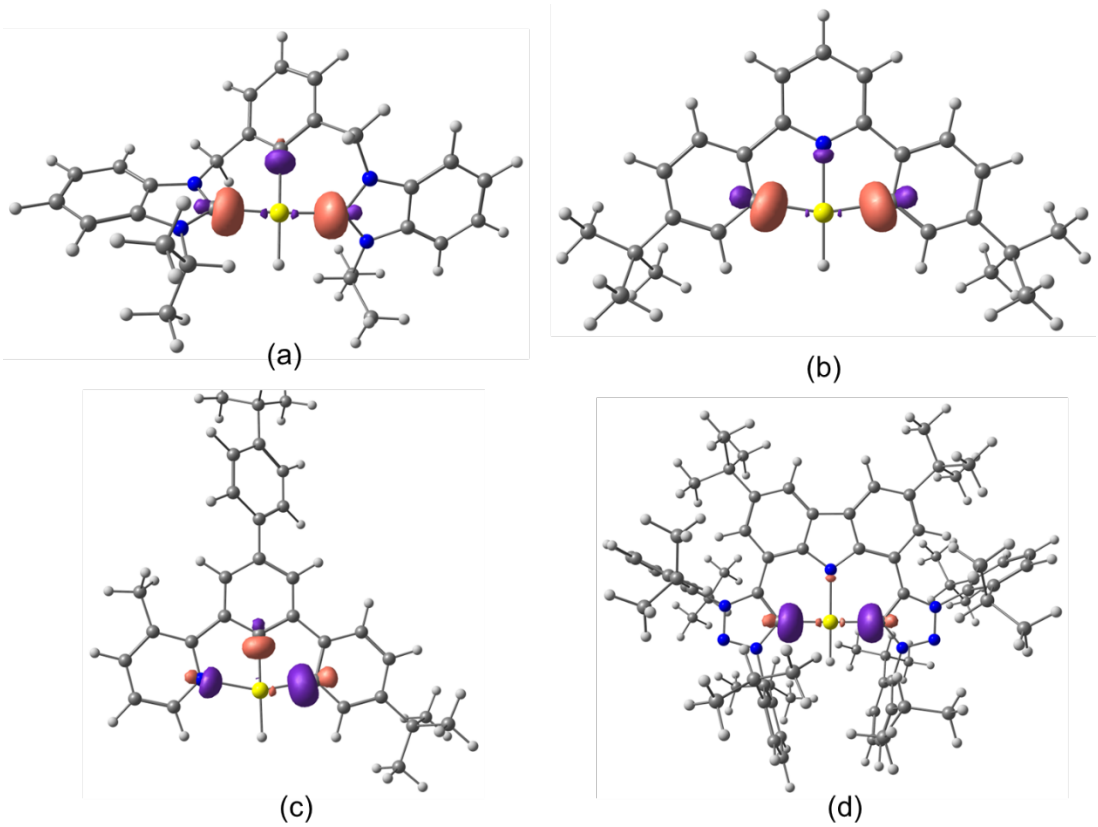

Figure S117. EFO describing the sigma donation from the pincer ligand to the Au atom in a) **12a**, as well as in the pincer Au(III)–H complexes described by b) Bochmann, c) Nevado, and d) Bezuidenhout.. Isocontour set to 0.1.

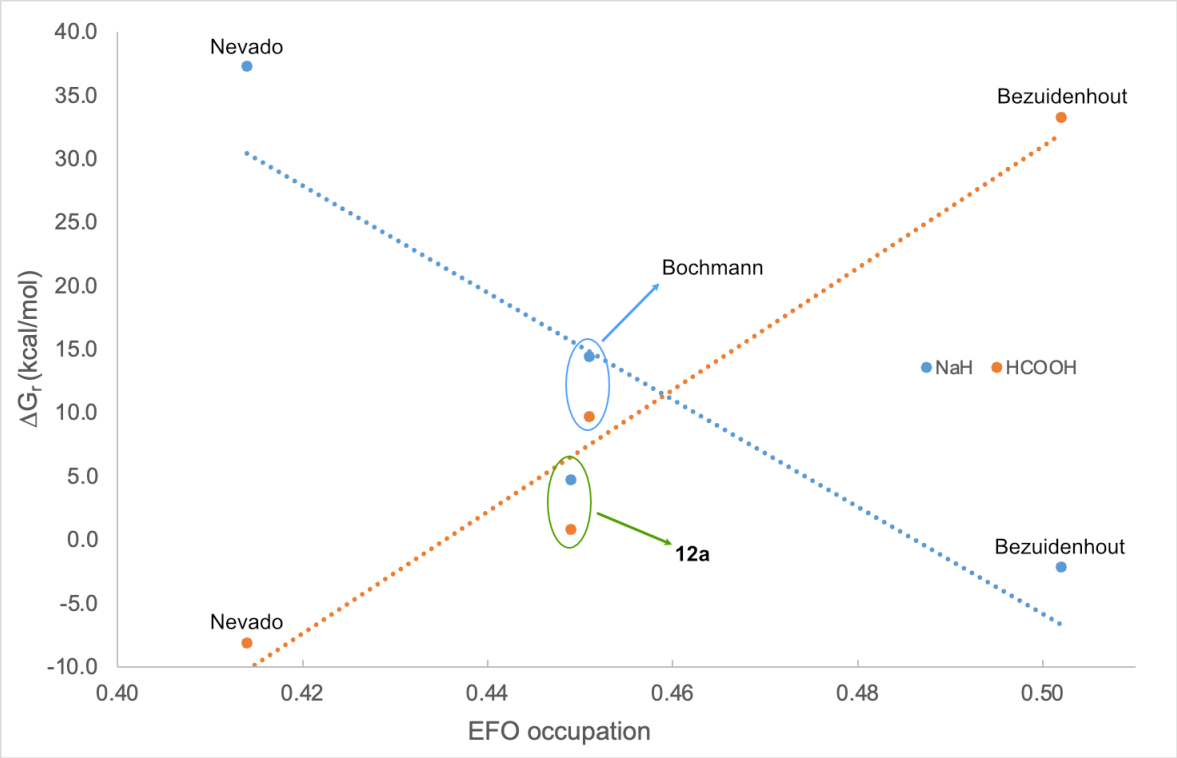

Figure S118. Graph of ΔG_r *vs* EFO occupation (see Table 1 of the main text).

10 References

(1) Starikova, O. V.; Dolgushin, G. V.; Larina, L. I.; Ushakov, P. E.; Komarova, T. N.; Lopyrev, V. A. Synthesis of 1,3-Dialkylimidazolium and 1,3-Dialkylbenzimidazolium Salts. *Russ. J. Org. Chem.* **2003**, *39* (10), 1467-1470.

(2) Liu, Q.-X.; Yin, L.-N.; Feng, J.-C. New N-heterocyclic carbene silver(I) and mercury(II) 2-D supramolecular layers by the π–π stacking interactions. *J. Organomet. Chem.* **2007**, *692* (17), 3655-3663.

(3) *Frisch, M. J.; Trucks, G. W.; Schlegel, H. B.; Scuseria, G. E.; Robb, M. A.; Cheeseman, J. R.; Scalmani, G.; Barone, V.; Petersson, G. A.; Nakatsuji, H.; Li, X.; Caricato, M.; Marenich, A. V.; Bloino, J.; Janesko, B. G.; Gomperts, R.; Mennucci, B.; Hratchian, H. P.; Ortiz, J. V.; Izmaylov, A. F.; Sonnenberg, J. L.; Williams; Ding, F.; Lipparini, F.; Egidi, F.; Goings, J.; Peng, B.; Petrone, A.; Henderson, T.; Ranasinghe, D.; Zakrzewski, V. G.; Gao, J.; Rega, N.; Zheng, G.; Liang, W.; Hada, M.; Ehara, M.; Toyota, K.; Fukuda, R.; Hasegawa, J.; Ishida, M.; Nakajima, T.; Honda, Y.; Kitao, O.; Nakai, H.; Vreven, T.; Throssell, K.; Montgomery Jr., J. A.; Peralta, J. E.; Ogliaro, F.; Bearpark, M. J.; Heyd, J. J.; Brothers, E. N.; Kudin, K. N.; Staroverov, V. N.; Keith, T. A.; Kobayashi, R.; Normand, J.; Raghavachari, K.; Rendell, A. P.; Burant, J. C.; Iyengar, S. S.; Tomasi, J.; Cossi, M.; Millam, J. M.; Klene, M.; Adamo, C.; Cammi, R.; Ochterski, J. W.; Martin, R. L.; Morokuma, K.; Farkas, O.; Foresman, J. B.; Fox, D. J. Gaussian 16, Rev. A.03*, Gaussian Inc.: Wallingford, CT, 2016.

(4) Adamo, C.; Barone, V. Toward reliable density functional methods without adjustable parameters: The PBE0 model. *J. Chem. Phys.* **1999**, *110* (13), 6158-6170.

(5) Grimme, S.; Antony, J.; Ehrlich, S.; Krieg, H. A consistent and accurate ab initio parametrization of density functional dispersion correction (DFT-D) for the 94 elements H-Pu. *J. Chem. Phys.* **2010**, *132* (15), 154104.

(6) Becke, A. D.; Johnson, E. R. A density-functional model of the dispersion interaction. *J. Chem. Phys.* **2005**, *123* (15), 154101.

(7) Grimme, S.; Ehrlich, S.; Goerigk, L. Effect of the damping function in dispersion corrected density functional theory. *J. Comput. Chem.* **2011**, *32* (7), 1456-1465.

(8) Hylland, K. T.; Schmidtke, I. L.; Wragg, D. S.; Nova, A.; Tilset, M. Synthesis of substituted (N,C) and (N,C,C) Au(III) complexes: the influence of sterics and electronics on cyclometalation reactions. *Dalton Trans.* **2022**, *51* (13), 5082-5097.

(9) Langseth, E.; Scheuermann, M. L.; Balcells, D.; Kaminsky, W.; Goldberg, K. I.; Eisenstein, O.; Heyn, R. H.; Tilset, M. Generation and Structural Characterization of a Gold(III) Alkene Complex. *Angew. Chem. Int. Ed.* **2013**, *52* (6), 1660-1663.

(10) Holmsen, M. S. M.; Nova, A.; Balcells, D.; Langseth, E.; Øien-Ødegaard, S.; Heyn, R. H.; Tilset, M.; Laurenczy, G. trans-Mutation at Gold(III): A Mechanistic Study of a Catalytic Acetylene Functionalization via a Double Insertion Pathway. *ACS Catalysis* **2017**, *7* (8), 5023-5034.

(11) Figgen, D.; Peterson, K. A.; Dolg, M.; Stoll, H. Energy-consistent pseudopotentials and correlation consistent basis sets for the 5d elements Hf–Pt. *J. Chem. Phys.* **2009**, *130* (16), 164108.

(12) Figgen, D.; Rauhut, G.; Dolg, M.; Stoll, H. Energy-consistent pseudopotentials for group 11 and 12 atoms: adjustment to multi-configuration Dirac–Hartree–Fock data. *Chem. Phys.* **2005**, *311* (1), 227-244.

(13) Marenich, A. V.; Cramer, C. J.; Truhlar, D. G. Universal Solvation Model Based on Solute Electron Density and on a Continuum Model of the Solvent Defined by the Bulk Dielectric Constant and Atomic Surface Tensions. *J. Phys. Chem. B* **2009**, *113* (18), 6378-6396.
(14) Grimme, S. Supramolecular Binding Thermodynamics by Dispersion-Corrected Density Functional Theory. *Chem. Eur. J.* **2012**, *18* (32), 9955-9964.
(15) Luchini, G.; Alegre-Requena, J. V.; Funes-Ardoiz, I.; Paton, R. S. GoodVibes: automated thermochemistry for heterogeneous computational chemistry data [version 1; peer review: 2 approved with reservations]. *F1000Research 2020 9*, 291.
(16) Reed, A. E.; Weinhold, F. Natural bond orbital analysis of near-Hartree–Fock water dimer. *J. Chem. Phys.* **1983**, *78* (6), 4066-4073.
(17) P. Salvador, E. R.-C., M. Montilla, L. Pujal, M. Gimferrer. APOST-3D: Chemical Concepts from Wavefunction Analysis. *J. Chem. Phys.* **2024**, 160, 172502.